VOLUME 87 NO. ST1
JANUARY 1961

JOURNAL of the

Structural Division

PROCEEDINGS OF THE

AMERICAN SOCIETY
OF CIVIL ENGINEERS

BASIC REQUIREMENTS FOR MANUSCRIPTS

Original papers and discussions of current papers should be submitted to the Manager of Technical Publications, ASCE. Authors should indicate the technical division to which the paper is referred. The final date on which a discussion should reach the Society is given as a footnote with each paper. Those who are planning to submit material will expedite the review and publication procedures by complying with the following basic requirements:

1. Titles must have a length not exceeding 50 characters and spaces.

2. A summary of approximately 50 words must accompany the paper, a 300-word synopsis must precede it, and a set of conclusions must end it.

3. The manuscript (an original ribbon copy and two duplicate copies) should be double-spaced on one side of 8½-inch by 11-inch paper. Three copies of all illustrations, tables, etc., must be included.

4. The author's full name, Society membership grade, and footnote reference stating present employment must appear on the first page of the paper.

5. Mathematics are recomposed from the copy that is submitted. Because of this, it is necessary that letters be drawn carefully, and that special symbols be properly identified. The letter symbols used should be defined where they first appear, in the illustrations or in the text, and arranged alphabetically in an Appendix.

6. Tables should be typed (an original ribbon copy and two duplicate copies) on one side of 8½-inch by 11-inch paper. Specific illustrations and explanation must be made in the text for each table.

7. Illustrations must be drawn in black ink on one side of 8½-inch by 11-inch paper. Because illustrations will be reproduced with a width of between 3-inches and 4½-inches, the lettering must be large enough to be legible at this width. Photographs should be submitted as glossy prints. Explanations and descriptions must be made within the text for each illustration.

8. The desirable average length of a paper is about 12,000 words and the absolute maximum is 18,000 words. As an approximation, each full page of typed text, table, or illustration is the equivalent of 300 words.

9. Technical papers intended for publication must be written in the third person.

10. The author should distinguish between a list of "Reading References" and a "Bibliography," which would encompass the subject of his paper.

Reprints from this Journal may be made on condition that the full title of the paper, name of author, page reference, and date of publication by the Society are given. The Society is not responsible for any statement made or opinion expressed in its publications.

This Journal is published monthly by the American Society of Civil Engineers. Publication office is at 2500 South State Street, Ann Arbor, Michigan. Editorial and General Offices are at 33 West 39 Street, New York 18, New York. $4.00 of a member's dues are applied as a subscription to this Journal. Second-class postage paid at Ann Arbor, Michigan.

The index for 1959 was published as ASCE Publication 1960-10 (list price $2.00); indexes for previous years are also available.

Journal of the

STRUCTURAL DIVISION

Proceedings of the American Society of Civil Engineers

STRUCTURAL DIVISION
EXECUTIVE COMMITTEE

Emerson J. Ruble, Chairman; Nathan D. Whitman, Jr., Vice Chairman; Robert D. Dewell; Theodore R. Higgins; John D. Haltiwanger, Secretary

COMMITTEE ON PUBLICATIONS
Gerald F. Borrmann, Chairman; Phil M. Ferguson; Abbott Frank; William J. Hall; Roy G. Johnston; William T. K. May; William H. Munse; Sidney Shore; George S. Vincent

CONTENTS

January, 1961

Papers

Page

Static and Dynamic Analysis of Guy Cables
by Donald L. Dean 1

Lateral Inelastic Buckling of Tied Arches
by Chin Fung Kee 23

Analysis of Structures by Combining Redundants
by Peter P. Gillis and Kurt H. Gerstle 41

Recent Trends in Ultimate Strength Design
by Phil M. Ferguson 57

Moment-Distribution Constants from Cardboard Analogs
by Otakar Ondra 73

(over)

Copyright 1961 by the American Society of Civil Engineers.

DISCUSSION

Page

Matrix Solution of Beams with Variable Moment of Inertia, by Ming L. Pei. (October, 1959. Prior discussion: December, 1959, January, April, 1960. Discussion closed.)
Ming L. Pei (closure) 105

Ultimate Load Theory for Concrete Frame Analysis, by A.L.L. Baker. (November, 1959. Prior discussion: May, June, 1960. Discussion closed.)
by A. L. L. Baker (closure) 111

Analysis of Rigid Frames by Electronic Computation, by Ardis White. (November, 1959. Prior discussion: November, 1959, June, 1960. Discussion closed.)
by Ardis White (closure) 113

Vierendeel Bents with Nonprismatic Members, by S. L. Lee and F. P. Wiesinger. (December, 1959. Prior discussion: May, 1960. Discussion closed.)
by S. L. Lee and F. P. Wiesinger (closure) 115

Discontinuity Stresses in Beams on Elastic Foundations, by Joseph Penzien. (April, 1960. Prior discussion: None. Discussion closed.)
by R. S. Alwar 117

Reinforced Concrete Pavements for Airports, by August W. Compton, (May, 1960. Prior discussion: None. Discussion closed.)
by Gordon K. Ray and William G. Westall 119

Stability Problems of Compressed Steel Members and Arch Bridges, by Georg Wastlund. (June, 1960. Prior discussion: None. Discussion closed.)
by S. O. Asplund 125

Dynamic Response of Elastic Plastic Frames, by Joseph Penzien. (July, 1960. Prior discussion: None. Discussion closed.)
by A. A. Eremin 127

Errata 129

Journal of the
STRUCTURAL DIVISION
Proceedings of the American Society of Civil Engineers

STATIC AND DYNAMIC ANALYSIS OF GUY CABLES

By Donald L. Dean,[1] M. ASCE

SYNOPSIS

Guy cables are analyzed for static and dynamic conditions, and examples are solved to illustrate the formulas derived. Cable sag is accounted for in a more exact manner than has been previously accomplished without causing additional complexity in the resulting expressions.

INTRODUCTION

The work presented in this paper was completed in 1955 in an unpublished study[2] of flexible towers. It has been available to many engineers and firms. Comments by several engineers resulted in the preparation of this paper. Although the presentation is directed toward guyed towers, it is believed that the formulas will prove useful for other needs such as the analysis of transmission lines and unloaded back stays for suspension bridges.

In the design and construction of many structures, such as towers to support antennas that radiate information at line-of-sight frequencies, the lateral support is furnished by guys composed of steel strand cables. Because these cables are also responsible for a major portion of the structure's axial loads, it is useful to have accurate and reliable formulas which relate the variables associated with hanging cables, such as the change in cable tension as a function

Note.—Discussion open until June 1, 1961. To extend the closing date one month, a written request must be filed with the Executive Secretary, ASCE. This paper is part of the copyrighted Journal of the Structural Division, Proceedings of the American Society of Civil Engineers, Vol. 87, No. ST 1, January, 1961.

[1] Prof. and Chmn. of Civ. Engrg., Univ. of Delaware, Newark, Del.

[2] "A Static and Dynamic Analysis of Tall Flexible Towers," by D. L. Dean, Ph. D. Dissertation, Univ. of Mich., 1955.

of the tower movement. In some special cases, formulas developed by considering cables as straight two-force members are sufficient. However, it is usually necessary to consider their sag.

In existing analyses[3,4,5,6] of guy cables, the geometry is assumed to be parabolic. This assumption introduces errors that are quite small in some instances, such as the formula for cable length if the chord is nearly horizontal. If the chord is not horizontal, however, symmetry (with respect to the chord mid-point) is lost and the approximation introduces significant errors. The parabola-for-catenary approximation is not made in this paper. The formulas derived by adhering to the properties of the catenary are as simple as those based upon the properties of the parabola. Therefore, the inaccuracies in the latter are not warranted.

In the static analysis that follows, cable movements and load changes are assumed to occur slowly (as compared with natural frequencies). In the dynamic analysis, the inertia of the cables is considered.

When the tower vibrates normal to its axis, the guys experience longitudinal and transverse components of the movement. If the tower movement is not in the plane of the guy, there are two components of transverse cable vibration. Preliminary computations indicate that the natural frequencies of towers and their guys are of the same order of magnitudes for lateral vibration. Therefore, in computing the lateral resistance that guys offer to tower movements, the inertia of the guys should be considered. The frequencies of the modes of longitudinal vibration of guys are not of the same order of magnitude as those of towers, and need not be included in the computation of the longitudinal resistance offered to tower movements.

The ratio of the fundamental frequency of longitudinal vibration to lateral vibration of a cable is $\frac{1}{\sqrt{\epsilon}}$, where ϵ is the cable strain. For cables used as guys, the ratio is about 40. Thus, the tower movement is slow enough, as compared with the fundamental frequencies of vibration, so that a static analysis is sufficient for longitudinal motion.

Notation.—The letter symbols adopted for use in this paper are defined where they first appear, in the illustrations or in the text, and are arranged alphabetically, for convenience of reference, in the Appendix.

STATIC ANALYSIS

Curve Equations and Properties.—The cable is considered to be perfectly flexible so that the differential equation of the cable curve can be written by summing the vertical forces which act on an element. Some of the details of the derivation of the equation for the cable curve follow.

---

3 "Structural Frameworks," by C. T. Morris, John Wiley and Sons, New York, Chapman and Hall Ltd., London, 1943.

4 "Length, Tension, and Sag of Stay Ropes," by T. Walmsley, Inst. of Civ. Engrg., No. 19, 1924.

5 "Design of Multi-Level Guyed Towers," by E. Cohen and H. Perrin, Proceedings, ASCE, Vol. 83, No. ST 5, September, 1957.

6 "Amplification of Stress and Displacement in Guyed Towers," by R. S. Rowe, Proceedings, ASCE, Vol. 84, No. ST 6, October, 1958.

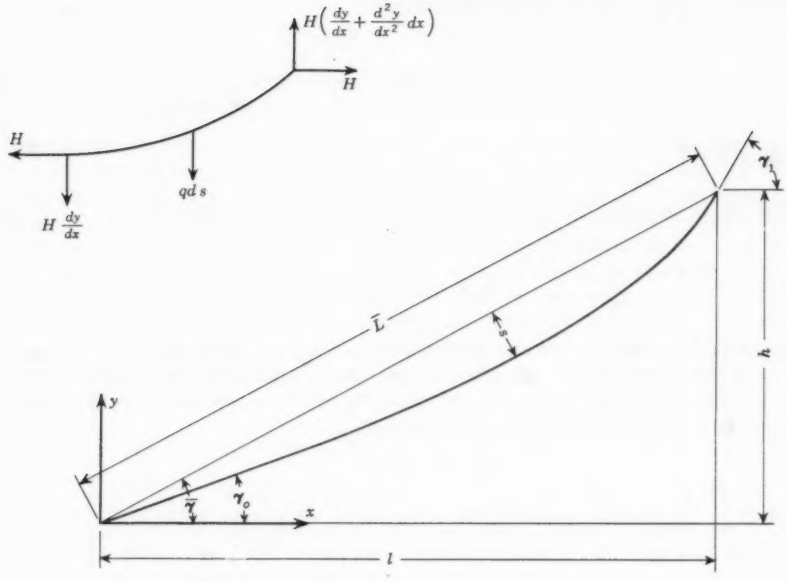

FIG. 1.—HANGING CABLE AND ELEMENT

Referring to Fig. 1,

$$H\frac{d^2y}{dx^2}\,dx = q\,ds \qquad \ldots\ldots\ldots\ldots\ldots\ldots (1)$$

$$\frac{d^2y}{dx^2} = \frac{q}{H}\left[1+\left(\frac{dy}{dx}\right)^2\right]^{1/2} \qquad \ldots\ldots\ldots\ldots\ldots (2)$$

$$\frac{dy}{dx} = \sinh\left(\frac{q}{H}x + a_1\right) \qquad \ldots\ldots\ldots\ldots\ldots\ldots (3)$$

and

$$y = \frac{H}{q}\cosh\left(\frac{q}{H}x + a_1\right) + a_2 \qquad \ldots\ldots\ldots\ldots (4)$$

The integration constants a_1 and a_2 are evaluated from the boundary conditions $y = 0$ at $x = 0$ and $y = h$ at $x = l$.

$$a_2 = -\frac{H}{q}\cosh a_1 \qquad \ldots\ldots\ldots\ldots\ldots\ldots (5a)$$

and

$$a_1 = \sinh^{-1}\left[\frac{q\,h}{2\,H\sinh r}\right] - r, \qquad \ldots\ldots\ldots\ldots (5b)$$

in which $r = \frac{q\,l}{2\,H}$. Eq. 4 can be rewritten

$$y = \frac{2H}{q} \sinh (r\bar{x} + a_1) \sinh r\bar{x}, \quad \ldots\ldots\ldots\ldots (6)$$

in which $\bar{x} = \frac{x}{l}$.

The cable tension, T, at any point, x, is $H \frac{ds}{dx}$. From Eq. 3,

$$T = H \cosh \left(\frac{q}{H}\, x + a_1\right) \quad \ldots\ldots\ldots\ldots (7)$$

Eq. 3 can be used to obtain the total length of the cable shown in Fig. 1, in terms of the other cable variables H, l, h, and q. Such an expression will furnish the key relations needed to express changes in one variable in terms of changes in the other variables, such as $\Delta l = f(\Delta H)$.

$$L = \int_o^l \frac{ds}{dx}\, dx = \int_o^l \cosh\left(\frac{q}{H}\, x + a_1\right) dx = \left[h^2 + \frac{4\,H^2}{q^2} \sinh^2 r\right]^{1/2} \ldots (8)$$

or

$$\sqrt{L^2 - h^2} = \frac{2\,H}{q} \sinh r \quad \ldots\ldots\ldots\ldots\ldots (9)$$

The slope of the cable curve at its upper and lower extremities is frequently needed. The slope of the cable at the ground, $\tan \gamma_o$, may be used with a sighting apparatus for setting the correct initial cable tension.

$$\tan \gamma_o = \sinh a_1 = \frac{q}{2\,H} \left[h \coth r - L\right] \ldots\ldots (10)$$

The slope of the cable at the tower, $\tan \gamma_1$, needed for the computation of tower loads is

$$\tan \gamma_1 = \sinh \left[2\,r + a_1\right] = \frac{q}{2\,H} \left[h \coth r + L\right] \ldots (11)$$

The maximum sag, denoted s and measured perpendicular to the chord (Fig. 1), may be desired. Occasionally this quantity is used as a criterion for establishing the initial erection stress for the guys, such as, $s < 0.015\,\bar{L}$ for a 1/2 in. coating of ice. At x_s, the horizontal distance to the point of maximum sag, $\frac{dy}{dx} = \frac{h}{l}$.

$$x_s = \frac{H}{q} \left[\sinh^{-1} \frac{h}{l} - a_1\right] \quad \ldots\ldots\ldots\ldots (12)$$

$$y_{(x_s)} = \frac{H}{q} \left[\cosh \sinh^{-1} \frac{h}{l} - \cosh a_1\right] = \frac{H}{q} \left[\sec \bar{\gamma} - \cosh a_1\right] \ldots (13)$$

and

$$s = x_s \sin \bar{\gamma} - y_{(x_s)} \cos \bar{\gamma} \quad \ldots\ldots\ldots\ldots \quad (14)$$

The dimensionless parameter, $r = \frac{q1}{2H}$, and hyperbolic functions involving r appear in the formulae presented. The term r has physical significance as the ratio between the vertical force necessary to support one-half the weight of the horizontal projection of a cable and the total horizontal force acting on the cable. In guy cables, or cables functioning as guys, r is usually quite small, rarely exceeding 0.5. Therefore, sinh r, cosh r, and tanh r can be replaced by a few terms of their respective series without a meaningful loss of accuracy. It will often be convenient and helpful to do this in the developments to follow, and many expressions will be simplified considerably by making such a substitution. An example is the constant a_1, which can be rewritten in a form that is easier to use numerically;

$$a_1 = \sinh^{-1}\left[\frac{h}{l\left(1 + \frac{1}{6}r^2\right)}\right] - r \quad \ldots\ldots\ldots \quad (15)$$

Eq. 9 can also be changed to forms that make computations easier. This equation, relating the cable variables L, h, l, H, and q, serves as a basis for most of the work to follow in this section and is used in its exact form, as Eq. 9, in derivations. However, when it is to be used for computing L in terms of known values of H, l, h, and q, it is much more convenient to work with a modified form that can be derived as follows:

$$\sqrt{L^2 - h^2} = \frac{2H}{q} \sinh r \simeq l\left(1 + \frac{1}{6}r^2\right) \ldots\ldots\ldots (16a)$$

$$L^2 \simeq \bar{L}^2 + \frac{l^2 r^2}{3} \quad \ldots\ldots\ldots\ldots\ldots\ldots (16b)$$

and

$$L \simeq \bar{L} + \frac{l^2 r^2}{6\,\bar{L}} \quad \ldots\ldots\ldots\ldots\ldots\ldots (16c)$$

Eq. 16c was derived by consistently dropping all powers of r above the third. It is very easy to use and is sufficiently precise for most guys. In fact, it is identical in form with a formula presented for the same purpose by C. T. Morris and S. T. Carpenter,[3] however, since the authors of that work were using properties of the parabola instead of the catenary, their formula, expressed in the symbols of this study,

$$L = \bar{L} + \frac{l^4 r^2}{6\,\bar{L}^3}, \quad \ldots\ldots\ldots\ldots\ldots\ldots (16d)$$

is seen to be in error by a factor, $\cos^2 \bar{\gamma}$ for the amount added to the chord length.

Although Eq. 16c is adequate for normal computations with guys, it may not be precise enough for computing L for cables with excessive sag. For such

cables it may be necessary to retain additional terms in the expansion of sinh r. By retaining powers of r including the fifth, one obtains:

$$L = \overline{L} + \frac{l^2 r^2}{6 \overline{L}} + \frac{l^2 r^4}{45 \overline{L}} - \frac{l^4 r^4}{72 \overline{L}^3} \quad \ldots\ldots\ldots\ldots\ldots\ldots (16e)$$

Effects of Changes in Cable Parameters.—Each time a tower is loaded or undergoes a change of dimensions, some of the cable parameters must vary to maintain tower equilibrium. Therefore, to carry out a rational analysis of a guyed tower, one must have available formulae that accurately relate these parameters and their changes. The three main classes of these changes are as follows:

(1) l changes due to a transverse tower load, affecting H, L, and h.
(2) h and L change due to a variation in temperature, affecting H.
(3) q increases due to ice on the cable, affecting H, L, and h.

Eq. 9 is the relation between parameters that provides the information necessary to computate quantitative values for the three main cases described above. Cases 1 and 2 may be derived from the differential relation

$$dH = \frac{\partial H}{\partial l} dl + \frac{\partial H}{\partial L} dL + \frac{\partial H}{\partial h} dh \quad \ldots\ldots\ldots\ldots\ldots\ldots (17)$$

The partial derivatives needed in Eq. 17 are obtained from Eq. 9 and simplified to

$$\frac{\partial H}{\partial l} = \frac{12 H^3}{q^2 l^3} \left(1 + 0.4 r^2\right) \quad \ldots\ldots\ldots\ldots\ldots\ldots (18)$$

$$\frac{\partial H}{\partial L} = \frac{-12 H^3 L}{q^2 l^3 \sqrt{L^2 - h^2} \left(1 + 0.1 r^2\right)} \quad \ldots\ldots\ldots\ldots (19)$$

and

$$\frac{\partial H}{\partial h} = \frac{12 H^3 h}{q^2 l^3 \sqrt{L^2 - h^2} \left(1 + 0.1 r^2\right)} \quad \ldots\ldots\ldots\ldots (20)$$

Note that in deriving Eqs. 18, 19, and 20, hyperbolic functions were replaced by three terms of their series. Also, the second approximation,

$$\frac{1}{1 - Cr^2} = 1 + Cr^2 + C^2 r^4 + C^3 r^6 + \ldots \simeq 1 + C r^2 \quad \ldots\ldots\ldots\ldots (21)$$

was frequently used. If care is excerised with these two approximations, the errors will not be accumulative and in many instances an increase in accuracy can be obtained by causing one to partially cancel the other. For example, if four terms of the series were used instead of three, Eq. 18 would be written:

$$\frac{\partial H}{\partial l} = \frac{12 H^3}{q^2 l^3} \frac{1}{\left(1 - 0.4 r^2 + 0.162 r^4\right)} \quad \ldots\ldots\ldots\ldots (22)$$

The final form presented as Eq. 18 can be rewritten:

$$\frac{\partial H}{\partial l} = \frac{12\,H^3}{q^2\,l^3}\,\frac{1}{\left(1 - 0.4\,r^2 + 0.160\,r^4 - \ldots\right)} \quad \ldots\ldots(23)$$

Here, cancellation of the errors involved in the two approximations yielded four term accuracy with a three term approximation.

As Eqs. 18, 19, and 20 all contain the factor H^3, the integration of Eq. 17 can be performed as follows;

$$\int_{H_o}^{H} \frac{dH}{H^3} = \frac{12}{q^2} \int_{l_o}^{l} \frac{\left(1 + 0.4\,r^2\right) dl}{l^3} - \frac{12}{q^2\,l^3} \int_{L_o}^{L} \frac{L\,dL}{\sqrt{L^2 - h^2}\left(1 + 0.1\,r^2\right)}$$

$$+ \frac{12}{q^2\,l^3} \int_{h_o}^{h} \frac{h\,dh}{\sqrt{L^2 - h^2}\left(1 + 0.1\,r^2\right)} \quad \ldots\ldots(24)$$

where the variables with the subscript o indicate the initial values before change, or $\Delta H = H - H_o$; $\Delta l = l - l_o$; $\Delta h = h - h_o$; and $\Delta L = L - L_o$.

Since r contains H, it is not constant during the integration of the preceding expressions, however, according to the mean value theorem for integrals, there exists an intermediate value of r, denoted r_i, such that r can be replaced by r_i and treated as a constant during integration. The values of the integrals are not sensitive to small changes in r as $r^2 \ll 1$. If the initial and final values of r are known, r_i should be made the arithmetical mean of the two values, but when the initial and final values are not both known, it is necessary to approximate the value of r_i from practical considerations. Should an extremely poor guess be made, the computation can be repeated using the first result as a guide to a better approximation.

The integration of Eq. 17, as previously indicated after some algebraic simplification, yields, for

$$K = \frac{6}{r_o^2\,l}\left[\left(1 + 0.4\,r_i^2\right)\Delta l - \frac{L\,\Delta L - h\,\Delta h}{l\left(1 + \frac{1}{6}\,r_o^2\right)\left(1 + 0.1\,r_i^2\right)}\right] \quad \ldots\ldots(25)$$

When $K \ll 1$, Eq. 25 is easier to use in the form

$$H = \frac{H_o}{\sqrt{1 - K}} \quad \ldots\ldots(26a)$$

$$\Delta H = H_o\,\frac{K}{2}\left[1 + \frac{3}{4}\,K + \frac{5}{8}\,K^2 + \frac{35}{64}\,K^3 + \ldots\right] \quad \ldots\ldots(26b)$$

The terms ΔL and Δh are seldom known. Even in case 2, ΔL and Δh are not completely known, because a change in H causes a change in L and h due to the fact that the cable and tower are elastic. Therefore, it is necessary to be able to express ΔL and Δh as functions of ΔH in Eq. 26a before it can be used.

Some of the steps in the derivation of these expressions are as follows:

$$\Delta L = \frac{1}{A_c E_c} \int_L (T - T_o)\, ds = \frac{L^2 \Delta H}{l A_c E_c} \left[1 - \frac{1}{6} r_i^2 \left(4 - \frac{l^2}{L^2} \right) \right] \quad \ldots . \quad (27)$$

in which A_c and E_c are the area and modulus, of elasticity respectively, of the cable, and T and T_o are, respectively, the final and initial cable tensions. Note that as $r_i \to 0$, the result of Eq. 27 approaches the result obtained by considering the cable to be a straight two-force member.

An expression for Δh could include factors other than temperature; namely, compression of leg of tower due to change in cable stress or decrease in length due to bending. These factors could be considered, but since the effect of Δh is usually small as compared with other effects, the computations are not warranted. Therefore, it is the writer's recommendation that the cable stress and bending factors be approximated by assuming that the change in cable stress compresses or permits elongation of a member which has a cross-section equal to the area of the leg at the level of the cable connection and a length equal to h, the vertical projection of the cable.

From Eq. 11, the vertical component of cable force, V, is

$$V = \frac{q}{2} (h \coth r + L) \quad \ldots \ldots \ldots \ldots \ldots \ldots . (28)$$

and

$$dV = \frac{q^2 hl}{4H^2} \operatorname{csch}^2 r \, dH = \frac{h}{l} \left(1 - \frac{1}{3} r^2 \right) dH \quad \ldots \ldots \ldots \ldots \quad (29)$$

It should be noted that, as $r_i \to 0$, Eq. 29 gives results that approach those obtained by treating the cable as a two-force member, but the approach is from below instead of from above as one may expect.

Now that ΔV is known in terms of ΔH, one can make use of the relation $\Delta h = \frac{-h \Delta V}{A_l E_l}$ (A_l and E_l are the area and elastic modulus of the tower leg at the level of the cable connection) to obtain

$$\Delta h = \frac{-h^2}{l A_l E_l} \left(1 - \frac{1}{3} r_i^2 \right) \Delta H \quad \ldots \ldots \ldots \ldots \quad (30)$$

which can be used with Eq. 27 to complete an expression for K that will account for cable stretch and compression of the tower leg. For example, ΔH can be determined for a given value of Δl by using Eq. 26a, in which k is given as

$$K = \frac{6}{r_o^2 l} \left[\left(1 + .4\, r_i^2 \right) \Delta l - \frac{L^3 \left[1 - \frac{1}{6} \left(4 - l^2/L^2 \right) r_i^2 \right] \Delta H}{l^2 A_c E_c \left(1 + \frac{1}{6} r_o^2 \right) \left(1 + .1\, r_i^2 \right)} - \frac{h^3 \left(1 - \frac{1}{3} r_i^2 \right) \Delta H}{l^2 A_l E_l \left(1 + \frac{1}{6} r_o^2 \right) \left(1 + .1\, r_i^2 \right)} \right] \quad \ldots \ldots \ldots . (31)$$

As will be subsequently shown, this is easy to work with numerically.

Resultant of Several Cable Forces at One Level.—The purpose here is to extend the formulae developed thus far to the computation of the total resistance offered, by all guys attached to the tower at one level, to motion in any direction. Inspection of the formulae presented for the solution of a single guy, shows that the relation of guy resistance to tower motion is not linear. To evaluate the resistance to a given motion, one must employ a 'trial and error' procedure for solving the equations. This 'trial and error' approach is facilitated by having formulae expressing Δl as a function of ΔH for each cable instead of ΔH as a function of Δl as previously given. The formulae are developed as follows:

$$dl = \frac{\partial l}{\partial H}\, dH + \frac{\partial l}{\partial L}\, dL + \frac{\partial l}{\partial h}\, dH \quad \ldots\ldots\ldots\ldots \quad (32)$$

$$\frac{\partial l}{\partial L} = \frac{L}{\sqrt{L^2 - h^2 \cosh r}} \simeq \frac{L}{l\left(1 + \frac{1}{6} r_o^2\right)\left(1 + 0.5\, r^2\right)} \quad \ldots\ldots \quad (33)$$

and

$$\frac{\partial l}{\partial h} = \frac{-h}{\sqrt{L^2 - h^2 \cosh r}} \simeq \frac{-h}{l\left(1 + \frac{1}{6} r_o^2\right)\left(1 + 0.5\, r^2\right)} \quad \ldots\ldots \quad (34)$$

Substituting Eqs. 18, 33, and 34, into Eq. 32 and integrating, one obtains

$$\Delta l = \frac{r_o^2\, l}{6\left(1 + 0.4\, r_i^2\right)} \left[1 - \frac{H_o^2}{H^2}\right] + \frac{L\,\Delta L - h\,\Delta h}{l\left(1 + \frac{1}{6} r_o^2\right)\left(1 + 0.5\, r_i^2\right)} \quad \ldots (35a)$$

By substituting the equations that express ΔL and Δh in terms of ΔH into Eq. 35a, the following working equation is obtained:

$$\Delta l = \frac{r_o^2\, l}{6\left(1 + 0.4\, r_i^2\right)} \left[1 - \frac{H_o^2}{H^2}\right]$$

$$+ \frac{\left[1 - \frac{1}{6}\left(4 - l^2/L^2\right) r_i^2\right] L^3\, \Delta H/(A_c\, E_c) + \left(1 - \frac{1}{3} r_i^2\right) h^3\, \Delta H/(A_l\, E_l)}{l^2\left(1 + \frac{1}{6} r_o^2\right)\left(1 + 0.5\, r_i^2\right)} \quad (35b)$$

Numerical examples of the use of Eq. 35b will subsequently be presented to determine the tower movement necessary for a group of guys to develop a given total resistance in a specified direction.

In a detailed study of the efficiency of various cable arrangements, it is necessary to investigate the effect on the tower of wind from different directions. Such an investigation is complicated by the fact that the relation between Δl

and ΔH is not linear for cable guys. As the modulus of elasticity for the cable was held constant in the derivation of Eq. 27, the mathematical model is elastic but nonlinear, that is, loading and unloading occur along the same curve and the order of loading is immaterial.

A tower guyed by straight two-force members has a mathematical model that is both linear and elastic. The direction of tower movement, in this case, depends only on the direction of the wind force and is not effected by its magnitude. If the force is applied in either of the orthogonal "principal" directions, the movement is parallel to the applied force. If, in addition, the "spring constants" in these two directions are equal, as in the case of a guying system with two axes of symmetry, the tower movement is parallel to the applied force for all directions.

In the case of a tower guyed with cables having nonlinear sag effects, the direction of the tower movement is a function of the magnitude as well as the direction of the applied force and the movement is along a curved path as the magnitude of the applied force increases. The tower movement is straight and parallel to the applied force only if the force is along an axis of symmetry.

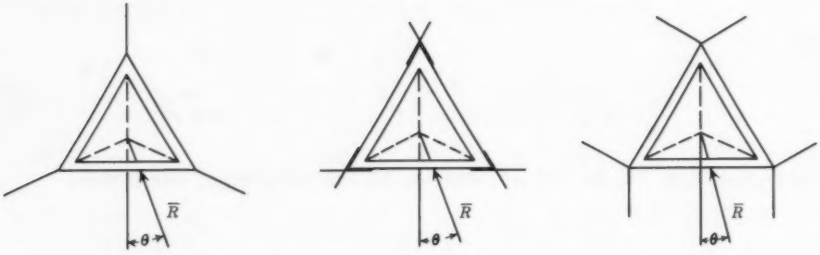

(a) (b) (c)

FIG. 2.—THREE COMMON GUY ARRANGEMENTS

Fig. 2 shows three common guy arrangements employed in the construction of tall towers. The loading is at an angle, θ. In none of these examples would the movement of the center of the tower be along the line of action of R for a general angle, θ. However, in any of the three cases shown, if θ equals 0° or 60° and cable properties are symmetrical, a condition of total symmetry exists and the tower movement will be along the line of action R.

Before proceeding with numerical examples, it is necessary to discuss a method for determining Δl for a guy whose horizontal projection is not parallel to the tower movement. If the cable projection and line of movement intersect at some angle, ϕ, then for a tower movement, y, that is very small as compared with the horizontal cable projection, l, one can usually write $\Delta l = y \cos \phi$, that is, Δl is taken as the component of y along the cable projection; however, the component of y perpendicular to the cable projection, $y \sin \phi$, does cause a small increase in the projected length of the cable $\frac{1}{2l}(y \sin \phi)^2$, and for precise computations, it may be necessary to consider this addition, that is

$$\Delta l = y \cos \phi + \frac{1}{2l}(y \sin \phi)^2 \quad \ldots\ldots\ldots \quad (36)$$

Numerical Examples.—Assuming the following constants: l = 950 ft; h = 1349 ft; A_c = 2.42 sq in.; $E_c = 24.10^3$ ksi; q = 9.0 plf; A_l = 26.4 sq in.; $E_l = 30.10^3$ ksi; H_o = 35.3 k; $r_o = \frac{q\,l}{2\,H_o} = 0.1211$; $r_o^2 = 0.0147$; and $\overline{L} = \sqrt{l^2 + h^2} = 1649.94$ ft; then

$$L_o = \overline{L} + \frac{l^2 r_o^2}{6\,\overline{L}} + \frac{l^2 r_o^4}{45\,\overline{L}} - \frac{l^4 r_o^4}{72\,\overline{L}^3} = 1649.94 + 1.34 + 0.003 - 0.0005 = 1651.28 \text{ ft}$$

Four examples will be worked in this section illustrating the use of cable formulas developed in previous sections. The physical constants given are those of the top cables that support an existing tower.

1) Find the effect on H_o of a temperature drop of 40°F. Eq. 26b can be used for the trial solution to this problem, where Eq. 25 can be applied. The change in H will be small as the decrease in L and h are cancelling effects, so r_i^2 will be taken equal to r_o^2, that is, $r_i^2 = 0.0147$. Taking the coefficient of expansion for steel, α, equal to $6.7.10^{-6}$/F°, and using the Eqs. 27 and 30, one obtains

$$\Delta L = \alpha\, L(-40°) + \frac{L^2}{l\,A_c\,E_c}\left[1 - \frac{1}{6}\left(4 - l^2/L^2\right) r_i^2\right] \Delta H = -0.442 + 0.0489\,\Delta H$$

$$\Delta h = \alpha\, h(-40°) - \frac{2\,h^2}{l\,A_l\,E_l}\left(1 - \frac{1}{3}\,r_i^2\right) \Delta H = -0.362 - 0.0048\,\Delta H$$

In the expression for Δh, the factor 2 was inserted to account for the fact that two cables are attached to each leg, as in Fig. 2(c).

With $\Delta l = 0$, the working formula for K is

$$K = 4.53.10^{-4}\,[-L\,\Delta L + h\,\Delta h] = 0.109\,[1 - 0.361\,\Delta H]$$

Note that the equation being solved for ΔH also contains ΔH, so that a trial solution is called for. However, this may be obtained in three trials as follows:

Try ΔH = 1.0 k, the K = 0.0697 and

$\Delta H = (35.3)\left(\frac{0.0697}{2}\right)(1.0553) = 1.30$ k.

Try ΔH = 1.20 k, then K = 0.0616 and ΔH = 1.14 k.

Now interpolating to make the difference between the trial value and the result zero, one obtains ΔH = 1.167 k, which yields ΔH = 1.167 k if substituted into the working formula.

2) Find the additional effect of an increase of q due to ½ in. ice on the entire structure.

Here the increase in q will be dealt with separately and then the result will be corrected to account for cable stretch and tower compression. If L, h and l

are held constant, the relationship between H and q is linear, that is,

$$\Delta H = H \frac{\Delta q}{q} \quad \ldots\ldots\ldots\ldots\ldots\ldots \quad (37)$$

For 1/2 in. of ice, $\Delta q = 1.55$ or $\Delta H = (36.5)\left(\frac{1.55}{9}\right) = 6.3$ kips. This result must be decreased to account for the stretch of the cable and the shortening of the tower due to the net change in H. In addition, there is a negative effect from the amount the tower compresses due to its own ice load. This was computated separately as $\Delta h = -0.0176$ ft. Therefore,

$$r_o = 0.1171;\ K = -4.84.10^{-4}\ [L\ \Delta L - h\ \Delta h]\ ;\ \Delta L = 0.0489\ \Delta H;$$

$$\Delta h = -0.0176 - 0.0048\ \Delta H;\ \text{or}\ K = -0.0422\ [\Delta H + 0.272]$$

Guess a net $\Delta H = 3.5$ k, then $K = -0.149$ and

$$\Delta H = (36.5 + 6.3)\left(\frac{-0.149}{2}\right)(1 - 0.112 + 0.014 - 0.002) = -2.8\text{k},$$

or the net $\Delta H = 6.3 - 2.8 = 3.5$k as assumed

Thus, with ice on the cable, H = 40 kips and r = 0.125. Then the vertical component of cable stress, V, is obtained from Eq. 28 as

$$V = \frac{q}{2}[h \coth r + L] = 66.0 \text{ kips}$$

3) Find the additional effect of $\Delta l = 2.5$ ft.

Here the change in H is probably going to be on the order of magnitude of H so that Eq. 26a should be used. Since all the changes in h and L are functions of ΔH only, the definition for K given in Eq. 31 should be used.

$$K = 0.404\left[\left(1 + 0.4\ r_1^2\right)\Delta l - 0.0892\left(1 - 0.713\ r_1^2\right)\Delta H\right]$$

Guess $\Delta H = 15.1$, then $r_1^2 = r_o^2\left(\frac{40}{40 + 7.6}\right)^2 = 0.011$ and

$$K = 0.404\ [(1.0044)(2.5) - (0.0892)(0.9921)(15.1)] = 0.4746$$

giving $H = \frac{40}{\sqrt{1 - .4746}} = 55.18$ or $\Delta H = 15.2$ kips

4) Find the motion of the tower necessary for the guys to develop a given net horizontal reactive force and show tangential equations relating the forces and moments to the tower motion. This example will be based on the same initial conditions as used in example three.

In Fig. 3, all six cables have identical properties, but are numbered as 1 or 2 to distinguish between the cables whose horizontal projections are parallel to the line of action of the force and those whose horizontal projections intersect it at 60°. The subscripts 1 and 2 in the following equations refer to cables 1 and 2 in Fig. 3.

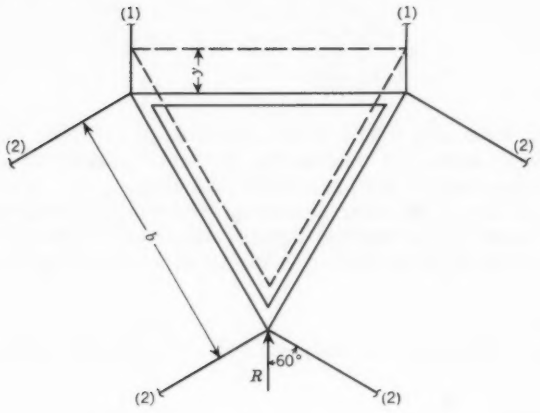

FIG. 3.—SYMMETRICAL GUY LOAD

$$R = 4(\Delta H_2 \cos 60°) - 2(\Delta H_1) = 2(\Delta H_2 - \Delta H_1)$$

$$\Delta l_1 = -y;\ \Delta l_2 = \left[y \cos 60° + \frac{1}{2\,l} (y \sin 60°)^2 \right] = \frac{y}{2} \left[1 + \frac{3}{4} \frac{y}{l} \right]$$

The recommended procedure, for finding y and the cable stresses caused by R, is as follows: (a) guess ΔH_2 and compute the corresponding ΔH_1, that is, $\Delta H_1 = \Delta H_2 - \frac{R}{2}$; (b) compute Δl and Δl_2 to check for consistency, that is,

$$\frac{2\,\Delta l_2}{\left(1 + \frac{3}{4} \frac{y}{l}\right)} + \Delta l_1 = 0 \quad \ldots\ldots\ldots\ldots\ldots \quad (38)$$

For this example, R = 60.1 kips; H_o = 40 kips; and $r_o^2 = 0.01562$. Substituting into Eq. 35b yields

$$\Delta l = \frac{2.47}{\left(1 + 0.4\, r_i^2\right)} \left[1 - \frac{H_o^2}{H^2} \right] + (0.0891) \left(1 - 1.1\, r_i^2\right) \Delta H$$

Guess $\Delta H_2 = 14.5$, then $\Delta H_1 = -15.55$.

$$\left(r_i^2\right)_1 = (0.01562) \left(\frac{40}{40 - 7.8}\right)^2 = 0.024;\ \left(r_i^2\right)_2 = (0.01562) \left(\frac{40}{40 + 7.3}\right)^2 = 0.011$$

$$\Delta l_1 = \frac{2.47}{1.0096} \left[1 - \left(\frac{40}{24.45}\right)^2 \right] + (0.0891)\,(0.9736)\,(-15.55) = -5.44 \text{ ft}$$

$$\Delta l_2 = \frac{2.47}{1.0044} \left[1 - \left(\frac{40}{54.5}\right)^2 \right] + (0.0891)\,(0.9878)\,(14.5) = 2.41 \text{ ft.}$$

Then checking for consistency,

$$\frac{2(2.41)}{1+\frac{3}{4}\frac{5.4}{950}} - 5.44 = (-.64) \neq 0$$

A similar trial with $\Delta H_2 = 15.3$ nets a residual of (+0.06). Interpolating to make the residual zero, one obtains the correct results: $\Delta H_2 = 15.23$ kips; $\Delta H_1 = -14.82$ kips; and y = 5.00 ft for R = 60.1 kips.

As a result of the above tower movement, the vertical components of stress in cables 2 increase and the vertical components of stress in cables 1 decrease. This causes a moment to be applied to the tower that may be computed as follows:

$$M = \frac{b\sqrt{3}}{6}\left[2\left(2\,\Delta V_2\right) - 2\left(\Delta V_1 + \Delta V_2\right)\right] = \frac{b\sqrt{3}}{3}\left[\Delta V_2 - \Delta V_1\right] \quad \ldots . \quad (39)$$

For this example,

$$M = 4\sqrt{3}\left[\Delta V_2 - \Delta V_1\right].$$

From Eq. 29,

$$\Delta V = \frac{h}{l}\left[1 - \frac{1}{3}r_i^2\right]\Delta H$$

or $\Delta V_1 = -20.85$, $\Delta V_2 = 21.53$ and M = 293.5 kip-ft.

In order to obtain information on the tangent to the curve relating R and y, the preceding computations are repeated for R = 62.0, giving $\Delta H_2 = 15.91$, $\Delta H_1 = -15.09$, M = 302.5 and y = 5.20 ft. Therefore, in the range near R = 60.1 kips, the function R versus y for the guy system shown, f(y), can be written: f(y) = 9.5 y + 12.6. In this range the external moment may be written

$$M = g(y) = 45\,y + 68.5.$$

Also, the axial load below this guy system has been increased to

$$\Delta P = 4\Delta V_2 + 2\Delta V_1 = 44.42 \text{ kips}$$

DYNAMIC ANALYSIS

Forced Vibration of Guy Cables.—By solving for the equations of motion for a vibrating guy cable, it is proposed to determine the variations in horizontal force exerted on the tower when the support point is executing harmonic motion. For small vibrations, out-of-plane lateral vibrations have the same equations as in-plane vibrations, however, for convenience of presentation, the work here will be devoted to in-plane lateral vibrations.

The coordinates ϵ and η in Fig. 4 are chosen along the arc and perpendicular to the arc of the cable in its static equilibrium position. Summing forces on an element of cable in a direction perpendicular to its equilibrium position, that is, in the direction η, one obtains

$$-T\,\frac{\partial\,\eta}{\partial\,\epsilon} + \left(T + \frac{\partial\,T}{\partial\,\epsilon}\,d\epsilon\right)\left(\frac{\partial\,\eta}{\partial\,\epsilon} + \frac{\partial^2\eta}{\partial\,\epsilon^2}\,d\epsilon\right) = \rho\,d\epsilon\,\frac{\partial^2\eta}{\partial t^2} \quad \ldots \quad (40)$$

where ϵ and η are the coordinates shown in Fig. 4, ρ is the mass per unit length of cable, and T is the tension on the element when the cable is in its equilibrium

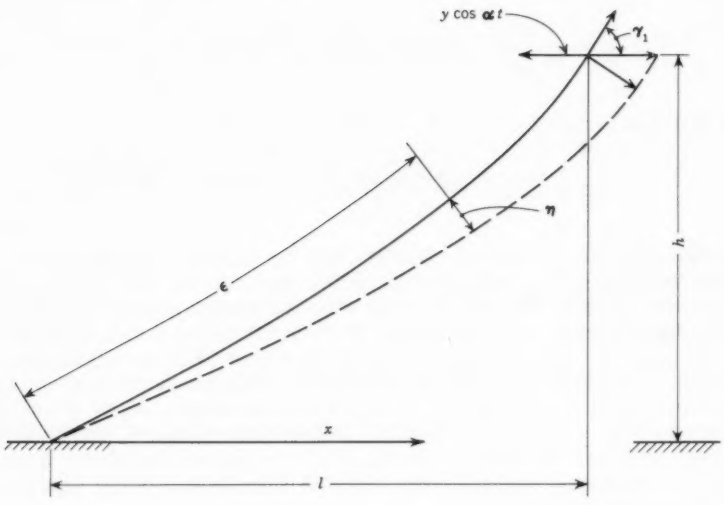

FIG. 4.—CABLE WITH VIBRATING SUPPORT

position. For small cable vibrations, the second order terms on the left side of the equation can be ignored, with the result

$$\frac{\partial}{\partial \epsilon}\left(T\frac{\partial \eta}{\partial \epsilon}\right) = \rho\frac{\partial^2 \eta}{\partial t^2} \quad \ldots\ldots\ldots\ldots\ldots\ldots \quad (41)$$

From Eq. 3,

$$\frac{d\epsilon}{dx} = \cosh\left(\frac{q\,x}{H} + a_1\right) \quad \ldots\ldots\ldots\ldots\ldots\ldots \quad (42)$$

or

$$\epsilon = \frac{H}{q}\left[\sinh\left(\frac{qx}{H} + a_1\right) - \sinh a_1\right] \quad \ldots\ldots\ldots\ldots \quad (43)$$

and from Eq. 7, $T = H\cosh\left(\frac{qx}{H} + a_1\right)$, substitution into Eq. 41 yields,

$$\frac{H}{\cosh\left(\frac{q\,x}{H} + a_1\right)}\frac{\partial^2 \eta}{\partial x^2} = \rho\frac{\partial^2 \eta}{\partial t^2} \quad \ldots\ldots\ldots\ldots \quad (44)$$

It is assumed that all points on the cable are executing harmonic motion so that the variables in Eq. 44 can be separated as follows: $\eta = \overline{\eta} \cos \alpha t$ where $\overline{\eta}$ is a mode shape function of x only. Substituting into Eq. 44,

$$\frac{d^2\overline{\eta}}{d\overline{x}^2} + \beta^2 \cosh \left(2r\overline{x} + a_1\right) \overline{\eta} = 0$$

in which $\overline{x} = x/l$ and

$$\beta^2 = \frac{l^2 \rho \alpha^2}{H} \quad \ldots\ldots\ldots\ldots\ldots\ldots \quad (45)$$

By expanding the hyperbolic function into its series, it is possible to obtain a series solution to the ordinary differential equation, Eq. 45, however, the series solution is quite difficult to work with and such a general solution is not actually needed here. What is needed is the solution for a vibrating cable that is functioning as a guy, that is, a cable whose tension varies only slightly along its length. The problem of the vibration of a cable whose tension, or density, or combination of the two varies slowly along its length can be solved by the W-K-B (Wentzel-Kramers-Brillouin)[7] method that is used in wave mechanics and other branches of physics. In Eq. 45, the variable coefficient appears in front of the dependent variable, $\overline{\eta}$, so that the form is that of the equation for a cable of varying density.

The governing differential equation for the vibration of a varying density cable is in the form

$$y'' + \gamma^2 \sigma^2 y = 0 \quad \ldots\ldots\ldots\ldots\ldots\ldots \quad (46)$$

in which σ^2 is a function of x representing the variation in density. If σ^2 does not vary rapidly in the range under consideration, the solution, according to the W-K-B method, is

$$y = C_{1,2}\, \sigma^{-1/2} \exp \pm i \gamma \int \sigma \, dx. \quad \ldots\ldots\ldots\ldots \quad (47)$$

Adapting this solution to Eq. 45 and making use of the boundary condition, $\overline{\eta} = 0$ at $\overline{x} = 0$, one obtains

$$\overline{\eta} = \frac{c}{\left[\cosh \left(2\, r\, \overline{x} + a_1\right)\right]^{1/4}} \sin \left[\beta \int_0^{\overline{x}} \sqrt{\cosh \left(2\, r\, \overline{x} + a_1\right)}\, d\overline{x} \right] \quad \ldots\ldots \quad (48)$$

in which c is an integration constant to be evaluated by the boundary condition at $\overline{x} = 1$, or the solution to Eq. 44 is

$$\eta(\overline{x},t) = \frac{c}{\left[\cosh \left(2\, r\, \overline{x} + a_1\right)\right]^{1/4}} \sin \beta D(\overline{x}) \cos \alpha t \quad \ldots\ldots\ldots (48a)$$

7 "Mechanics," by J. C. Slater and N. H. Frank, 1st Ed., McGraw-Hill Book Co., New York, 1947.

in which $D_{(x)}$ is a function of $\bar{x}$ as indicated by the integral in Eq. 48. This integral does not seem to be a standard function, however it can be evaluated as follows:

$$D_{(\bar{x})} = \int_0^{\bar{x}} \sqrt{\cosh\left(2r\bar{x} + a_1\right)}\, d\bar{x} = \frac{z}{r\sqrt{2}}\left[1 + \frac{z^2}{12} - \frac{z^4}{32}\right.$$

$$\left. + \frac{13\, z^6}{(16)(56)} - \frac{47\, z^8}{(256)(24)} + \frac{399\, z^{10}}{(256)(352)} - \cdots\right]\Bigg|_{z(o)}^{z(\bar{x})} \quad \ldots\ldots (49)$$

in which

$$z_o = \sqrt{\cosh a_1 - 1} \quad \ldots\ldots\ldots\ldots (50a)$$

and

$$Z_{(x)} = \sqrt{\cosh\left(2r\bar{x} + a_1\right) - 1} \quad \ldots\ldots\ldots\ldots (50b)$$

The boundary condition at $\bar{x} = 1$ is

$$\eta_{(1,t)} = y \sin \gamma_1 \cos \alpha t \ldots\ldots\ldots\ldots (51)$$

in which $y \cos \alpha t$ is the tower motion at the support point and $\tan \gamma_1$, is the slope of the guy at the tower when it is in its equilibrium position. The substitution of this boundary condition into Eq. 48a yields

$$c = \frac{y \sin \gamma_1 \left[\cosh\left(2r + a_1\right)\right]^{1/4}}{\sin \beta D_{(1)}} \quad \ldots\ldots\ldots (52)$$

Eq. 48a is the equation of motion for a guy cable that is being vibrated about its equilibrium position by a forced harmonic motion at its upper end. While this result is of interest, it is not the objective sought. The problem is to determine the force on the tower as it imparts the transverse motion, $y \sin \gamma_1 \cos \alpha t$, to the upper end of the cable. In general, this force is equal to $T \frac{\partial \eta}{\partial \epsilon}$ at the point in question.

$$T \frac{\partial \eta}{\partial \epsilon} = \frac{H}{l} \frac{\partial \eta}{\partial \bar{x}} \quad \ldots\ldots\ldots\ldots\ldots (53)$$

and from Eq. 48a,

$$\frac{H}{l} \frac{\partial \eta}{\partial \bar{x}} = \frac{(H/l)\, c \sin \beta D_x}{\left[\cosh\left(2\, r\, \bar{x} + a_1\right)\right]^{1/4}} \left[\beta \sqrt{\cosh\left(2\, r\, \bar{x} + a_1\right)} \cot \beta D_x\right.$$

$$\left. - \frac{r}{2} \tanh\left(2\, r\, \bar{x} + a_1\right)\right] \cos \alpha t \quad \ldots\ldots\ldots\ldots (54a)$$

or

$$\frac{H}{l}\frac{\partial \eta}{\partial \bar{x}}\Bigg|_{\bar{x}=1} = \frac{H}{l}\, y \sin\gamma_1 \left[\beta\sqrt{\cosh(2r + a_1)}\ \cot\beta D_x - \frac{r}{2}\tanh(2r + a_1)\right]\cos\alpha t \quad \ldots\ldots\ldots\ldots (54b)$$

The expression $\frac{H}{l}\frac{\partial \eta}{\partial \bar{x}}$ at $\bar{x} = 1$ represents the transverse force that the tower must exert on the cable to impart a lateral motion of $y \sin\gamma_1 \cos\alpha t$. The tower also imparts a longitudinal cable motion of $y \cos\gamma_1 \cos\alpha t$ which can be accounted for by using the static equations developed in the first section of this paper. The amplitude of the longitudinal motion can be represented by its horizontal and vertical components, that is,

$$\Delta l = y \cos^2\gamma_1 \quad \ldots\ldots\ldots\ldots\ldots\ldots (55a)$$

and

$$\Delta h = y \cos\gamma_1 \sin\gamma_1 \quad \ldots\ldots\ldots\ldots (55b)$$

By making use of the Eqs. 18 and 20, one finds that the amplitude of the horizontal force that the tower must exert on the cable to impart the longitudinal component of its motion is

$$\frac{\partial H}{\partial l}\Delta l + \frac{\partial H}{\partial h}\Delta h = \frac{3H}{r^2 l}\, y \left[(1 + 0.4\, r^2)\cos^2\gamma_1 + \frac{h}{l}(1 - 0.267\, r^2)\cos\gamma_1 \sin\gamma_1\right] \quad \ldots\ldots\ldots (55c)$$

Combining this with the horizontal component of the previously stated transverse force, one obtains the expression for the additional horizontal force that the tower must exert on the guy to impart a horizontal motion, $y \cos\alpha t$, at its upper end;

$$\Delta H = \left[\frac{H}{l}\sin^2\gamma_1\left[\beta\sqrt{\cosh(2r + a_1)}\ \cot\beta D_{(1)} - \frac{r}{2}\tanh(2r + a_1)\right] + \frac{3H\cos^2\gamma_1}{r^2 l}\left[(1 + .4r^2) + \frac{h}{l}(1 - .267\, r^2)\tan\gamma_1\right]\right] y\cos\alpha t \quad \ldots (56)$$

Illustrative Example.—The following will serve to illustrate the numerical use of Eq. 56 and its application to groups of guys for finding the total dynamic resistance they offer to tower movement at a support point.

The same guy system will be used here as in the previous illustrative examples. As shown in Fig. 5, the tower is assumed to be oscillating so as to cause symmetrical changes in the guy stresses. The line of action of the resultant forces is parallel to the horizontal projection of the cables denoted 1 and intersects the projection of the cables denoted 2 at 60°, that is, the 1 cables are experiencing only an in-plane forced horizontal vibration of y cos α t and the 2 cables are experiencing both an in-plane motion y cos 60° cos α t and an out-of-plane motion of y sin 60° cos α t.

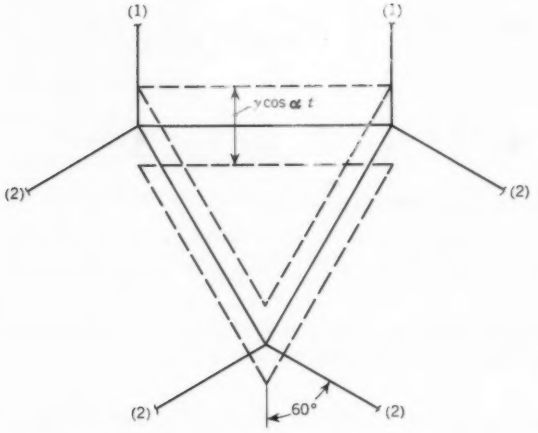

FIG. 5.—SYMMETRICAL VIBRATION OF TOWER AT SUPPORT POINT

In Eq. 56, the first term accounts for the transverse component of cable motion and the second term gives the static force necessary to impart the longitudinal component of motion. Because only the first term is used in expressing the force necessary to impart out-of-plane motion, it is convenient to rewrite Eq. 56 using compacted notation for the two terms, that is,

$$\Delta H = \left[T_{(r,\alpha)} + L_{(r)} \right] y \cos \alpha t \quad \ldots\ldots\ldots (57)$$

Then it may be seen that the resultant force in the direction of the line of movement of the tower is

$$R = \left[2 \left[T_{(r,\alpha)} + L_{(r)} \right] \Big|_1 + 4 \left[T_{(r,\alpha)} + L_{(r)} \right] \Big|_2 \cos^2 60° + 4\, T_{(r,\alpha)} \Big|_2 \sin^2 60° \right] y \cos \alpha t \quad \ldots\ldots\ldots\ldots\ldots (58a)$$

If the tower is vibrating about a vertical equilibrium position, then $T_{(r,\alpha)}$ and and $L_{(r)}$ are the same for cables 1 and 2 and the expression may be simplified

to

$$R = \bar{f}_{(y)} = \left[6\, T_{(r,\alpha)} + 3\, L_{(r)}\right]\, y \cos \alpha t \quad \ldots\ldots (58b)$$

A similar expression may also be obtained for the dynamic moment caused by the changes in the vertical components of the guy forces as the support point oscillates. Only in-plane vibrations will cause changes in the vertical components of the guy forces, so by the use of Eq. 29, one obtains

$$\Delta V_1 = \frac{h}{l}\left(1 - \frac{1}{3} r^2\right) \left(T_{(r,\alpha)} + L_{(r)}\right)\, y \cos \alpha t \quad \ldots\ldots\ldots (59a)$$

and

$$\Delta V_2 = \frac{h}{l}\left(1 - \frac{1}{3} r^2\right) \left(T_{(r,\alpha)} + L_{(r)}\right)\, \frac{y}{2} \cos \alpha t \quad \ldots\ldots\ldots (59b)$$

The moment, $\bar{g}_{(y)}$, may be expressed as

$$\bar{g}_{(y)} = b \frac{\sqrt{3}}{2} \frac{h}{l} \left(1 - \frac{1}{3} r^2\right) \left[T_{(r,\alpha)} + L_{(r)}\right]\, y \cos \alpha t \quad \ldots\ldots (60)$$

For a numerical example, take H = 40.0 kips; r = .125; h = 1349 ft; l = 950 ft; $\gamma_1 = 1.0255$; and q = .01055 kips per ft. Then

$$a_1 = \sinh^{-1} \frac{h}{l\left(1 + \frac{1}{6} r^2\right)} - r = 1.02242; \quad \beta = 1 \frac{\sqrt{q}}{\sqrt{g_a H}} \alpha = 2.7206\, \alpha;$$

$$z_o = \sqrt{\cosh a_1 - 1} = 0.75497; \quad z_1 = \sqrt{\cosh\left(2r + a_1\right) - 1} = 0.96169$$

$$D_{(1)} = 1.3186; \quad T_{(r,\alpha)} = 0.1161\, \alpha \cot (3.5873\, \alpha) - 0.00164; \quad L_{(r)} = 7.259;$$

$$\bar{f}_{(y)} = \left[0.6966\, \alpha \cot (3.5873\, \alpha) + 21.766\right] y \cos \alpha t$$

and

$$\bar{g}_{(y)} = \left[1.704\, \alpha \cot (3.5873\, \alpha) + 106.53\right] y \cos \alpha t$$

APPENDIX.—NOTATION

H	horizontal component of cable force
q	cable weight per unit length
x,y	cable coordinates (origin at lower extremity)

l,h	horizontal and vertical projections of cable length
γ_o, γ_1, $\bar{\gamma}$	cable slope angles for lower and upper extremity and chord, respectively
L, $\bar{L}$	cable length and chord length
a_1, a_2, c	constants of integration
r	cable parameter equal to $\frac{q\,l}{2\,H}$
A_c E_c, A_l E_l	areas and moduli of elasticity for cable and tower leg, respectively
R	cable group force resultant
η, ϵ	normal and arc coordinates
T	cable force
ρ	mass density of cable
β	dynamic cable parameter
D	special integral function for dynamic solution

Journal of the
STRUCTURAL DIVISION
Proceedings of the American Society of Civil Engineers

LATERAL INELASTIC BUCKLING OF TIED ARCHES

By Chin Fung Kee[1]

SYNOPSIS

This paper is an extension of previous works.[2,3] It concerns the same structure - the tied or stabbogen arch - and deals with its lateral stability when the elastic limit is exceeded. The behavior of the arch in the light of existing inelastic buckling theories is discussed and a theoretical method for computing the inelastic buckling load is produced.

The theoretical analysis is followed by an experimental study with two main objects - the first to verify the results of computation, and the second to examine the validity of a method of plotting suggested by R. V. Southwell for certain types of elastic buckling, when extended beyond the original conception to problems of inelastic buckling.

INTRODUCTION

The problem of buckling is one of stability and not of flexural stresses, and is a phenomenon peculiar to perfect structural members that are subject to compressive loads. The general basis of structural design is the evaluation of stresses on the tacit assumption that equilibrium exists between the external and the internal forces. The permissible stresses, therefore, determine the

Note.—Discussion open until June 1, 1961. To extend the closing date one month, a written request must be filed with the Executive Secretary, ASCE. This paper is part of the copyrighted Journal of the Structural Division, Proceedings of the American Society of Civil Engineers, Vol. 87, No. ST 1, January, 1961.

[1] Senior Lecturer in Engrg., Univ. of Malaya, Kuala Lumpur, Malaya.

[2] "The Lateral Buckling of Tied Arches," by W. G. Godden, Part III, Proceedings, I.C.E., August, 1954.

[3] "The Design of the Unbraced Stabbogen Arch," by Chin Fung Kee, The Structural Engineer, Journal I, Struct. E., September, 1959.

safety and strength of the members. The strength of certain compressive members, like the ideal column and the ideal stabbogen arch, however, is not governed by the avoidance of a certain working stress or of a fraction thereof, but by the critical load at which a peculiar state of unstable equilibrium occurs. This critical load is called the buckling load. The inception of buckling is the result of a sudden breakdown of the internal resistance of the compressive member regardless of whether or not the maximum stress exceeds that of the material at the proportional limit at the instant of failure. If it takes place when the maximum stress is below the limit to which Hooke's law remains applicable, the buckling is said to be elastic; if it occurs when the proportional limit has been exceeded, the phenomenon is referred to as inelastic buckling. The latter case will arise in the case of "stiff" or non-slender arch ribs and in arch ribs of certain metals, like light alloys which do not have a constant modulus of elasticity throughout the working range of stress.

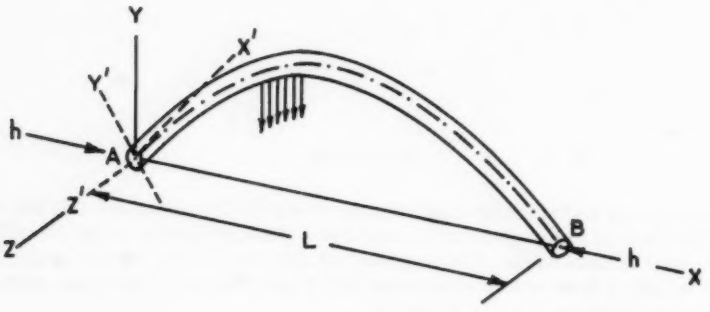

FIG. 1

Notation.—The letter symbols adopted for use in this paper are defined where they first appear, in the illustrations or in the text, and are arranged alphabetically, for convenience of reference, in the Appendix.

THE STABBOGEN ARCH

The arches concerned in this paper are known as stabbogen or tied arches. The shape of the arches in elevation is parabolic and it is assumed that there is no bending moment in the vertical plane XAY (Fig. 1) - an assumption which is only valid if the hangers are inextensible. The arches are loaded through the hangers which may be referred to as "wire-hangers" because they are assumed to take tension only and have a comparatively small flexural rigidity. The chord to which the hangers are connected is assumed to be absolutely rigid. The load may be considered as applied by means of a horizontal thrust H applied at the ends of the arch instead of through the hangers.

INELASTIC BUCKLING THEORIES AND THEIR APPLICATION TO THE STABBOGEN ARCH

The inelastic buckling load may be defined as the smallest horizontal end thrust at which the lateral deflected form of equilibrium of the originally ideal

arch, resulting from a small lateral disturbing force H', becomes stable. Unlike the elastic case, it is not sufficient to define it as the smallest load at which the original straight form (in plan) of the ideal arch becomes unstable, for while in the elastic case, the arch resumes its originally straight form with the removal of H', no such resumption is possible once the elastic limit is exceeded.[4]

The distribution of stress over any cross-section of the arch rib will depend on the history of loading of H'. If it is applied before any of the compressive stresses reach the proportional limit, the stresses due to bending and to direct compression increase simultaneously. On the other hand, if it is applied when the compressive stresses have exceeded the elastic limit, the superimposition of the bending stresses will result in a reduction of stress over the convex side (in plan) and an increased compressive stress on the concave side. Stress reversal or decrement occurs.

Under the first process of loading, the tangent modulus theory applies. Under this theory, it is assumed that the compressive stress, and therefore the tangent modulus is constant over the whole section under consideration. To the second mode of loading, Von Karman's double modulus theory is applicable. For simplicity, the tangent modulus E_t is assumed to be constant over the inelastic portion of the section. For the equilibrium of the internal forces, it can be shown that E_t/E is equal to the ratio of the cross-sectional areas to the left and right of the axis N-N.[5] The axis N-N is the axis of bending and is the line along which the stress has not changed with the superimposition of the bending stress. The reduced modulus E_r is given by

$$E_r = \left(E\, I_1 + E_t\, I_2\right)/I \quad \ldots\ldots\ldots\ldots\ldots\ldots (1)$$

in which I_1 and I_2 are the moments of inertia of the cross-sectional areas separated by the line N-N, with reference to this line as the axis.

EVALUATION OF THE ELASTIC BUCKLING LOAD

A theoretical method for computing the elastic buckling load for the tied arch was produced by W. G. Godden.[2] It makes use of the energy criterion for stability, that is: that at the critical load, the work done by the external forces is equal to the increase in the strain energy acquired by the system. A deflected form in plan is given by the equation

$$z = \sin \frac{\pi x}{L} - \frac{1}{3} \sin \frac{3 \pi x}{L} \quad \ldots\ldots\ldots\ldots (2)$$

in which L is the span of the arch. This is the simplest expression of the lateral deformation satisfying all the boundary conditions of an arch encastre at the ends - also referred to as end conditions A in this paper. The ends of the arch are fixed about both the x' and the y' axes, but free to rotate about the z' axis (Fig. 1).

If λ is the shortening of the chord AB due to deformation of the arch in the XAZ plane, and H is the horizontal thrust, then the work done by H is λ H. The

---

4 "Inelastic Column Theories and an Analysis of Experimental Observations," by C. T. Wang, Journal of Aeronautical Science, May, 1947.

5 "Buckling Strength of Metal Structures," by F. Bleich, 1952.

increase in the strain energy of the system as a result of the deformation is

$$\frac{1}{2\,B_2}\int_0^S M^2\,ds + \frac{1}{2CJ}\int_0^S T^2\,ds$$

in which B = EI and CJ is the torsional rigidity. Therefore, at the critical load,

$$\lambda H = \frac{1}{2\,B_2}\int_0^S M^2\,ds + \frac{1}{2\,C\,J}\int_0^S T^2\,ds$$

$$= \frac{1}{2B_2}\left[\int_0^S M^2\,ds + \gamma\int_0^S T^2\,ds\right] \quad \ldots\ldots\ldots (3)$$

in which $\gamma = B_2/C\,J$. It can be shown that[2]

$$\lambda = \frac{1}{2}\int_0^L \left[\frac{dz}{dx} - \frac{z}{y}\frac{dy}{dx}\right]^2 dx \quad \ldots\ldots\ldots (4)$$

This integral is computed numerically by dividing the span L of the arch rib into twelve equal sections, giving the result

$$\lambda = 30.6936/L \quad \ldots\ldots\ldots\ldots\ldots\ldots (5)$$

The term λ is independent of the rise-span ratio, and is only inversely proportional to L. The same value of λ can therefore be used for arches of different rise-span ratios.

It is also not possible to integrate the right hand side of Eq. 3 directly, and it has to be computed in the same way as in the evaluation of λ. Table 1 gives part of the calculation for an arch with a rise-span of 0.12.

THE VALUE OF THE ELASTIC BUCKLING LOAD H_{cr}

Applying the results obtained from Table 1 and Eq. 5 to Eq. 3, the value of the elastic buckling load for an arch with a rise-span ratio f = 0.12, is given by

$$30.6936\,\frac{H}{L} = (2)\,\frac{1}{2\,B_2}\,(0.3496 + 0.0057\,\gamma)\,L\,H^2$$

Therefore,

$$H_{cr} = \frac{30.6936}{(0.3496 + 0.0057\,\gamma)}\,\frac{B_2}{L^2} \quad \ldots\ldots\ldots (6)$$

METHOD OF COMPUTING THE INELASTIC BUCKLING LOAD BY SUCCESSIVE APPROXIMATION

In contrast to the inelastic buckling of a column subject only to an axial compressive load, the stresses and therefore, the values of the tangent modulus E_t and the inelastic modulus of rigidity C_t vary along the length of the arch rib. Therefore Godden's method cannot be directly applied as in the elastic case because E_t and C_t are not constant.

If h is the value of the inelastic buckling load, then the average compressive stress f_c at any section P of the arch rib is equal to $(h \cos \theta + V \sin \theta)/A$, in which θ is the angle of inclination of the tangent at P to the horizontal. The value of f_c is least at the crown C of the arch, and increases to its maximum at the ends A and B. Hence, the value of the tangent modulus E_t is greatest at C, and decreases to its minimum at A and B. The flexural rigidity $E_t I$, therefore varies along the arch. Hence, the problem of evaluating the inelastic buckling load is reduced to one of computing the buckling load of an equivalent arch with a non-uniform flexural rigidity. This equivalent arch cannot, however, be determined until the value of the inelastic buckling load h is known, since the flexural rigidity at each section of the arch rib is dependent on the

TABLE 1[a].—PART OF COMPUTATION FOR ARCH

Section (1)	M[b] (2)	T[c] (3)	M^2 (4)	T^2 (5)	ds/dx (6)	$M^2 ds/dx$ (7)	$T^2 ds/dx$ (8)
A	H x 0	H x 0	H^2 x 0	H^2 x 0	-	H^2 x 0	H^2 x 0
	0.1155	0.0019	0.0133	0.0000	1.0929	0.0146	0.0000
1	0.2100	0.0074	0.0441	0.0001	1.0770	0.0475	0.0001
	0.2682	0.0158	0.0719	0.0003	1.0628	0.0765	0.0003
2	0.2802	0.0257	0.0785	0.0006	1.0498	0.0824	0.0007
	0.2410	0.0361	0.0581	0.0013	1.0386	0.0603	0.0014
3	0.1623	0.0428	0.0263	0.0018	1.0284	0.0271	0.0019
	0.0484	0.0465	0.0023	0.0022	1.0198	0.0024	0.0022
4	-0.0821	0.0459	0.0067	0.0021	1.0128	0.0068	0.0021
	-0.2104	0.0400	0.0443	0.0016	1.0072	0.0446	0.0016
5	-0.3178	0.0297	0.1010	0.0009	1.0032	0.1013	0.0009
	-0.3892	0.0151	0.1515	0.0002	1.0008	0.1516	0.0002
6	-0.4142	0	0.1716	0	1.0000	0.1716	0

$$\sum_{0}^{6} M^2 ds = 0.3496\ H^2$$

$$\sum_{0}^{6} T^2 ds = 0.0057\ H^2$$

[a] End condition A f = 0.12
[b] M denotes bending moment in the arch rib about the axis y'; and
[c] T denotes torque in arch rib about the axis x'.

value of h. A value of h can, however, be assumed first in order to determine the value of E_t at each section of the equivalent arch, the buckling load of which is then computed by the Godden method. If the value of the buckling load so obtained is equal to that of h, then the value of h is the required buckling load.

In assuming a value of h, one is guided by the limits: (1) h is less than H_{cr}, since at no section of the arch is the value of the tangent modulus greater than E; and (2) h is greater than the buckling load of an arch with a constant flexural rigidity $E_t I$, if E_t is the tangent modulus corresponding to the average compressive stress $(H_{cr} \cos \theta + V \sin \theta)/A$ at the ends A and B.

The method of computing the inelastic buckling load by successive approximation may be outlined as follows:

Step I - The Upper Bound.—An estimate of the inelastic buckling load is first obtained by substituting the value of the elastic modulus E of the material in

the formula obtained by Godden's method for the elastic case,

$$H_{cr} = K \frac{E I}{L^2} \quad \ldots\ldots\ldots\ldots\ldots\ldots\ldots\ldots (7)$$

in which K is a constant depending on the rise-span ratio of the arch.[3] Eq. 7 gives the upper bound for the approximation of h, since the value of the tangent modulus at every section along the arch is less than E.

Step II - The Lower Bound.—From the stress-strain curve, the tangent modulus E_t corresponding to the compressive stress $(H_{cr} \cos \theta + V \sin \theta)/A$ is found. (A is the cross-sectional area of the arch rib.) This value of E_t is lower than the tangent modulus at any section of the arch, and, hence, the lower limit of h is obtained by substituting this value of E_t for E in Eq. 7. This load will be denoted by H_1. The inelastic buckling load should have a value lying between H_{cr} and H_1.

TABLE 2[a]

Section (1)	sin θ (2)	cos θ (3)	V (4)	M^2 ds/dx (5)	T^2 ds/dx (6)	V sin θ (7)	H cos θ + V sin θ (8)
A	0.4329	0.9014	0.4800H	0.00000H^2	0.00000H^2	0.20729H	1.10869H
	0.4036	0.9150	0.4400	0.01457	0.00000	0.17758	1.09258
1	0.3714	0.9285	0.4000	0.04750	0.00005	0.14856	1.07706
	0.3387	0.9409	0.3600	0.07645	0.00027	0.12193	1.06283
2	0.3048	0.9523	0.3200	0.08242	0.00069	0.09754	1.04984
	0.2695	0.9629	0.2800	0.06032	0.00135	0.07546	1.03836
3	0.2335	0.9724	0.2400	0.02709	0.00188	0.05604	1.02844
	0.1960	0.9806	0.2000	0.00239	0.00220	0.03920	1.01980
4	0.1582	0.9874	0.1600	0.00683	0.00214	0.02531	1.01271
	0.1192	0.9929	0.1200	0.04459	0.00161	0.01430	1.00720
5	0.0802	0.9968	0.0800	0.10132	0.00088	0.00642	1.00322
	0.0401	0.9992	0.0400	0.15160	0.00023	0.00160	1.00080
6	0	1.0000	0	0.17156	0	0	1.00000

[a] End condition A f = 0.12. This table applies to both the double and the tangent modulus theories.

(The computations indicate that by substituting the tangent modulus corresponding to the compressive stress H_{cr}/A instead of that corresponding to $(H_{cr} \cos \theta + V \sin \theta)/A$, for E in Eq. 7, a closer approximation is obtained.)

Step III.—Using the values of H_1, the values of the tangent moduli at the various cross-sections along the arch can be found. These values are then used in the summation of $\frac{M^2}{E_t I} \frac{ds}{dx}$ and $\frac{T^2}{E_t I} \frac{ds}{dx}$ to give a closer approximation H_2 of the inelastic buckling load.

As is shown in the accompanying examples, it is hardly necessary to repeat Step III more than twice before a very close approximation of the inelastic buckling load is obtained.

THE INELASTIC BUCKLING LOAD BY THE TANGENT MODULUS AND THE DOUBLE MODULUS THEORIES

In the method previously outlined, since the tangent modulus is used in the summation of $\frac{M^2}{E_t} \frac{ds}{dx}$ and $\frac{T^2}{E_t} \frac{ds}{dx}$, the inelastic buckling load so obtained is

the tangent modulus load h_t. If E_r is used instead of E_t, the double modulus load h_r is obtained. The former is obviously the quicker to evaluate as the tangent modulus E_t can be directly read from the stress-strain relationship for any given stress, while the evaluation of E_r is more involved. The inelastic buckling load obtained by the double modulus theory is larger than that derived by the tangent modulus theory as E_r is always greater than E_t.

THE VALUE OF THE INELASTIC MODULUS OF RIGIDITY C_t

No definite information is available concerning the relationship between the tangent modulus of rigidity C_t and the tangent modulus E_t. Different values have been used.

(a) $C_t = C\sqrt{E_t/E}$ - This expression is used in the theory of local buckling of plate elements. The term C is the elastic modulus of rigidity and E_t the tangent modulus;

(b) $C_t = E_tC/E$ - This relationship simplifies the treatment of inelastic buckling;

(c) $C_r = E_rC/E$ - This is used by W. Ramberg and S. Levy.[6] The terms C_r and E_r are the equivalent moduli under the Double Modulus theory; and

(d) $C_r = E_t/E + \sqrt{(E_t/E)C/2}$ - This rather complicated expression is used by E. E. Lundquist.[7]

It was decided to apply the relationships given by (b) and (c) in computing the inelastic buckling loads under the tangent modulus and the double modulus theories respectively, since in each case, it would make the ratio of the lateral flexural to the torsional rigidities γ_t constant throughout both the elastic and the inelastic ranges. A comparison of the values of γ_t derived by (a) and those by either (b) or (c) for the model arches used in the experiments, is as follows:

E_t/E	γ_t By (b) or (c)	γ_t By (a)
0.9	1.316	1.248
0.8	1.316	1.175
0.7	1.316	1.110

The expressions M and T are independent of γ, and the effect of γ on the buckling load comes only from the evaluation of the right hand side of Eq. 3. Since the value of $\Sigma T^2 \delta s$ is small as compared to that of $\Sigma M^2 \delta s$, the effect of small variations in the value of γ on the buckling load is negligible, as is

6 "Instability of Extrusions Under Compressive Loads," by W. Ramberg and S. Levy, Journal of Aeronautical Science, 1945.

7 "On the Strength of Columns that Fail by Twisting," by E. E. Lundquist, Journal of Aeronautical Science, Vol. 4, 1937.

shown by the following results for a model arch with a rise-span ratio of 0.24:

γ_t	h_t, in pounds
1.316	156.11
1.248	156.25
1.175	156.35
1.110	156.55

THE VALUE OF THE VERTICAL SHEAR V

Let t_o be the hanger tension per unit x, then at any point $P(x_1, y_1)$ on the arch rib,

$$H y_1 - \left(\frac{1}{2} t_o L x_1 - \frac{1}{2} t_o x_1^2\right) = 0 \quad \ldots\ldots\ldots (8a)$$

because there is no resulting bending moment in the XAY plane. But

$$y_1 = 4 f x_1 (L - x_1)/L \quad \ldots\ldots\ldots\ldots\ldots\ldots (8b)$$

in which f is the rise span ratio. Therefore,

$$t_o = 8 H f/L \quad \ldots\ldots\ldots\ldots\ldots\ldots (8c)$$

The vertical shear force at P is given by,

$$V = \frac{1}{2} t_o L - t_o x_1$$
$$= 8 H f\left(\frac{1}{2} L - x_1\right)/L \quad \ldots\ldots\ldots\ldots\ldots (9)$$

The average compressive stress at P is $(H \cos \theta + V \sin \theta)/A$.

NUMERICAL EXAMPLES

In the following examples, the inelastic buckling loads are computed for model arches for which the span is 40 in. The tubular section has an external diameter of 3/8 in. and a wall thickness 0.022 in., the cross-sectional area, A, is 0.02442 sq in., I_y equals 0.0003814 in.,^{4} the value of E is 11.24 x 10^6 psi, and $\gamma_t = \gamma = 1.316$. The values of E_t are read directly from Fig. 2, which gives the relationship between the stress and the tangent modulus for the material of which the model arches are made. The value of n is obtained from Fig. 3, which gives the relationship between n and the ratio E_t/E for a tubular section. The values of I_1 and I_2 are taken from Fig. 4, which gives the variation of I_1 and I_2 with n for a tubular section of mean radius r and wall thickness t.

The integrals are computed by the mid-ordinate rule by dividing the span into twenty-four equal sections. The computations were done on a calculating machine.

Example No. 1 - The Inelastic Buckling Load by the Tangent Modulus Theory.—The rise-span ratio f was 0.12.

Step I[3]

$$H_{cr} = 86.1 E I/L^2 = 231.0 \text{ lb}$$

Step II

$$H_{cr}/A = 231.0/0.02442 = 9459 \text{ psi}$$

From Fig. 2, the value of E_t for this stress is 9.45×10^6 psi. Therefore,

$$H_1 = (86.1 \times 9.45 \times 10^6 \times 0.0003814)/40^2 = 194.0 \text{ lb}$$

Step III

$$H_1/A = 194.0/0.02442 = 7{,}942 \text{ psi}$$

$$H_2 = 202.0 \text{ lb (from Table 3)}$$

$$H_3 = 199.6 \text{ lb (from Table 3)}$$

Therefore,

$$h_t = \frac{1}{2}(H_2 + H_3) = 200.8 \text{ lb}$$

Example No. 2 - The Inelastic Buckling Load by the Double Modulus Theory.—The rise-span ratio is 0.12. Only the final approximation is given (Table 4).

$$H_2 = 213.5 \text{ lb}$$

$$H_3 = 211.4 \text{ lb (from Table 4);}$$

Therefore,

$$h_r = \frac{1}{2}(H_2 + H_3) = 212.45 \text{ lb}$$

Introduction.—The objects of the experimental study were to verify the computed values of the inelastic buckling loads, and to investigate the applicability of Southwell's method to cases beyond the proportional limit.

Though Southwell postulated his method for the case of the pin-ended strut,[8] the method was found to be valid in predicting the elastic buckling load of the stabbogen arch. Southwell indicated that his method would only apply within the elastic range, but C. T. Wang[4] has claimed its validity for predicting the inelastic buckling loads of columns. Wang applied the method to the experimental data obtained by Von Karman, Gerard and those of Horsfall and Sandorff, and it was found that the results gave good linear relationships between δ/P and δ, in which δ was the deflection resulting from a compressive load P. It was deemed that Southwell's method might have wider applications than at first realized, and that it might be applied to the prediction of buckling loads in structures where its use was "a liberty not justified by theory."

The Testing Bench.—The same testing bench as that used for the experiments in elastic buckling was employed.[2] The only modification was in the fixation of the ends of the model arches to the end-plates by means of tappering plugs.

The Model Arches.—Model arches of commercially pure aluminum were used because this material has (1) a comparatively large inelastic range, and (2) a low elastic limit as compared to that of structural steel, and its employment entailed very few modifications to the existing apparatus.

The section was of 24 gage with an external diameter of 3/8 in. The span of the arches had to be reduced from 60 in. (the span of the steel arches used in the experiments on elastic buckling), to 40 in. in order that buckling occurred beyond the elastic limit.

---

8 "On the Analysis of Experimental Observations In Problems of Elastic Stability," by R. V. Southwell, Proceedings, Royal Soc., London, Series A, Vol. 135, 1932.

The model arches were parabolic in elevation. Seven wire-hangers, spaced at equal intervals, were used. Each wire was wrapped round the boom of the arch and the ends were twined together before clamping them to the trolley. By this arrangement, the wire-hangers originated, very nearly, from their theoretical centers.

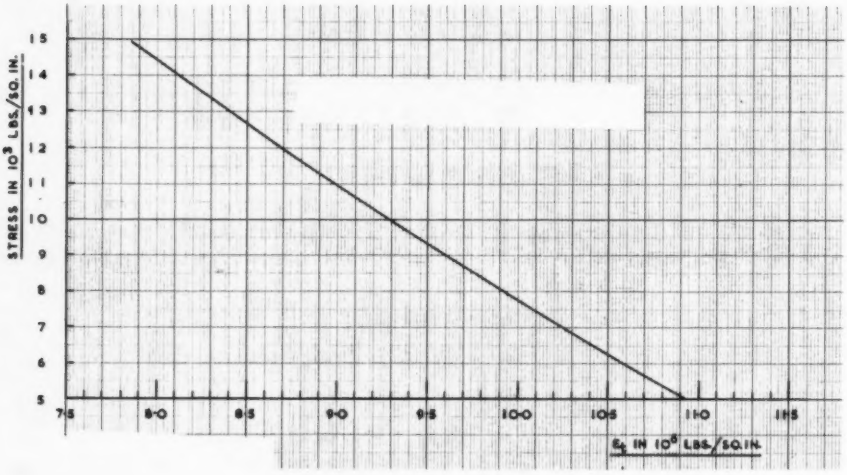

FIG. 2.—THE VARIATION OF E_t WITH STRESS

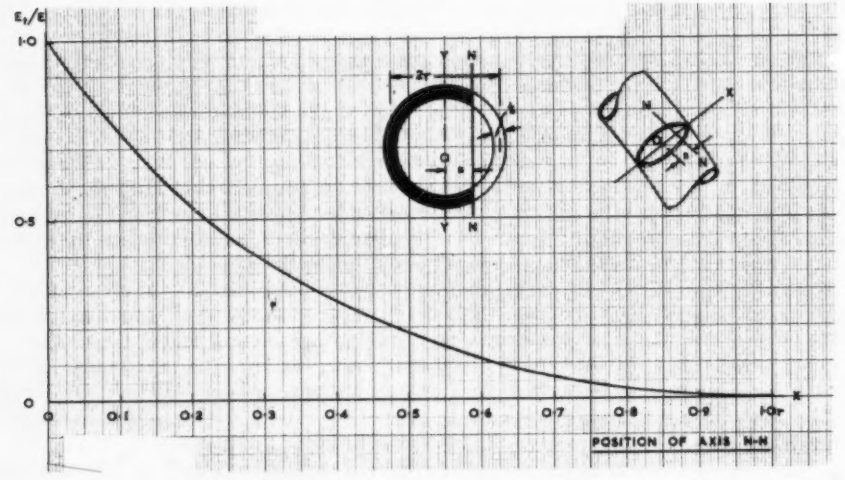

FIG. 3.—THE VARIATION OF n WITH E_t/E

Test Procedure.—As with the experiments in elastic buckling, the procedure in the tests was to observe lateral deflections with the corresponding end thrust measured on both the proving rings. To ascertain that the experimental obser-

TABLE 3.—EXAMPLE 1 (CONT.)

Section	Approximation using H_1 = 194 lb, H_1/A = 7942 psi				Approximation using H_2 = 202 lb, H_2/A = 8271 psi			
	$(H \cos\theta + V \sin\theta)/A$ in psi	E_t (x 10^6 psi)	$\frac{M^2\,ds}{E_t\,dx}$ (x 10^{-8})	$\frac{T^2\,ds}{E_t\,dx}$ (x 10^{-8})	$(H \cos\theta + V \sin\theta)/A$ in psi	E_t (x 10^6 psi)	$\frac{M^2\,ds}{E_t\,dx}$ (x 10^{-8})	$\frac{T^2\,ds}{E_t\,dx}$ (x 10^{-8})
A	8805	9.660	0	0	9170	9.534	0	0
	8677	9.696	0.15027	-	9037	9.580	0.15209	-
1	8554	9.740	0.48768	0.00051	8908	9.620	0.49376	0.00052
	8441	9.777	0.78194	0.00276	8791	9.660	0.79141	0.00280
2	8338	9.808	0.84033	0.00704	8683	9.695	0.85013	0.00712
	8247	9.840	0.61301	0.01372	8588	9.730	0.61994	0.01387
3	8168	9.860	0.27475	0.01907	8506	9.756	0.27768	0.01927
	8099	9.890	0.02417	0.02224	8435	9.778	0.02444	0.02250
4	8043	9.910	0.06892	0.02159	8376	9.792	0.06975	0.02185
	7999	9.922	0.44941	0.01623	8331	9.812	0.45444	0.01641
5	7968	9.930	1.02034	0.00886	8298	9.820	1.03177	0.00896
	7948	9.940	1.52515	0.00231	8278	9.828	1.54253	0.00023
6	7942	9.940	1.72596	0	8271	9.832	1.74491	0

$$2 \times \frac{1}{2} \sum_{0}^{6} M^2/E_t \, ds = 3.54938$$

$$2 \times \frac{1}{2} \gamma_t \sum_{0}^{6} T^2/E_t \, ds = 0.07524$$

$$H_2 = \frac{30.6936 \times 0.0003814 \times 10^8}{3.62462 \times 1600}$$

$$= 202.0 \text{ lb}$$

$$2 \times \frac{1}{2} \sum_{0}^{6} M^2/E_t \, ds = 3.59011$$

$$2 \times \frac{1}{2} \gamma_t \sum_{0}^{6} T^2/E_t \, ds = 0.07471$$

$$H_3 = \frac{30.6936 \times 0.0003814 \times 10^8}{3.66482 \times 1600}$$

$$= 199.6 \text{ lb}$$

TABLE 4[a].—EXAMPLE 2 (CONT.)

Section	$(H \cos\theta + V \sin\theta)/A$, psi	$E_t \times 10^6$ psi	E_t/E	n	$I_1 \times r^3 t$	$I_2 \times r^3 t$	$E_t I_2/E \times r^3 t$	$E_r I \times r^3 t$	$\frac{M^2}{E_r I}\frac{ds}{dx} \times 1/r^3 t$	$\frac{T^2}{E_r I}\frac{ds}{dx} \times 1/r^3 t$
A	9693	9.368	0.8335	0.050r	1.363	1.797	1.498	2.861	0	0
	9552	9.410	0.8372	0.053	1.367	1.793	1.501	2.868	0.00508	0.00000
1	9417	9.456	0.8413	0.051	1.373	1.784	1.501	2.874	0.01653	0.00002
	9292	9.496	0.8448	0.050	1.377	1.780	1.504	2.881	0.02654	0.00009
2	9179	9.530	0.8479	0.049	1.381	1.776	1.506	2.887	0.02855	0.00023
	9078	9.564	0.8509	0.047	1.388	1.767	1.504	2.892	0.02086	0.00045
3	8992	9.592	0.8534	0.047	1.388	1.767	1.508	2.896	0.00935	0.00063
	8916	9.620	0.8559	0.046	1.392	1.763	1.509	2.901	0.00082	0.00074
4	8854	9.640	0.8577	0.045	1.395	1.759	1.509	2.904	0.00235	0.00072
	8806	9.652	0.8587	0.044	1.398	1.754	1.506	2.904	0.01535	0.00054
5	8771	9.670	0.8603	0.044	1.398	1.754	1.509	2.907	0.03485	0.00030
	8750	9.675	0.8608	0.044	1.398	1.754	1.510	2.908	0.05213	0.00008
6	8743	9.675	0.8608	0	1.398	1.754	1.510	2.908	0.05900	0

$$2 \times \frac{1}{2} \sum_{0}^{6} \frac{M^2}{E_r I} \delta_s = 0.12086/r^3 t; \qquad \gamma_t \times 2 \times \frac{1}{2} \sum_{0}^{6} \frac{T^2}{E_r I} \delta_s = 0.00250/r^3 t;$$

$$\text{Therefore } H_3 = \frac{30.6936 \times 0.00001209 \times 11.24 \times 10^6}{0.12336 \times 1600}$$

$$= 211.4 \text{ lb}$$

[a] Approximation using $H_2 = 213.5$ lb; Therefore $H_2/A = 8{,}743$ psi.

vations made corresponded to stresses beyond the elastic limit, a quick stress analysis and observations to ensure the presence of permanent set were made.

The Southwell plot was obtained by using the values of $(z - z_1)$ and $(z - z_1)/(H - H_1)$ instead of those of z and z/H. The term $(z - z_1)$ was the amount by which the lateral deflections were increased when the load was increased from H_1 to H. The initial load H_1 had to be sufficiently large so that the observations taken corresponded to stresses beyond the elastic range.

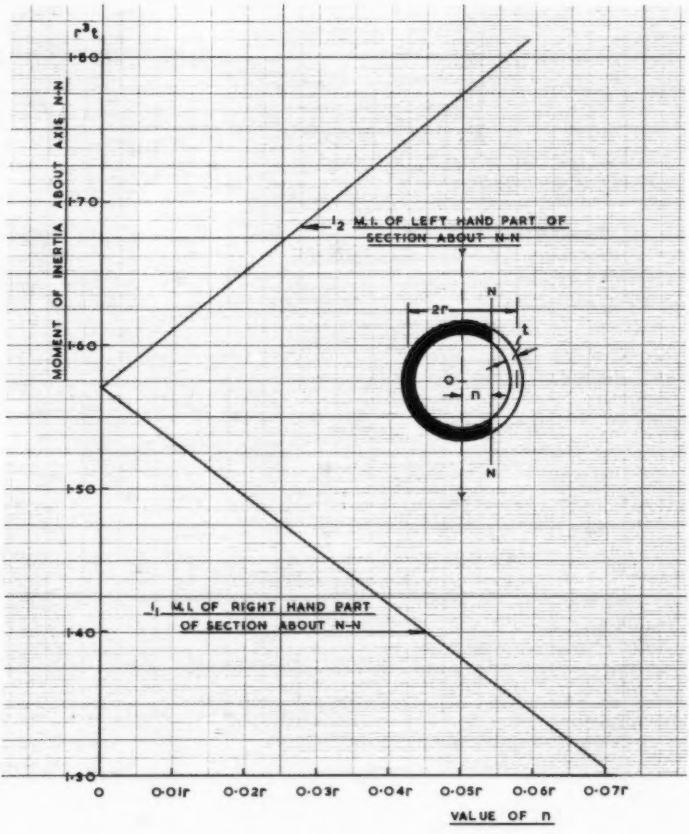

FIG. 4

General Results.

The Southwell Plot.—The Southwell plot is fairly linear if plotted over a range of stress within which there is a negligible difference in the value of E_t. Fig. 5 gives the results of tests No. 18 and No. 22. For those plotted over a range of stress where the difference in the tangent modulus is appreciable, there is a gradual but distinct departure from the linear relationship as is shown in Fig. 6. This deviation is in the direction of decreasing inverse slope, which indicates the registration of a measurable reduction in the value of E_t.

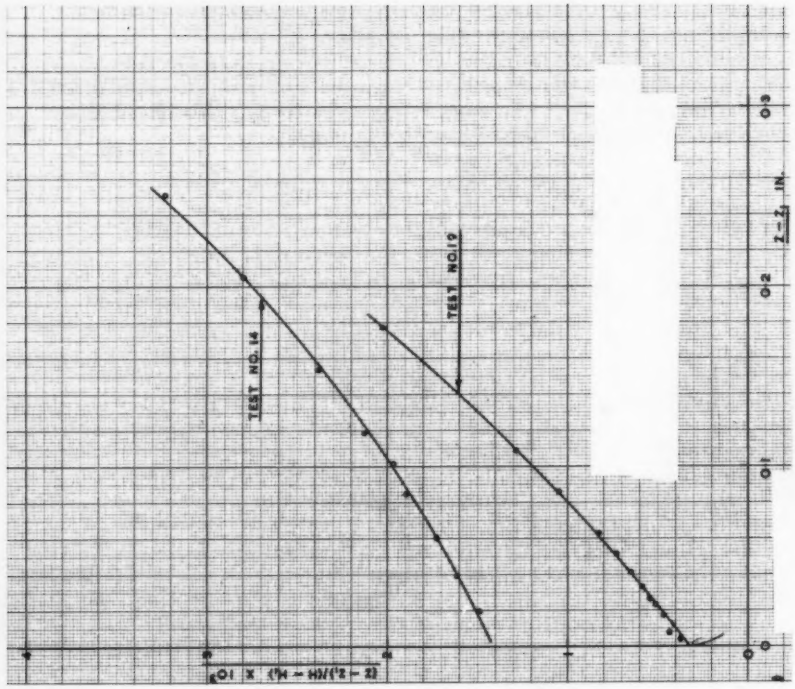

FIG. 6.—SOUTHWELL PLOTS SHOWING A GRADUAL BUT DISTINCT CURVATURE IN THE DIRECTION OF DECREASING INVERSE SLOPE INDICATING MEASURABLE DECREASES IN E_t

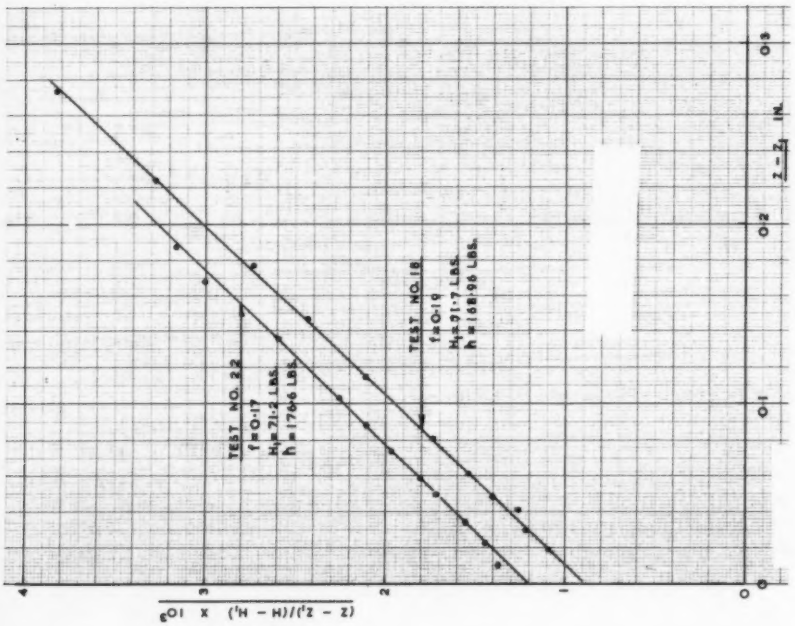

FIG. 5.—SOUTHWELL PLOTS

The Value Of The Inelastic Buckling Loads.—The inelastic buckling loads as assessed from the Southwell plots are only approximate and may be sufficiently accurate for design purposes. Table 5 gives some of the experimental results in comparison with those evaluated by calculation under the tangent modulus and the double modulus theories. The percentage error given in Table 5 is that based on the buckling loads computed on the tangent modulus theory.

As is indicated in Fig. 7, which gives the plot of the results, the experimental results for the buckling loads are more closely related to those obtained by

TABLE 5.—COMPARISON OF RESULTS

f (1)	Double Modulus Load-h_r (lbs) (2)	Tangent Modulus Load-h_t (lbs) (3)	Experimental Result (lbs) (4)	Percentage Error (5)
0.08	223.5	211.2	219.6	3.96
0.12	212.5	200.8	209.6	4.38
0.14	205.6	192.6	185.5	3.71
0.16	198.2	186.7	186.9	0.00
0.20	180.2	171.8	163.7	4.71

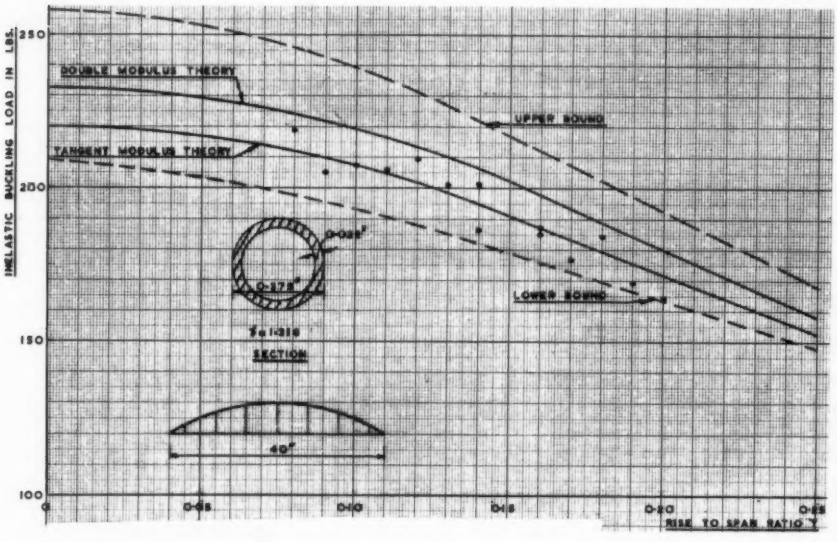

FIG. 7.—EXPERIMENTAL RESULTS AND THEORETICAL CURVES

the tangent modulus theory than those evaluated under the double modulus theory. This is obvious because as a result of unavoidable eccentricities such as imperfect alinement of the arch rib and a non-axial application of the horizontal end thrust, an arch under test will deflect laterally as soon as a load is applied. This results in a simultaneous increase in the stresses due to both bending and to direct compression complying thereby with the assumptions of the tangent modulus theory.

Conclusion.—The method of successive approximation gives the value of the inelastic buckling load accurate enough for design purposes. The inelastic buckling load obtained by the tangent modulus theory is lower than that evaluated by the double modulus theory, and is, therefore, the safer load to use in design. The tangent modulus load, apart from being the easier one to evaluate, gives a closer estimate of the actual buckling load.

Southwell's experimental method is only useful for predicting an approximation of the inelastic buckling load if the arches are of material which has a comparatively small variation in the tangent modulus. Because of its larger scatter, the Southwell plot lacks the advantage of serving as a check against possible experimental errors due, for example, to slip in the wire-hangers and to local instability. The test specimens have to be of greater perfection than is necessary with those that buckle within the elastic range in order that the experimental load reached is a large proportion of the inelastic buckling load. The usefulness of Southwell's method for predicting inelastic buckling loads is, therefore, greatly limited.

ACKNOWLEDGMENTS

Acknowledgment is due A. H. Naylor and to W. G. Godden for their encouragement and criticism, and to the staff of the Engineering Department Workshop, Queen's University, Belfast, Northern Ireland, where the work described in this paper was carried out, for their unfailing cooperation and suggestions on constructional details.

APPENDIX. NOTATION

A	Cross-sectional area of arch rib;
$B = EI$	Flexural rigidity; hence $B_2 = EI_y$;
CJ	Torsional rigidity;
E	Modulus of elasticity;
E_r	Reduced modulus;
E_t	Tangent modulus;
f	Rise-span ratio;
$\gamma = B_2/CJ$	for the elastic range; hence γ_t for the inelastic range;
H	Horizontal component of thrust in the arch rib;
H_{cr}	Critical value of H in the elastic range; that is the elastic horizontal buckling load;
h	The inelastic horizontal buckling load;
h_r	The inelastic horizontal buckling load by the double modulus theory;
h_t	The inelastic horizontal buckling load by the tangent modulus theory;

L	Span of arch;
λ	Shortening of the chord AB;
M	Bending moment in the arch rib about the axis y';
n	Displacement of the axis N-N from the centroidal axis Y-Y (double modulus theory);
r	Mean radius of tubular section;
r_y	$= I_y/A$
S	Length of the arch rib measured along the center line;
s	Distances from the origin A measured along the center line of the arch;
T	Torque in the arch rib about the axis x';
t	Thickness of tube;
θ	$= \tan^{-1}(dy/dx)$
V	Resultant vertical shearing force on chord AB;
x, y, z	Rectangular co-ordinates;
x', y'	Axis tangential and normal respectively to the center line of the arch in the plane XAY; and
z'	Axis perpendicular to the XAY plane.

Journal of the
STRUCTURAL DIVISION
Proceedings of the American Society of Civil Engineers

ANALYSIS OF STRUCTURES BY COMBINING REDUNDANTS

By Peter P. Gillis[1] and Kurt H. Gerstle[2]

SYNOPSIS

A method of analysis of elastic structures that avoids the solution of large systems of simultaneous equations is examined. This method is applicable to structures of any type or degree of indeterminacy and, in special cases, reduces to the well known elastic center and column analogy methods.

The underlying theory is presented, its use is indicated by examples, its physical meaning is discussed, and its relation to the better known special methods is shown.

INTRODUCTION

Among the many refinements proposed for the analysis of statically indeterminate structures, several methods have in the past been suggested that avoid the solution of large systems of simultaneous equations.

Among early investigators, Mueller-Breslau (1897),[3] Mueller (1907),[4] and Gruening (1921)[5] proposed the application of redundants in such combinations as to result in a diagonalized set of compatibility conditions, in which each equation contains one unknown explicitly. This method is generally applicable to

Note.—Discussion open until June 1, 1961. To extend the closing date one month, a written request must be filed with the Executive Secretary, ASCE. This paper is part of the copyrighted Journal of the Structural Division, Proceedings of the American Society of Civil Engineers, Vol. 87, No. ST 1, January, 1961.

[1] Research Asst., Brown Univ., Providence, R. I.
[2] Assoc. Prof. of Civ. Engrg., Univ. of Colorado, Boulder, Colo.

[3] "Zentralblatt der Bauverwaltung," by H. Mueller-Breslau, 1897, p. 513.
[4] "Zentralblatt der Bauverwaltung," by H. Mueller-Breslau, 1907, p. 23.
[5] "Der Eisenbau," M. Gruening, 1921, p. 305.

elastic structures of any type or degree of indeterminacy, and results in a direct and simple set of operations suitable for tabular or computer computation. In cases in which either the degree of indeterminacy or the number of loading conditions is large, this method provides a significant reduction in the amount and complexity of computation.

For the special case of flexural structures of the closed circuit type, it can be shown that this approach is equivalent to the well known elastic center or column analogy methods of analysis. These more specialized procedures have received much attention in the literature of recent decades and are commonly used when many loading conditions are to be considered.

It is the purpose of this paper to direct attention to the more general formulation of the method, to demonstrate its applicability to the analysis of various structures, and to establish its relationship with the more widely known procedures.

OUTLINE AND APPLICATION OF THE METHOD

This classical method of analyzing elastic structures consists of the reduction of an indeterminate structure to a determinate form by removing a number of restraints (redundants) equal to the degree of indeterminacy and then reapplying these redundants in such amounts as to satisfy the conditions of geometry. This procedure leads to a set of simultaneous equations for the redundants, of the form

$$\begin{aligned}
&X_1\,\delta_{11} + X_2\,\delta_{12} + X_3\,\delta_{13} + \cdots + X_m\,\delta_{1m} - \Delta_1 = 0\\
&X_1\,\delta_{21} + X_2\,\delta_{22} + X_3\,\delta_{23} + \cdots + X_m\,\delta_{2m} - \Delta_2 = 0\\
&\quad\vdots\qquad\quad\vdots\qquad\quad\vdots\qquad\qquad\vdots\\
&X_1\,\delta_{m1} + X_2\,\delta_{m2} + X_3\,\delta_{m3} + \cdots + X_m\,\delta_{mm} - \Delta_m = 0
\end{aligned} \qquad \ldots(1)$$

The set Eq. 1 is solved for the X's and the internal forces are then found by superposition of the individual effects.

The proposed method is an orthogonalization procedure, by means of which all interaction coefficients are eliminated, thus leading to a system of equations of the form of Eq. 2

$$\begin{aligned}
&X'_1\,\delta'_{11} && && - \Delta'_1 = 0\\
&&X'_2\,\delta'_{22} && - \Delta'_2 = 0\\
&&&X'_3\,\delta'_{33} && - \Delta'_3 = 0\\
&&&&&\vdots\\
&&&&X'_m\,\delta'_{mm} && - \Delta'_m = 0
\end{aligned} \qquad \ldots(2)$$

To establish this method, use will be made of the principle of virtual work because of its power and generality. However, the necessary equations are also derivable from other considerations.

The principle of virtual work asserts that during any virtual displacement of an elastic body the net work done by all the forces is zero. The internal and external forces must be in equilibrium, and the virtual displacement must be small and compatible with the conditions of constraint.

For clarity of exposition, an application of the method to analysis of a rather simple truss will first be shown and compared with the classical analysis and

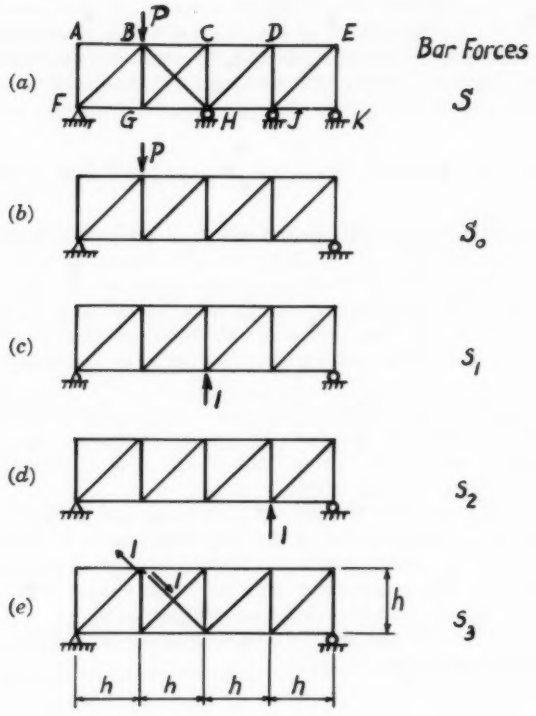

FIG. 1

then generalized. Consider the three times redundant, pin jointed truss of Fig. 1 (a). The member forces S in this structure may be thought of as resulting from superposition of the forces S_o due to the external loads on the determinate truss, and the forces $x_n s_n$ due to the redundants, where x_n is the value of the nth redundant, and s_n represents the member forces due to a unit value of this redundant. We therefore write

$$S = x_1 s_1 + x_2 s_2 + x_3 s_3 + S_o \quad \ldots\ldots\ldots\ldots\ldots\ldots (3)$$

Denoting by α the flexibility (compliance) of any bar ($\alpha = L/A\,E$) the corresponding elongations are

$$\Delta L = \alpha S = \alpha(x_1 s_1 + x_2 s_2 + x_3 s_3 + S_o) \quad \ldots\ldots\ldots\ldots\ldots (4)$$

With unyielding supports, the deflections at points of supports vanish, whereas the deflection of the load point is Δ.

Consider next the truss of Fig. 1 (c) with a unit load as shown equilibrated by bar forces s_1 and reactions that can be computed from statics. Suppose this force system in equilibrium is subject to a virtual displacement equal to the actual displacement of the truss of Fig. 1 (a) (that is assumed small in usual structural practice and is compatible with the constraint conditions). Then the net work done is zero. As neither the unit load nor reactions do any work during this displacement, we have

$$\Sigma \alpha S s_1 = 0 = x_1 \Sigma \alpha s_1^2 + x_2 \Sigma \alpha s_2 s_1 + x_3 \Sigma \alpha s_3 s_1 + \Sigma \alpha S_o s_1 \quad \ldots (5)$$

The summation extends over all the members of the truss. This equation contains the unknowns x_1, x_2 and x_3. Two similar equations can be obtained by application of virtual work to the equilibrium systems of Figs. 1 (d) and 1 (e) subject to virtual displacements equal again to the actual displacements of the truss of Fig. 1 (a). In this fashion, a set of equations of the form of Eq. 1 are set up, that can be solved simultaneously for the unknown values of the redundants.

It should be noticed that in this classical analysis the truss systems of Figs. 1 (c), 1 (d) and 1 (e) were chosen strictly for convenience. In order to reduce the resulting set of equations to the form of Eq. 2, it is necessary to make a more appropriate choice of systems.

In particular, new systems of redundants are applied to the determinate form of the truss that are combinations of the unit redundants of Figs. 1 (c) to 1 (e). These systems will be called combined unit redundants although in general only one of the forces of the combination will have unit value. The bar forces due to the nth combined unit redundant will be designated S_n.

The first combined unit redundant will be chosen equal to the one of Fig. 1 (c). The corresponding member forces are

$$S_1 = s_1 \quad \ldots\ldots\ldots\ldots\ldots\ldots (6a)$$

The second combined unit redundant is a combination of those of Figs. 1 (c) and 1 (d) such that the member forces are

$$S_2 = C_{21} S_1 + s_2 \quad \ldots\ldots\ldots\ldots\ldots (6b)$$

The third combined unit redundant is a combination of all three and results in member forces

$$S_3 = C_{31} S_1 + C_{32} S_2 + s_3 \quad \ldots\ldots\ldots\ldots (6c)$$

The coefficients C_{ij} are constants yet to be determined.

As in establishing Eq. 3 superposition asserts that the member forces in the actual truss are

$$S = X_1 S_1 + X_2 S_2 + X_3 S_3 + S_o \quad \ldots\ldots\ldots (7)$$

Here X_n represents the value of the nth combined unit redundant. The corresponding elongations are now expressed by

$$\Delta L = \alpha S = \alpha (X_1 S_1 + X_2 S_2 + X_3 S_3 + S_o) \ldots\ldots (8)$$

Applying virtual work, we subject each of the combined unit redundant systems to a virtual displacement equal to the actual displacement of the real truss. As before, none of the external forces or reactions of the redundant systems do any work during the displacement and we obtain

$$\Sigma \alpha S S_1 = 0 = X_1 \Sigma \alpha S_1^2 + X_2 \Sigma \alpha S_2 S_1 + X_3 \Sigma \alpha S_3 S_1 + \Sigma \alpha S_o S_1 \ldots (9a)$$

$$\Sigma \alpha S S_2 = 0 = X_1 \Sigma \alpha S_1 S_2 + X_2 \Sigma \alpha S_2^2 + X_3 \Sigma \alpha S_3 S_2 + \Sigma \alpha S_o S_2 \ldots (9b)$$

and

$$\Sigma \alpha S S_3 = 0 = X_1 \Sigma \alpha S_1 S_3 + X_2 \Sigma \alpha S_2 S_3 + X_3 \Sigma \alpha S_3^2 + \Sigma \alpha S_o S_3 \ldots (9c)$$

The summations again extend over all members of the truss.

Eqs. 9 constitute a set of the form of Eq. 1. According to the proposed scheme, we must now make the cross terms vanish, that is

$$\Sigma \alpha S_1 S_2 = 0 \quad \ldots\ldots\ldots\ldots\ldots (10a)$$

$$\Sigma \alpha S_1 S_3 = 0 \quad \ldots\ldots\ldots\ldots\ldots (10b)$$

and

$$\Sigma \alpha S_2 S_3 = 0 \quad \ldots\ldots\ldots\ldots\ldots (10c)$$

This is accomplished by suitably choosing the coefficients C_{ij} in Eq. 6. Substituting the expressions from Eqs. 6a and 6b into Eq. 10a yields

$$\Sigma \alpha S_1 (C_{21} S_1 + s_2) = 0 = C_{21} \Sigma \alpha S_1^2 + \Sigma \alpha S_1 s_2 \ldots (11a)$$

This will be satisfied if we choose

$$C_{21} = \frac{-\Sigma \alpha S_1 s_2}{\Sigma \alpha S_1^2} \quad \ldots\ldots\ldots\ldots (11b)$$

Similarly, substitution from Eq. 6 into Eq. 10b gives

$$\Sigma \alpha S_1 (C_{31} S_1 + C_{32} S_2 + s_3) = 0 = C_{31} \Sigma \alpha S_1^2 + C_{32} \Sigma \alpha S_1 S_2 + \Sigma \alpha S_1 s_3 \ldots (11c)$$

The second term, by Eq. 10a, here is zero so this equation will be satisfied if we choose

$$C_{31} = \frac{-\Sigma \alpha S_1 s_3}{\Sigma \alpha S_1^2} \quad \ldots\ldots\ldots\ldots (11d)$$

Finally, substitution into Eq. 10c gives

$$\Sigma \alpha S_2 (C_{31} S_1 + C_{32} S_2 + s_3) = 0 = C_{31} \Sigma \alpha S_2 S_1 + C_{32} \Sigma \alpha S_2^2 + \Sigma \alpha S_2 s_3 \quad \ldots (11e)$$

The first term here is zero by Eq. 10a so we need only choose

$$C_{32} = \frac{-\Sigma \alpha S_2 s_3}{\Sigma \alpha S_2^2} \quad \ldots\ldots\ldots\ldots (11f)$$

Beginning with the known member forces S_1 the constant C_{21} can be computed from Eq. 11b and then forces S_2 can be determined from Eq. 6b. Having obtained S_2 the constants C_{31} and C_{32} can be computed from Eq. 11d and 11f.

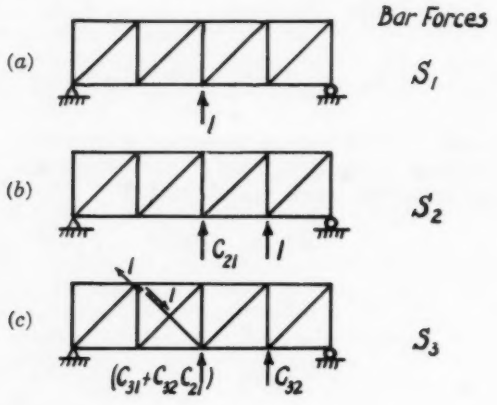

FIG. 2

With these, the forces S_3 can be determined from Eq. 6c. The combined unit redundants producing S_1, S_2, and S_3 are shown in Fig. 2.

Eqs. 9 are now reduced to the explicit form

$$X_1 \Sigma \alpha S_1^2 + \Sigma \alpha S_o S_1 = 0 \quad \ldots\ldots\ldots\ldots (12a)$$

$$X_2 \Sigma \alpha S_2^2 + \Sigma \alpha S_o S_2 = 0 \quad \ldots\ldots\ldots\ldots (12b)$$

and

$$X_3 \Sigma \alpha S_3^2 + \Sigma \alpha S_o S_3 = 0 \quad \ldots\ldots\ldots\ldots (12c)$$

The multipliers X_n are found from Eq. 12 and substituted into Eq. 7 to obtain the member forces. It should be noted that the coefficients C_{mn} depend only

on the nature of the structure. For analysis of any other loading condition, only Eqs. 12 and 7 are required.

Table 1 shows the numerical calculation of the solution of the truss under the load of Fig. 1. For simplicity the flexibility α of the members has been taken equal for all members.

Columns 1, 2, and 3 give member forces due to unit redundants as determined by statics. Columns 4 to 13 comprise the work of finding the coefficients C_{mn} and the member forces due to the combined unit redundants. Columns 15 to 17 enable determination of the X_n's, and columns 18 to 21 produce the final member forces.

Analyses for other loading conditions now require only repetition of the work of columns 14 to 21.

GENERAL THEORY

To formulate this method in a more comprehensive manner, it is convenient to consider an m times statically indeterminate structure. Call the internal stresses s or S, and the corresponding strains δ. These stresses may be due to axial force, shear force, bending, torsion, or any combinations thereof, providing all normal stresses at any point are unidirectional.

The structure is made statically determinate by removing m restraints. In order that no external work will be done by interior redundants, removal of internal constraints is never accompanied by removal of members. That is, internal members are cut or hinged so that equal and opposite forces or moments can be applied at points infinitely close together. Therefore, the only external work that can be done by a combined unit redundant system during its virtual displacement will be due to yielding of supports.

Unit values of the m removed redundants produce internal stresses s_1, s_2, ... s_m, respectively in the determinate structure. From these redundants, a set of combined unit redundants that produce internal stresses S_1, S_2, ... S_m, is constructed according to the scheme;

$$
\begin{aligned}
S_1 &= s_1 \\
S_2 &= C_{21} S_1 + s_2 \\
S_3 &= C_{31} S_1 + C_{32} S_2 + s_3 \qquad \text{. . . . . (13)} \\
&\vdots \\
S_m &= C_{m1} S_1 + C_{m2} S_2 + \ldots + C_{m(m-1)} S_{m-1} + s_m
\end{aligned}
$$

Beginning with C_{21}, the coefficients for each successive S_n are computed according to

$$
C_{ij} = - \frac{\int \alpha \, S_j \, s_i \, dV}{\int \alpha \, S_j^2 \, dV} , \qquad i > j \qquad \text{. . . . . (14)}
$$

TABLE 1

BAR	1 s_1 S_1	2 s_2	3 s_3	4 αS_1^2	5 $\alpha S_1 S_2$	6 $C_{21} S_1$	7 S_2	9 $\alpha S_1 s_3$	10 αS_2^2	11 $C_{31} S_1$	11 $C_{31} S_1$	12 $C_{32} S_2$
AB	0	0	0	0	0	0	0	0	0	0	0	0
BC	0.500	0.250	-0.707	0.250	0.125	-0.292	-0.042	-0.354	0.030	0.002	-0.147	-0.003
CD	1.000	0.500	0	1.000	0.500	-0.583	-0.083	0	0	0.007	-0.294	-0.006
DE	0.500	0.750	0	0.250	0.375	-0.292	0.458	0	0	0.209	-0.147	0.034
FG	-0.500	-0.250	0	0.250	0.125	0.292	0.042	0	0	0.002	0.147	0.003
GH	-1.000	-0.500	-0.707	1.000	0.500	0.583	0.083	0.707	-0.059	0.007	0.294	0.006
HJ	-0.500	-0.750	0	0.250	0.375	0.292	-0.458	0	0	0.209	0.147	-0.034
JK	0	0	0	0	0	0	0	0	0	0	0	0
AF	0	0	0	0	0	0	0	0	0	0	0	0
BG	-0.500	-0.250	-0.707	0.250	0.125	0.292	0.042	0.354	-0.030	0.002	0.147	0.003
CH	-0.500	-0.250	-0.707	0.250	0.125	0.292	0.042	0.354	-0.030	0.002	0.147	0.003
DJ	0.500	-0.250	0	0.250	-0.125	-0.292	-0.542	0	0	0.293	-0.147	-0.041
EK	0.500	0.750	0	0.250	0.375	-0.292	0.458	0	0	0.209	-0.147	0.034
BF	0.707	0.354	0	0.500	0.250	-0.412	-0.058	0	0	0.003	-0.208	-0.004
BH	0	0	1.00	0	0	0	0	0	0	0	0	0
CG	0.707	0.354	1.00	0.500	0.250	-0.412	-0.058	0.707	-0.058	0.003	-0.208	-0.004
DH	-0.707	0.354	0	0.500	-0.250	0.412	0.766	0	0	0.587	0.208	0.058
EJ	-0.707	-1.060	0	0.500	0.750	0.412	-0.648	0	0	0.420	0.208	-0.049
SUM				6.000	3.500			1.768	-0.147	1.955		

$$C_{21} = -\frac{3.500}{6.000} \qquad C_{31} = -\frac{1.768}{6.000} = -.294$$

$$C_{32} = -\frac{-.147}{1.955}$$

$$= +.075$$

in which α represents an appropriate elastic coefficient of proportionality between stress and strain. The integration extends over the entire structure. This gives an orthogonal set of redundants such that

$$\int \alpha S_i S_j \, dV = 0 \quad \text{for} \quad i \neq j \qquad \ldots\ldots\ldots\ldots (15)$$

Call the internal stresses produced in the determinate structure by applied loads S_o. By superposition, the internal stresses in the actual structure are

$$S = X_1 S_1 + X_2 S_2 + \ldots + X_m S_m + S_o \qquad \ldots\ldots\ldots (16)$$

and from Hooke's Law the corresponding strains are

$$\delta = \alpha S + \delta_t = \alpha \left(X_1 S_1 + X_2 S_2 + \ldots + X_m S_m + S_o\right) + \delta_t, \qquad \ldots (17)$$

in which the δ_t term denotes internal strains due to temperature changes, and so on. The multipliers X_1, X_2, $\ldots$ X_m are found by applying the principle

TABLE 1.—*CONTINUED*

13 S_3	14 αS_3^2	15 S_o	16 $\alpha S_o S_2$	17 $\alpha S_o S_2$	18 $\alpha S_o S_3$	19 $X_1 S_1$	20 $X_2 S_2$	21 $X_3 S_3$	22 S
0	0	0	0	0	0	0	0	0	0
-0.857	0.732	-0.750P	-0.375P	-0.031P	0.643P	0.250P	0	0.436P	-0.064P
-0.300	0.090	-0.500P	-0.500P	-0.042P	0.150P	0.500P	0	0.153P	0.153P
-0.113	0.012	-0.250P	-0.125P	-0.114P	0.028P	0.250P	0	0.057P	0.057P
0.150	0.022	0.750P	-0.375P	0.031P	0.112P	-0.250P	0	-0.076P	0.424P
-0.407	0.166	0.500P	-0.500P	0.042P	-0.204P	-0.500P	0	0.207P	0.207P
0.113	0.012	0.250P	-0.125P	-0.114P	0.028P	-0.250P	0	-0.057P	-0.057P
0	0	0	0	0	0	0	0	0	0
0	0	0	0	0	0	0	0	0	0
-0.557	0.310	-0.250P	0.125P	-0.010P	0.139P	-0.250P	0	0.284P	-0.216P
-0.557	0.310	-0.250P	0.125P	-0.010P	0.139P	-0.250P	0	0.284P	-0.216P
-0.188	0.036	-0.250P	-0.125P	0.136P	0.047P	0.250P	0	0.096P	0.096P
-0.113	0.012	-0.250P	-0.125P	-0.114P	0.028P	0.250P	0	0.057P	0.057P
-0.212	0.045	-1.060P	-0.750P	0.061P	0.224P	0.354P	0	0.108P	-0.598P
1.000	1.000	0	0	0	0	0	0	-0.509P	-0.509P
0.788	0.619	0.354P	0.250P	-0.021P	0.279P	0.354P	0	-0.401P	0.307P
0.266	0.072	0.354P	-0.250P	0.271P	0.094P	-0.354P	0	-0.135P	-0.135P
0.159	0.026	0.354P	-0.250P	-0.229P	0.056P	-0.354P	0	-0.081P	-0.081P
	3.464		-3.000P	0.002P	1.763P				

$$X_1 = -\frac{-3.000P}{6.000} = .500P$$

$$X_2 = -\frac{.002P}{1.955} = -.001P \sim 0$$

$$X_3 = -\frac{1.763P}{3.464} = -.509P$$

of virtual work to each of the equilibrium systems S_1, S_2, S_3, ... S_m subject to a virtual displacement equal to the actual displacement of the real structure. In view of Eq. 15, and including the effect of support settlements, this gives

$$X_1 \int \alpha S_1^2 \, dV + \int \alpha S_o S_1 \, dV + \int \delta_t S_1 \, dV + \Sigma R_{1p} \Delta_p = 0$$

$$X_2 \int \alpha S_2^2 \, dV + \int \alpha S_o S_2 \, dV + \int \delta_t S_2 \, dV + \Sigma R_{2p} \Delta_p = 0 \quad \ldots\ldots (18)$$

$$\vdots$$

$$X_m \int \alpha S_m^2 \, dV + \int \alpha S_o S_m \, dV + \int \delta_t S_m \, dV + \Sigma R_{mp} \Delta_p = 0$$

The work resulting from yielding of the pth support by an amount Δ_p is included in the last term of Eq. 18. This work is equal to the product of the external force or moment at the pth support of the appropriate equilibrium system, and the corresponding settlement Δ_p. Calling the external force or moment at point p for system s_n, r_{np} and for system S_n, R_{np} it can be seen that these are the

same for system S_1 as for system s_1, or $R_{1p} = r_{1p}$. For system S_2, the support reactions are those for s_2 plus C_{21} times those for S_1, or $R_{2p} = C_{21} R_{1p} + r_{2p}$. For system S_3 they are those for system s_3 plus C_{31} times those for S_1 plus C_{32} times those for S_2, or $R_{3p} = C_{31} R_{1p} + C_{32} R_{2p} + r_{3p}$. Generalizing, the equation

$$R_{np} = C_{n1} R_{1p} + C_{n2} R_{2p} + \ldots + C_{n(n-1)} R_{(n-1)p} + r_{np} ;$$

$$C_{ni} = 0 \text{ for } n \leq i \quad \ldots\ldots\ldots\ldots\ldots\ldots (19)$$

allows for the successive determination of each R_{np}.

Each X is computed from Eq. 18, and the internal stresses of the structure are then obtained from Eq. 16. For other loading conditions applied to the same structure, the analysis requires only Eqs. 18 and 16. It should be noted that in many analyses including influence line computations, the terms representing support settlement and temperature strains are customarily omitted because only the effects of live load are considered.

Integration to obtain the internal work can be simplified for structural members. Subject to the usual assumptions of structural theory, the state of stress at any cross section of a member can be completely described by specifying the bending moment, twisting moment, normal force and shear force that act at the section. Call these M, T, N, and V, respectively. The corresponding elastic strains are also specified because of Hooke's Law.

Consider now the work dW done in a slice of infinitesimal thickness dl at a cross section of a member in which the stresses of an equilibrium system S_i are specified by M_i, T_i, N_i and V_i. The strains due to a virtual displacement system S_j are specified by M_j, T_j, N_j and V_j. Integration over the cross section gives

$$dW = \left(\frac{M_i M_j}{E I} + \frac{T_i T_j}{C G} + \frac{N_i N_j}{A E} + \frac{k V_i V_j}{A G} \right) dl \quad \ldots\ldots\ldots (20)$$

Integration along the length of each member throughout the entire structure shows that

$$\int \alpha S_i S_j \, dV = \int \left(\frac{M_i M_j}{E I} + \frac{T_i T_j}{C G} + \frac{N_i N_j}{A E} + \frac{k V_i V_j}{A G} \right) dl \quad \ldots\ldots\ldots (21)$$

PHYSICAL INTERPRETATION

The physical significance of the proposed procedure may be suggested by a consideration of the deflection curves of the three times indeterminate continuous beam of Fig. 3. The statically determinate system selected is that of Fig. 3 (b), and according to Eqs. 13, the combined unit redundants are those of Figs. 3 (c) to 3 (e).

Considering now, in particular, the deflection curve of Fig. 3 (d), we see that the effect of selecting the coefficient C_{21} according to Eq. 14, is to annul the deflection at point 1. The deflection curve of Fig. 3 (e) due to the third combined unit redundant is a superposition of curves proportional to those of Figs. 3 (c) and 3 (d), and that due to the unit force at point 3, at which the amplitudes of the two first curves, specified by C_{31} and C_{32}, are such as to annul deflections at points 1 and 2.

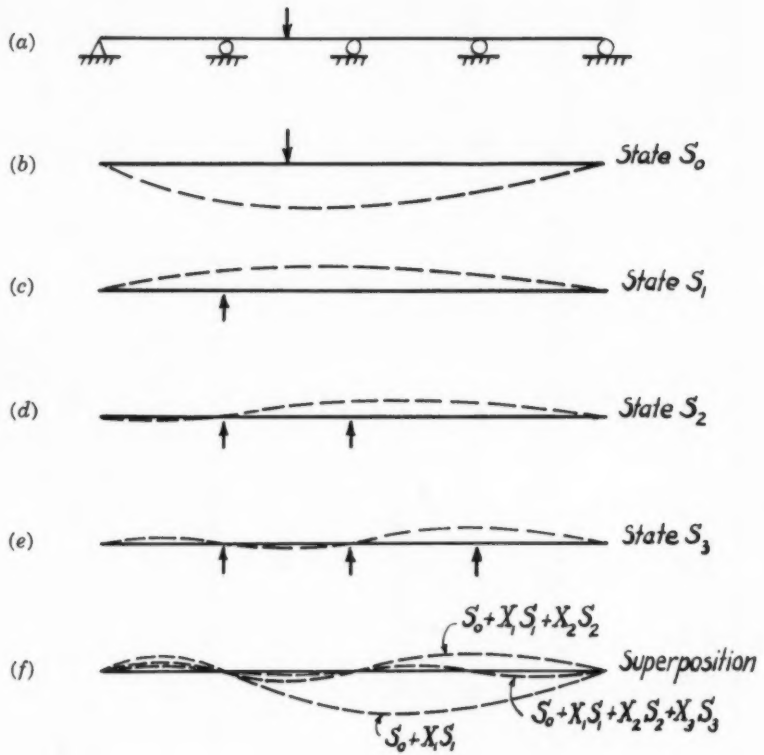
(a)
(b)
State S_0
(c)
State S_1
(d)
State S_2
(e)
State S_3
(f)
$S_0+X_1S_1+X_2S_2$
Superposition
$S_0+X_1S_1+X_2S_2+X_3S_3$
$S_0+X_1S_1$

FIG. 3

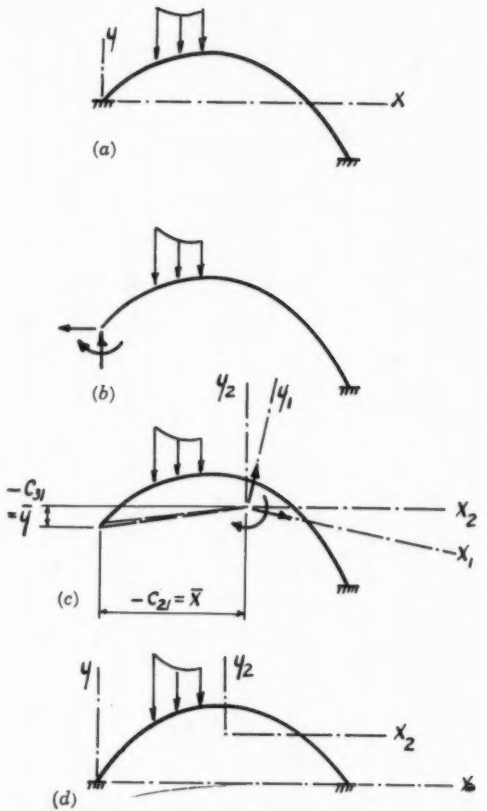
y
x
(a)
(b)
y_2
y_1
$-c_{31}$
$-\bar{y}$
x_2
x_1
(c)
$-c_{21}=\bar{x}$
y
y_2
x_2
(d)

FIG. 4

Consideration of the deflected shapes due to the redundant states S_1, S_2, S_3, shows that, of these states, only state S_1 will affect the deflection at point 1. The multiplier X_1 is accordingly selected to annul the deflection at point 1 due to the load (state S_0). Of the other redundant states, only state S_2 will affect the deflection at point 2, and X_2 is accordingly selected to annul the deflection at this point due to the states $(S_0 + X_1 S_1)$. The scheme is extended for additional redundants. Eqs. 18 provide for the selection of appropriate values of X_n, and Eq. 16 for the superposition of the states, that is also shown in the series of elastic curves of Fig. 3 (f).

It should be noted that the statically determinate system S_0 of Fig. 3 (b) was selected only for purposes of visualization. A more effective way of attacking the analysis of continuous beams or frames might often be to consider internal moments as redundants.

RELATION TO OTHER METHODS

To illustrate the application of the present method of flexural structures in which the work done by axial and shear forces can be neglected in comparison with that done by bending, and to show the relation of this method to the well known elastic center and column analogy methods, consider a fixed-ended arch type structure, as shown in Fig. 4.

Make the structure determinate as shown in Fig. 4 (b). The unit redundants are a moment and horizontal and vertical forces respectively, applied at the cut end, and the moments due to these are

$$m_1 = 1; \qquad m_2 = x; \qquad m_3 = y; \qquad \ldots (22)$$

The combined unit redundants are then selected according to Eq. 13 to give moments

$$M_1 = m_1 = 1 \quad \ldots (23a)$$

$$M_2 = C_{21} M_1 + m_2 = C_{21} + x \quad \ldots (23b)$$

and

$$M_3 = C_{31} M_1 + C_{32} M_2 + m_3 = C_{31} + C_{32} C_{21} + C_{32} x + y \quad \ldots (23c)$$

The coefficients here are computed, following Eq. 14, as

$$C_{21} = -\frac{\int \frac{x\, dl}{E I}}{\int \frac{dl}{E I}} \quad \ldots (24a)$$

$$C_{31} = -\frac{\int \frac{y\, dl}{E I}}{\int \frac{dl}{E I}} \quad \ldots (24b)$$

and

$$C_{32} = -\frac{\int (C_{21} + x)\frac{y\,dl}{E\,I}}{\int (C_{21} + x)^2 \frac{dl}{E\,I}} = -\frac{\int \frac{x\,y\,dl}{E\,I} - \left(\int \frac{x\,dl}{E\,I}\right)\left(\int \frac{y\,dl}{E\,I}\right) \Big/ \left(\int \frac{dl}{E\,I}\right)}{\int \frac{x^2 dl}{E\,I} - \left(\int \frac{x\,dl}{E\,I}\right)^2 \Big/ \left(\int \frac{dl}{E\,I}\right)} \quad \ldots\ldots (24c)$$

The multipliers X_n are computed according to Eq. 18, and the final moments are written by use of Eq. 16. It is, of course, not always necessary to compute the integrals analytically. Sometimes, as for instance in the case of linear structures and moment diagrams, it is more convenient to resort to graphical or geometrical methods.

It is instructive to show the relation of this method to the well-known elastic center method applicable to this type of structure. In that method, the coupling terms are eliminated by suitable choice of orientation and point of application of the redundants, namely along the axes with respect to which the quantities

$$\int \frac{x_1\,dl}{E\,I} = 0 \quad \ldots\ldots (25a)$$

$$\int \frac{y_1\,dl}{E\,I} = 0 \quad \ldots\ldots (25b)$$

and

$$\int \frac{x_1\,y_1\,dl}{E\,I} = 0 \quad \ldots\ldots (25c)$$

as shown on Fig. 4 (c). The axes thus defined can be identified as the centroidal principal axes x_1, y_1 of a conjugate structure the elements of which extend along the centerline of the structure a distance dl, and have a width normal to the centerline of $1/E\,I$. The centroid of this equivalent area is thus defined, in terms of the axes x, y of Fig. 4 (a), by the distances

$$\bar{x} = \frac{\int \frac{x\,dl}{E\,I}}{\int \frac{dl}{E\,I}} = -C_{21} \quad \ldots\ldots (26a)$$

and

$$\bar{y} = \frac{\int \frac{y\,dl}{E\,I}}{\int \frac{dl}{E\,I}} = -C_{31} \quad \ldots\ldots (26b)$$

We can further observe that the numerator of the expression for C_{32} (Eq. 24c) represents the product of inertia of the conjugate structure with respect to the centroidal x_2 and y_2 axes, and the denominator the moment of inertia with re-

spect to a centroidal y_2 axis, so that

$$C_{32} = -\frac{\int \frac{x_2\, y_2\, dl}{E\,I}}{\int \frac{x_2^2\, dl}{E\,I}} \quad \ldots\ldots\ldots\ldots\ldots\ldots \quad (26c)$$

For redundants applied along the principal axes, Eq. 24 and Eq. 25 result in

$$C_{21} = -\frac{\int \frac{x_1\, dl}{E\,I}}{\int \frac{dl}{E\,I}} = 0 \quad \ldots\ldots\ldots\ldots\ldots\ldots \quad (27a)$$

$$C_{31} = -\frac{\int \frac{y_1\, dl}{E\,I}}{\int \frac{dl}{E\,I}} = 0 \quad \ldots\ldots\ldots\ldots\ldots\ldots \quad (27b)$$

and

$$C_{32} = -\frac{\int \frac{x_1\, y_1\, dl}{E\,I}}{\int \frac{x_1^2\, dl}{E\,I}} = 0 \quad \ldots\ldots\ldots\ldots\ldots\ldots \quad (27c)$$

This shows that the elastic center method becomes a special case of the proposed method for which all coefficients C_{ij} vanish.

It also can be seen that if the x and y axes through the point of redundancy are taken parallel to the principal axes of the conjugate structure, then the coefficient C_{32}, being proportional to the centroidal product of inertia, will vanish. In particular, this occurs in symmetrical structures, thereby considerably simplifying the computations.

For this symmetrical case, it will be shown that the computations for the proposed method, for the elastic center method, and for the method of column analogy become identical.

Here, Eq's. 23 reduce to

$$M_1 = 1 \quad \ldots\ldots\ldots\ldots\ldots\ldots \quad (28a)$$

$$M_2 = C_{21} + x \quad \ldots\ldots\ldots\ldots\ldots\ldots \quad (28b)$$

and

$$M_3 = C_{31} + y \quad \ldots\ldots\ldots\ldots\ldots\ldots \quad (28c)$$

and the total moment is written as

$$M = X_1 + X_2\,(C_{21} + x) + X_3\,(C_{31} + y) + M_o \quad \ldots\ldots\ldots\ldots \quad (29)$$

in which M_o denotes the moment due to the applied load on the determinate structure.

Here the coefficients C_{21} and C_{31} are given by Eqs. 24a and 24b, and according to Eqs. 18,

$$X_1 = -\frac{\int \frac{M_o\, dl}{EI}}{\int \frac{dl}{EI}} \qquad \text{(30a)}$$

$$X_2 = -\frac{\int (C_{21} + x)\frac{M_o\, dl}{EI}}{\int (C_{21} + x)^2 \frac{dl}{EI}} = -\frac{\int (x-\bar{x})\frac{M_o\, dl}{EI}}{\int (x-\bar{x})^2 \frac{dl}{EI}} = -\frac{\int \frac{M_o\, x_2\, dl}{EI}}{\int \frac{x_2^2\, dl}{EI}} \qquad \text{(30b)}$$

and

$$X_3 = -\frac{\int (C_{31} + y)\frac{M_o\, dl}{EI}}{\int (C_{31} + y)^2 \frac{dl}{EI}} = -\frac{\int (y-\bar{y})\frac{M_o\, dl}{EI}}{\int (y-\bar{y})^2 \frac{dl}{EI}} = -\frac{\int \frac{M_o\, y_2\, dl}{EI}}{\int \frac{y_2^2\, dl}{EI}} \qquad \text{(30c)}$$

so that

$$M = -\frac{\int \frac{M_o\, dl}{EI}}{\int \frac{dl}{EI}} - \frac{\int \frac{M_o\, x_2\, dl}{EI}}{\int \frac{x_2^2\, dl}{EI}}\, x_2 - \frac{\int \frac{M_o\, y_2\, dl}{EI}}{\int \frac{y_2^2\, dl}{EI}}\, y_2 + M_o \qquad \text{(31)}$$

that will be recognized as the elastic center solution. Substituting the usual symbols for the integral expressions,[6] this can be written as

$$M = -\frac{P}{A} - \frac{M_{y2}}{I_{y2}}\, x_2 - \frac{M_{x2}}{I_{x2}}\, y_2 + M_o \qquad \text{(32)}$$

that is the column analogy form of the solution.

CONCLUDING REMARKS

The present treatment is a specialization of the Gram-Schmidt Method of Orthogonalization.[7]

In the modern literature, a general treatment of the use of orthogonal states of stress in structural analysis and elasticity has been presented by Prager.[8] In that paper, a geometrical approach based on the representation of states of

[6] "Statically Interdeterminate Structures," by C. K. Wang, 1953.

[7] "Methods of Mathematical Physics," by R. Courant and D. Hilbert, 1953, p. 4.

[8] "The Extremum Principles of the Mathematical Theory of Elasticity and Their Use in Stress Analysis," by W. Prager, Univ. of Washington Engrg. Sta., Bulletin No. 119, 1951.

stress by vectors in function space is used, and extended to devise an approximate method by means of which a correct solution can be bracketed to within any desired degree of accuracy. Morkovin and Kincaid have examined the simplifications due to orthogonalization of stress states.[9] They, however, restricted their observations to symmetrical structures under bending moments only.

For structures of a high degree of indeterminacy, some advantages are offered by the Peach Method,[10] that uses matrix methods to construct from the set $s_1, s_2, \ldots s_m$ an orthonormal set $S_1, S_2, \ldots S_m$ that in addition to fulfilling Eq. 15 has the property

$$\int \alpha \, S_i \, S_j \, dV = 1 \quad \text{for} \quad i = j, \ldots\ldots\ldots\ldots (33)$$

thereby simplifying Eqs. 18.

ACKNOWLEDGMENT

The authors express appreciation to William Prager, F. ASCE of Brown University, for suggesting this topic. The last named author also expresses appreciation to the National Science Foundation for the grant of a Science Faculty Fellowship that enabled him to devote time to this subject and to the Division of Engineering of Brown University, Providence, Rhode Island for inspiration and help in writing this paper.

9 "An Application of Orthogonal Moments to Problems in Statically Interdeterminate Structures," by W. M. Kinkaid and V. Morkovin, Quarterly of Applied Mathematics, Vol. 1, 1943, p. 334.

10 "Bulletin of the American Mathematical Society," by M. O. Peach, Vol. 50, 1944, p. 556.

Journal of the
STRUCTURAL DIVISION
Proceedings of the American Society of Civil Engineers

RECENT TRENDS IN ULTIMATE STRENGTH DESIGN

By Phil M. Ferguson[1]

SYNOPSIS

For reinforced concrete members, load-stress curves show such irregularities at cracking load and near ultimate load that the attainment of reasonably accurate predictions of member capacity requires the use of ultimate strength theory.

Under ultimate strength theory, the designer must become familiar with load factors (and probability theory). Several load factor proposals have been presented, each calling for the use of reduced material strengths and an increase over working loads. In addition, American study has always used separate load factors for dead and live load.

The increasing use of strains and the convenient use of the rectangular stress block for concrete stresses seem to furnish the tools that the designer needs to develop a systematic "theory" of ultimate strength for either complicated or standard sections.

INTRODUCTION

When the reinforced concrete designer first moves into ultimate strength design, he finds new concepts and new specifications, and may feel ill at ease. He will be more efficient if he understands some of the background necessitating the change to ultimate strength methods and is aware of some of the trends that must become part of the ultimate strength picture.

Note.—Discussion open until June 1, 1961. Separate discussions should be submitted for the individual papers in this symposium. To extend the closing date one month, a written request must be filed with the Executive Secretary, ASCE. This paper is part of the copyrighted Journal of the Structural Division, Proceedings of the American Society of Civil Engineers, Vol. 87, No. 1, January, 1961.

1 Prof. of Civ. Engrg., Dept. of Civ. Engrg., Univ. of Texas, Austin 12, Tex.

This discussion is more philosophical than mathematical. It shows from the diversity of load-stress relationships why concepts based on working stress design are relatively inefficient tools. It indicates the probable increased role of the load factor concept in future design. Finally, it points out the necessity for a greater introduction of ultimate strain concepts into ultimate strength methods as new codes are prepared.

STRESS COMPLICATIONS

Ultimate strength design is relatively new in codes, but it is not a new idea. Fifty years ago a form of ultimate strength design almost became the official procedure for the first code written by the group that is now known as the

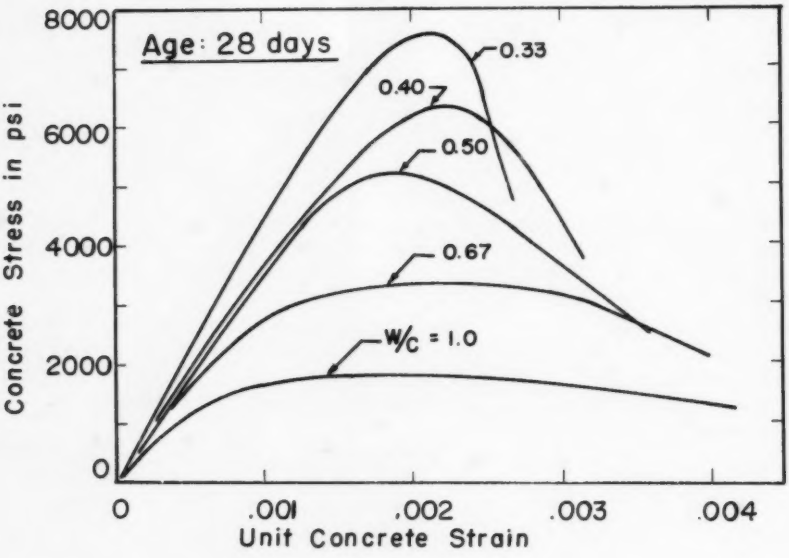

FIG. 1.—FLEXURAL STRESS-STRAIN CURVES

American Concrete Institute. Instead, the apparent simplicity of the straight-line stress distribution prevailed, and probably it did make the acceptance of reinforced concrete somewhat simpler. With allowable stresses suitably established, it has for many years yielded safe results, but it often resulted in rather unbalanced or non-uniform strengths.

The straight line theory has always presented difficulties to research engineers. In the laboratory they simply could not find the strains indicated by working stress type of computations. At least three factors have been involved in this lack of agreement.

First, concrete in tension is quite limited in capacity. In beams, this tension capacity is largely lost when loading is increased to the flexural cracking

state. However, with lightly reinforced beams, the cracking load can be as high as 50% to 60% of the ultimate load. Indeed, minimum reinforcing is often specified to prevent immediate failure as soon as the first flexural crack appears. Although ultimate strength design does not eliminate this problem, it focuses attention on ultimate rather than working load conditions; and flexural tension in concrete is rarely significant at ultimate load.

Second, the stress-strain curve for concrete in compression is not a straight line but, in a beam or column as in a cylinder, is greatly curved and includes a small downtrend beyond the peak, as indicated in Fig. 1. This pattern is well authenticated,[2] and it is not surprising that any straight line approximation gives unrealistic results.

Third, shrinkage stresses are often of significant magnitude and at working load are very difficult to assess. Fortunately, when the concrete once cracks in flexure the shrinkage stresses largely dissipate insofar as flexural strength computations are concerned. But shrinkage stresses greatly influence the cracking-load itself and, thus, their effect is quite noticeable in research. Whereas ultimate strength computations do not eliminate this problem, it is less important at ultimate loads.

Load-Stress Relationships.—Figs. 2 to 5, inclusive, indicate in a general way how widely f_c and f_s vary with loading. (These are not laboratory data but rather estimated curves based on several well established check points.) Figs. 2, 3 and 4 are based on f'_c = 3000 psi and intermediate grade steel (f_y = 40,000 psi), whereas Fig. 5 is more diagramatic. To facilitate comparisons, the axes in these figures are given in dimensionless units, with the ratio of load to ultimate load plotted vertically and the ratio of unit stress to ultimate stress for concrete (or unit stress to yield stress for steel) plotted horizontally. There is a major break at first cracking, particularly when percentage of steel is small. There is always a second irregularity near ultimate.

In the case of the prestressed concrete beam there is no sharp yield point for the steel, and the steel stress ratio plotted is simply that of f_s to the f_s that exists at beam failure. With prestress, the effects of cracking and of high concrete stress tend somewhat to move together toward the top of the curve.

The relationship between loads and stresses is more effectively presented in Figs. 6 and 7. From Fig. 6 note that, with medium of large steel percentages, a working load of roughly half of the ultimate load develops an f_s that seems to be reasonably proportional to load. However, for s small percentage of steel f_s varies far from linearly, and the same is true with prestress.

In Fig. 7, the variations in f_c at working load are wide and give little assistance in pointing toward the true ultimate moment. In the case of prestress, the dotted extension in Fig. 5 of the working f_c curve to ultimate (in which f_c/f'_c = 1.00) would be overly optimistic. In the case of p = 0.03 (Fig. 4), the dotted extension of the working f_c curve would show a very low value; working stress methods do yield this low answer, limited by a failure in compression. Thus, to the designer under working stress methods, the low apparent value of ultimate load might be increased by adding compression steel. In contrast, the actual behavior of this beam would be to fail in tension. Ultimate strength analysis indicates the tension failure and the considerably larger ultimate moment capacity. Hence, the addition of compression steel would add practically no strength.

---

[2] "Confirmation of Inelastic Stress Distribution in Concrete," by Eivind Hognestad, ASCE Proceedings Paper No. ST 2, Vol. 83, March, 1957.

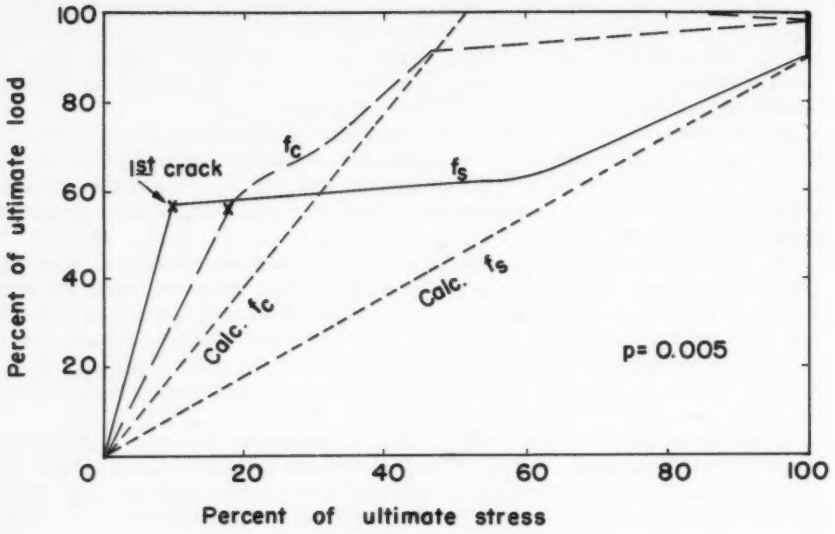

FIG. 2.—UNDERREINFORCED BEAM, LOAD-STRESS RELATIONS

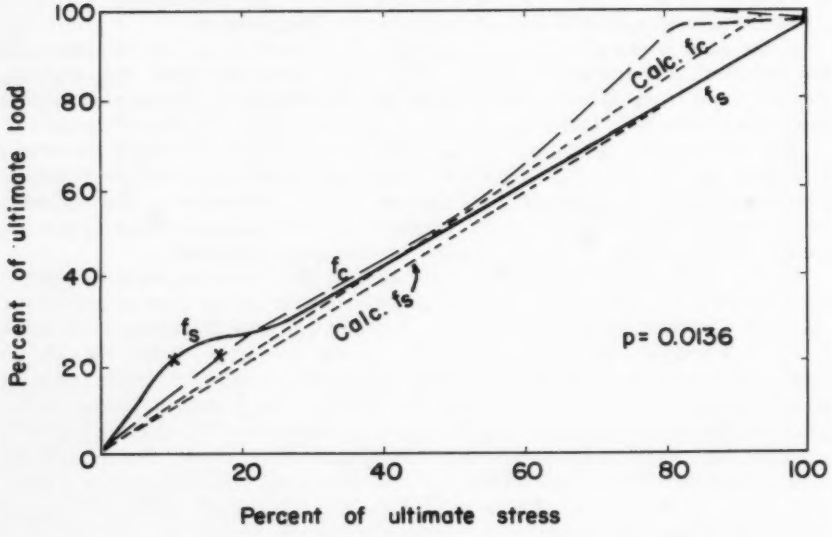

FIG. 3.—BALANCED BEAM, LOAD-STRESS RELATIONS

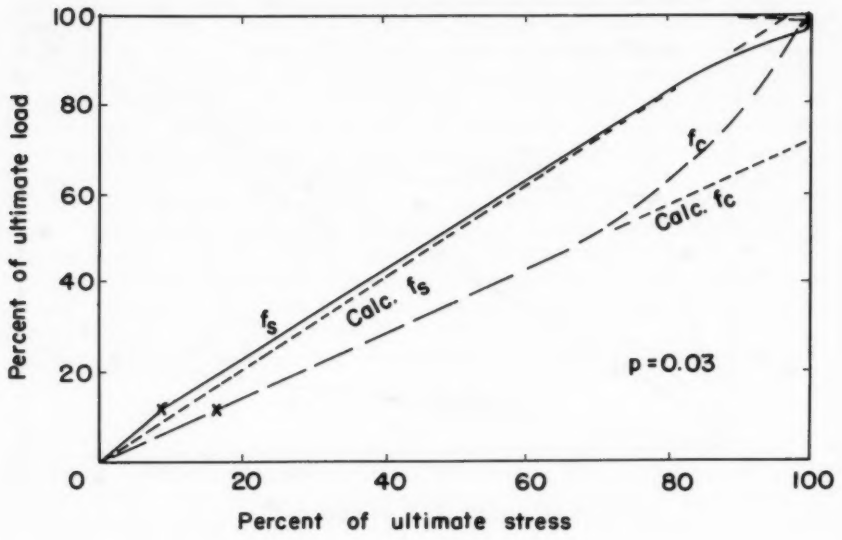

FIG. 4.—OVERREINFORCED BEAM, LOAD-STRESS RELATIONS

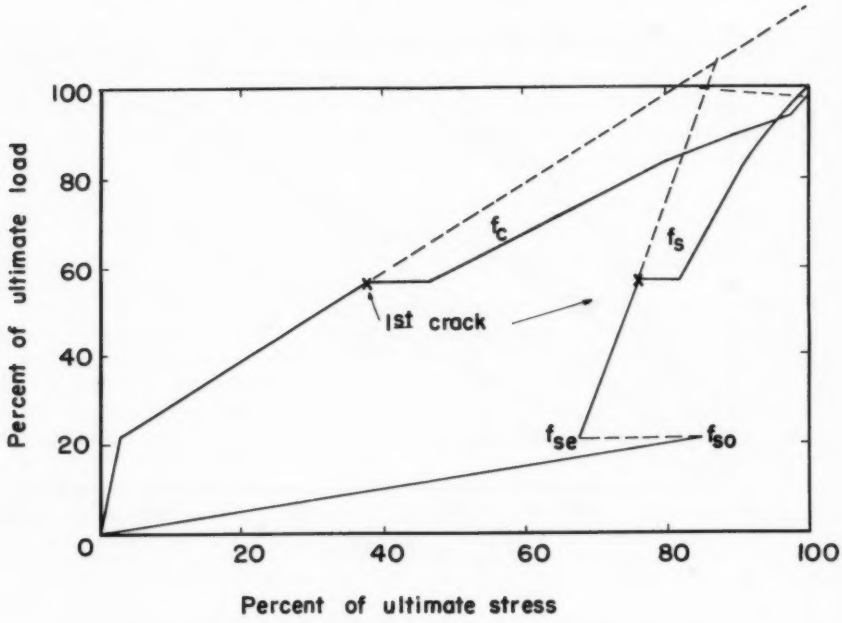

FIG. 5.—PRESTRESSED BEAM, LOAD-STRESS RELATIONS

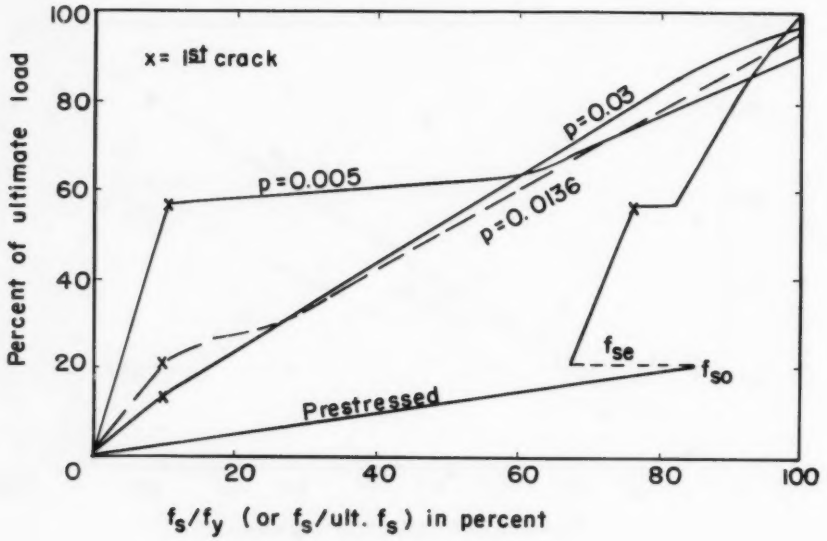

FIG. 6.—VARYING RELATIONSHIP BETWEEN f_s AND LOAD

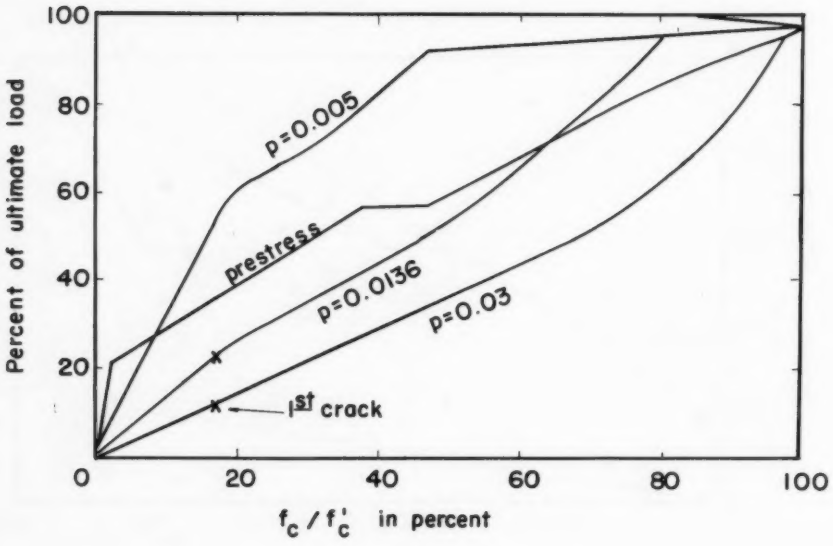

FIG. 7.—VARYING RELATIONSHIP BETWEEN f_c AND LOAD

Except to show the different curve shapes, the f_c curves for lower steel percentages in Fig. 7 have little meaning, because failures are in tension, as was shown in Fig. 6. It should be noted, however, that whether initial weakness is in compression or in tension, the final failure is always a crushing in compression. This is a key point in ultimate strength analysis. The extreme fiber stress is always less at failure than at slightly smaller loads, with the f'_c stress existing well inside the beam and the lower stress corresponding to the maximum strain (Fig. 1) at the extreme fiber.

One must conclude that working load and working stress patterns mask rather than point out the true ultimate load capacity. There are too many different shapes the load-stress curve can take. In extreme cases it can even point toward added compression steel in a situation in which only tension steel can add strength. This also suggests that the factors of safety under fixed allowable working stresses must vary considerably.

Consistent design thus almost demands analysis based on ultimate strength.

LOAD FACTORS

Although ultimate strength analysis is able to predict ultimate strengths rather closely, it introduces a new problem for the designer. Under working stress methods, committees from time to time have set up allowable working stresses that were assumed to give adequate factors of safety. Under ultimate strength design the designer must select proper load factors (or factors of safety).

Some load factors may ultimately be spelled out in codes, as is now the case in the ACI Building Code Appendix.[3] However, just as allowable stresses alone have never provided adequate protection in the case of a cantilever retaining wall (overloads are always considered), in like fashion no rigid set of load factors may really fit a novel design situation. For example, a load factor must increase the dead load to be carried by a beam, but, when the dead load acts as a stabilizing force on a retaining wall, the load factor should reduce it.

Much thought is currently going into the choice of proper load factors, and there are many variations in ideas presented. A few of these will be discussed briefly because the designer of the future will be under the necessity of understanding load factors in some detail.

Probability Theory for Load Factors.—A corollary of the need for understanding load factors is the need for understanding probability theory, at least in simple form. Consider a histogram of compressive cylinder strengths, that is, a plot of the number of specimens yielding each strength, as in Fig. 8 (taken from another publication.[4]) If there are a large number of specimens, the ordinates will form a curve that at least approximates a high point at the average or mean cylinder strength and that shows a series of decreasing numbers of specimens for both higher and lower values of strength. This curve is often approximated by the Gaussian (bell shaped) curve used in probability theory, as shown in Fig. 8.

---

[3] "Building Code Requirements for Reinforced Concrete (ACI 318-56)," an ACI Standard.

[4] "Recommended Practice for Evaluation of Compression Test Results of Field Concrete (ACI 214-57)," an ACI Standard.

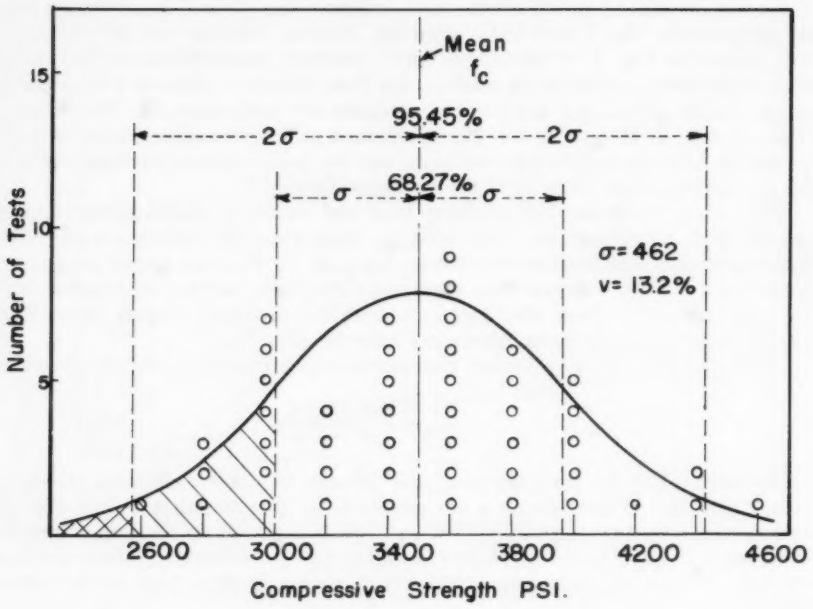

FIG. 8.—NORMAL FREQUENCY DISTRIBUTION OF STRENGTH DATA FROM 46 TESTS

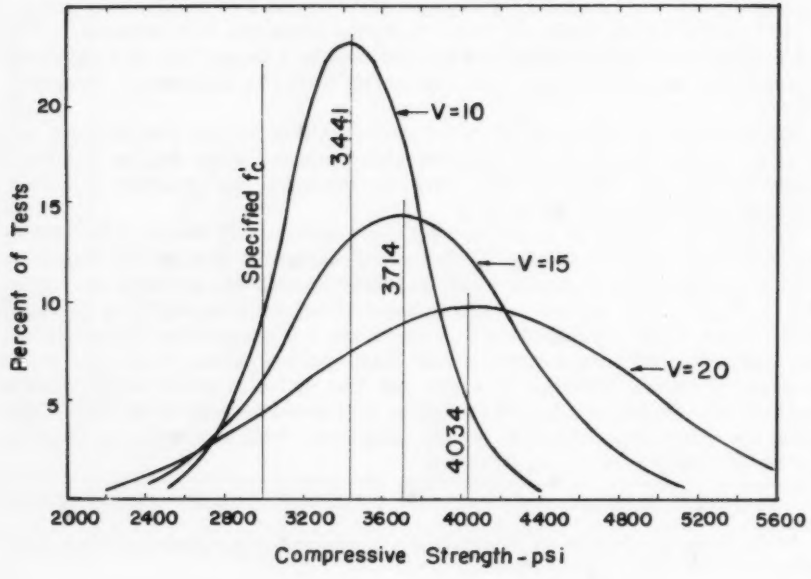

FIG. 9.—REQUIRED MEAN f_c FOR f'_c = 3000 psi

Another convenient concept used in probability theory is the standard deviation σ, defined as

$$\sigma = \frac{\Sigma (m - f'_c)^2}{N} \quad \ldots\ldots\ldots\ldots\ldots\ldots\ldots (1)$$

in which m is the mean (average) value of f'_c, $m - f'_c$ represents the difference between a given sample and the mean, and N is the number of samples. Possibly, a clearer way to visualize the standard deviation (in the case of a true Gaussian distribution) is to say it is the spread in values between the mean

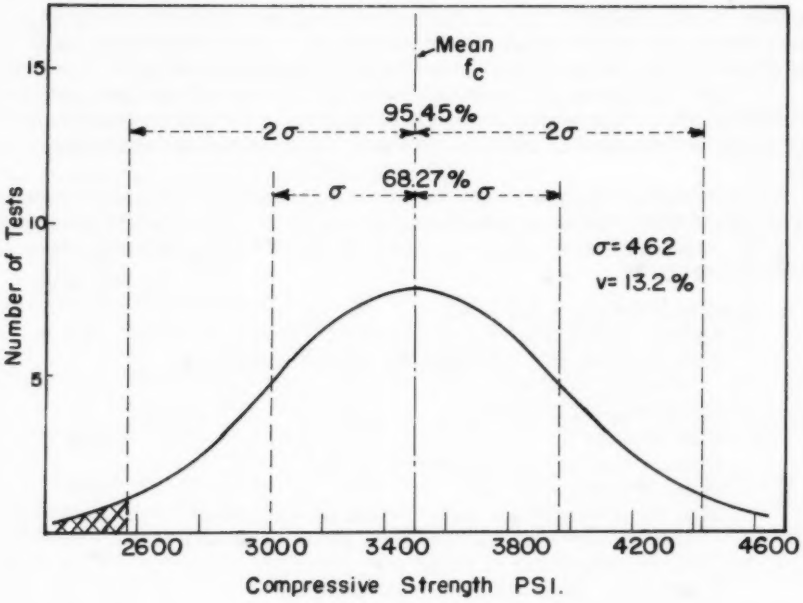

FIG. 10.—DESIGN STRENGTH RECOMMENDED BY BAKER

and the value that leaves below this range approximately 16% of the total specimens, as shown shaded in Fig. 8. If one goes 2 σ from the mean, the shaded area reduces to approximately 2.2% of the specimens as shown cross-hatched in Fig. 8 and 10. The shaded area measures the probability of a specimen having a strength less than the value at the limiting ordinate.

Well-controlled concrete will have a small standard deviation and a poorly-controlled concrete a large standard deviation. Both conditions are shown in Fig. 9 (from another publication[4], prepared to show the mean cylinder strengths required to give an f'_c of 3000 psi in accordance with the ACI Code requirement for ultimate strength design. This code requires that not more than one cylinder in ten may fall below the specified f'_c. Fig. 9 also shows a further probability term, called the variance and noted as V. The variance is

simply the standard deviation expressed as a percentage of the mean strength instead of as a range in psi (for an f'_c frequency curve). The larger V becomes, the higher must be the average f_c to secure a dependable given strength.

Baker's Factors of Safety.—Several years ago A. L. L. Baker, of England, proposed a system of factors of safety that involve both load factor and probability theory.[5] Two separate elements enter into his system, a reliable material strength and a separate factor of safety or load factor.

His discussion on reliable material strength relates primarily to concrete strength. He suggests that the assumed dependable cube strength be taken as the mean strength (of a large number of specimens) reduced by two standard deviations, as shown in Fig. 10. (For the normal Gaussian distribution, one standard deviation deduction would correspond to a 15.9% chance of smaller values; two standard deviations to a 2.2% chance of smaller values.) There is then only a 2.2% (or one in forty-five) chance that lower strengths will exist (assuming thet strengths vary according to the symmetrical Gaussian distribution.) He states that the two-standard -deviation reduction should not exceed 1500 psi "when the most efficient control is used" and 2000 psi for a medium control. This material specification is considerably stricter than the ACI Code definition of f'_c cylinder strength, as discussed in connnection with Fig. 9.

For his factor of safety (or load factor) Baker suggests values ranging from 1.25 to 2.00. These are established by adding to unity a weighted quantity ($\Sigma W/10$) representing six factors, some of which have indicated ranges as noted numerically:

	Example
1. Results of failure - 1.0 to 4.0	
Serious, either human or economic	4.0
Less serious, only the exposure of non-damageable material ----1.0	
2. Workmanship - 0.5 to 2.0	
Cast in place	2.0
Precast "factory manufactured" ---0.5	
3. Load conditions - 1.0 to 2.0	2.0
High for simple spans and overload possibilities; low for load combinations such as live load and wind	
4. Importance of member in structure	0.5
Beams may use lower value than columns	
5. Warning of failure	1.0
6. Depreciation of strength	0.5
Total = ΣW =	10.0

The numbers in the right hand column are suggested by Baker for the frame of an apartment building on good ground in an area in which workmanship and inspection are reliable. The column total is divided by 10 and added to unity to obtain his recommended factor of safety:

$$F = 1.0 + \Sigma W/10 = 1.0 + 10/10 = 2.0$$

---

[5] "The Ultimate-Load Theory Applied to the Design of Reinforced and Prestressed Concrete Frames," by A. L. L. Baker, Concrete Publications, London, 1956.

Torroja's Load Factors.—In 1957, Eduardo Torroja, as chairman of the International Council for Building Research, presented a report that (abstracted elsewhere[6] had for its opening statement:

Safety calculations should fix a satisfactorily low upper limit to the probability of collapse and (should) achieve a minimum value (total cost) for the (initial) cost of construction, the maintenance cost during the useful life, (and) the cost of a hypothetical insurance policy to cover accident risks, material losses, and possible loss of human life, (all) with consideration to possible criticism of public opinion and similar factors of a psychological nature. (Terms in parenthesis added by this author.)

This report carefully lists the possible errors in data used in design including: the size of loads, the way they are applied, and the way the structure is analyzed by the engineer; the actual strength of the materials used and any decrease in strength with time; variations in the quality of workmanship and the strictness of control; the permissible probability of failure; and the ductile or brittle failure behavior of the members as designed.

There is a strong position taken in favor of using a statistical or probability approach to safety, (1) reducing the assumed strength of materials, and (2) increasing the assumed working loads.

For materials, it is interesting to note that this report[6] suggests the use of a basic design strength computated as the mean strength reduced by the factor $(1 - \sigma)$ and further lowered by dividing this reduced strength by a factor of 1.5 to 1.6 for concrete or 1.15 to 1.20 for steel. The term σ is the standard deviation for the material.

With strengths so reduced, loads are to be multiplied by a basic factor of 1.25 that, in turn, is multiplied by other factors to represent less than ideal conditions. For example, with only average design and construction accuracy the factor becomes 1.65, with 15% more to be added if there is a very serious risk of danger in case of failure, as for a theatre, or a dam in a highly-populated area.

ACI Code on Load Factors.—American feeling on load factors seems to be developing along lines related to the above two plans, at least in the sense that reductions in nominal material strengths seem necessary (below those used to date). Also, increases above service loads are obviously essential. In addition, the original ACI Code Appendix provided different load factors for dead and live load. There is every evidence that the next ACI Code will continue this differentiation between dead and live load factors although probably in different fashion from the present code. Some differences should be expected, in that the present code uses only one combined factor to cover both material deficiencies and overload possibilities, whereas the next code will attempt to treat the two separately.

Another important variable to consider is construction accuracy. How should the designer allow for a vertical displacement of moment steel? One-quarter in. difference in a 3-in. slab is a large difference, and in a 24-in. beam is nearly negligible.

---

6 "Load Factors," by Edvardo Torroja, ACI Proceedings Paper No. 55, November, 1958, p. 567.

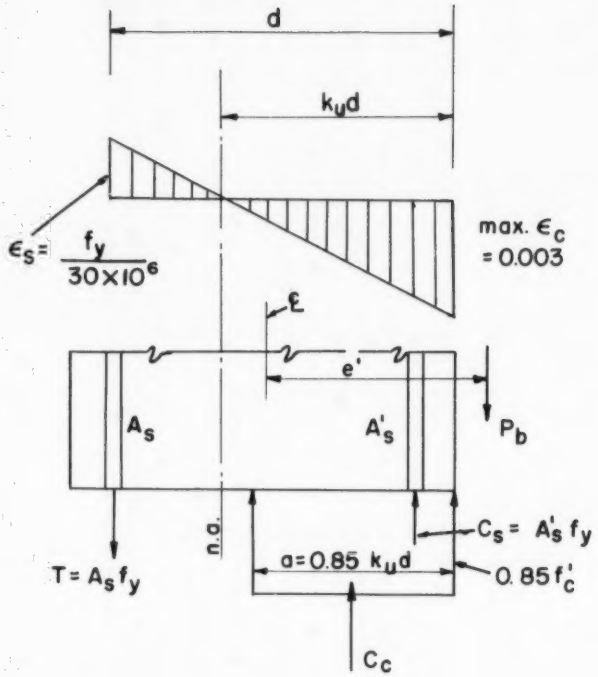

FIG. 11.—STRAINS AND LOADS FOR BALANCED COLUMN

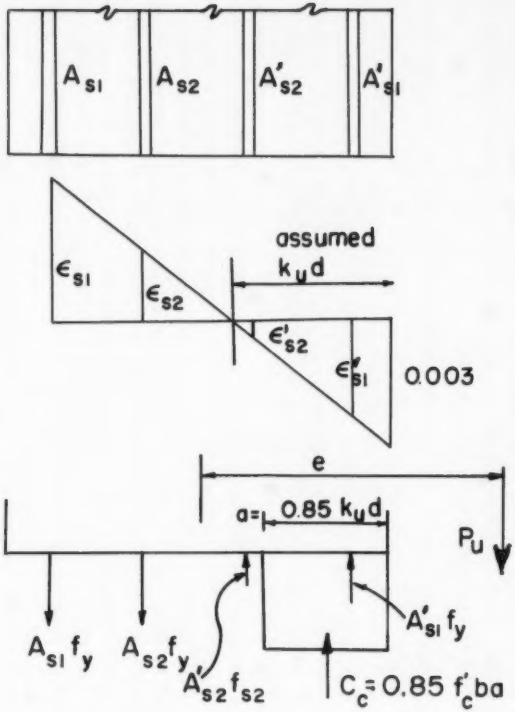

FIG. 12.—LOAD FOR AN ASSUMED NEUTRAL AXIS

Serious studies of load factors and related conditions are now being made by the ACI Code Committee in an attempt to limit the probability of failure in a sound statistical fashion.

STRAINS

Early discussion of ultimate strength theory, by Whitney, gave consideration to unit strains as a part of his explanation, but not as part of his method. The Joint ASCE-ACI Committee introduced the strain idea into the balanced column load P_b, using the strain triangles of Fig. 11 to establish the neutral axis depth.

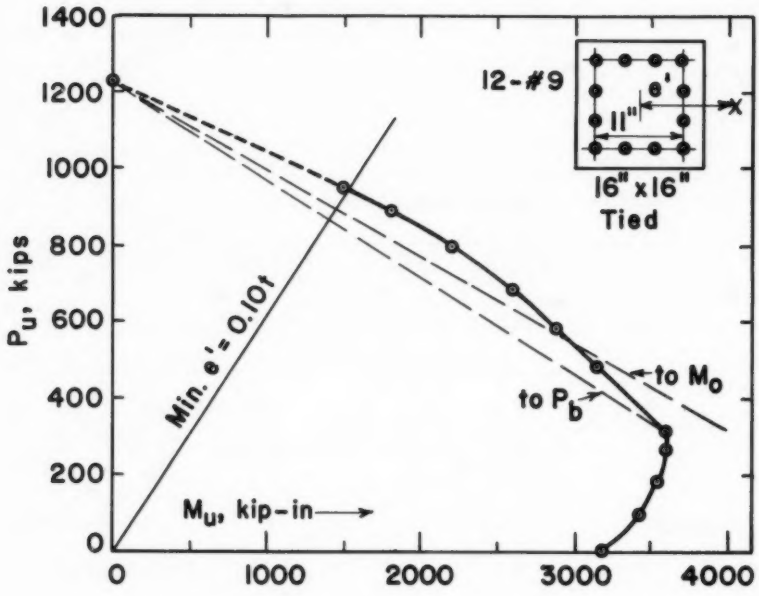

FIG. 13.—INTERACTION DIAGRAM, STEEL ALL FOUR SIDES

In effect, the rectangular stress block was taken with stress intensity of 0.85 f'_c and with depth $a = 0.85\ k_u\ d$ (for f'_c up to 5000 psi). Later experimental work, still unpublished, seems to confirm the fact that the depth of stress block can be taken as $0.85\ k_u\ d$, probably with some reduction for f'_c values greater than 4000 psi. This gives a most convenient relationship between strains and load.

Starting with an assumed neutral axis and an ultimate concrete strain of 0.003 in. per in. (as suggested by the ACI Building Code), it is very easy to establish the ultimate load and eccentricity for a column with steel in any arrangement, as in Fig. 12. One simply evaluates the strains (and thereby the stresses and loads) on each set of bars and the resultant compression on the concrete. The applied load must be equal and opposite to the resultant of these

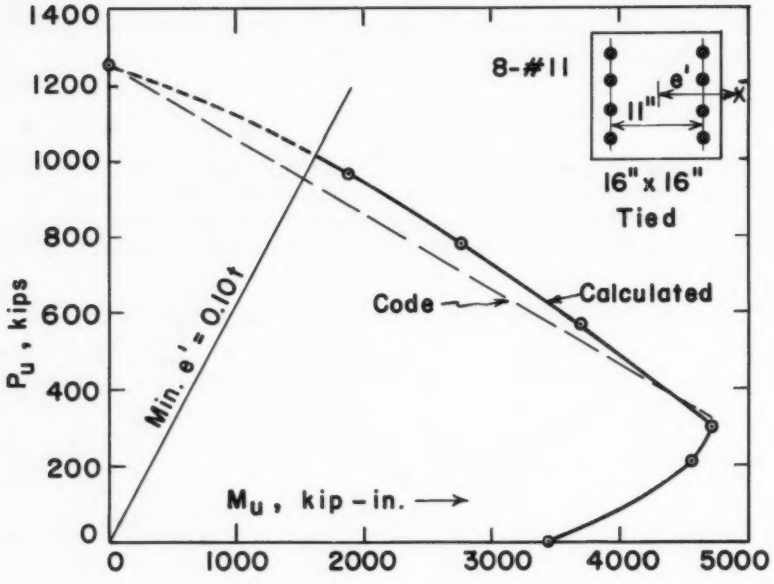

FIG. 14.—INTERACTION DIAGRAM FOR TIED COLUMN

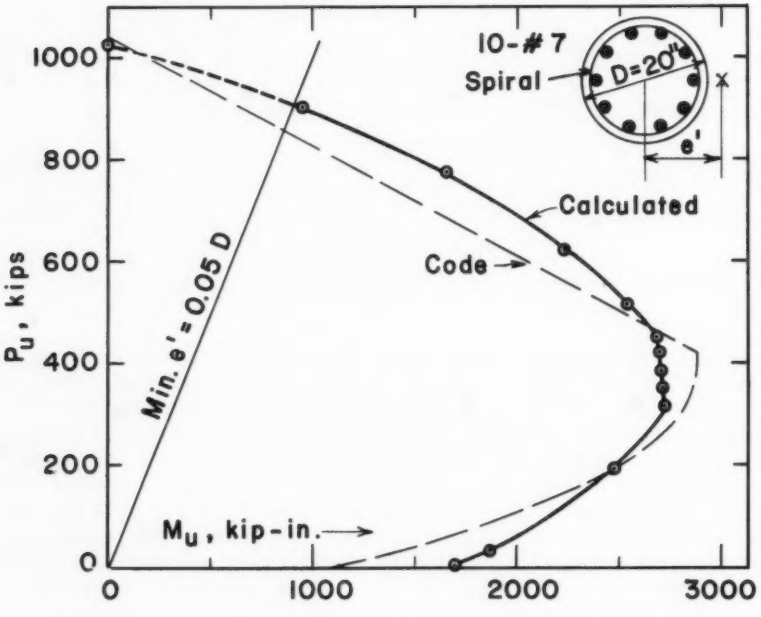

FIG. 15.—INTERACTION DIAGRAM FOR CIRCULAR COLUMN

internal forces, a simple problem in statics. With more research, the constants used may need some modification, but the method is simple and general. Figs. 13, 14, and 15 show column interaction diagrams prepared in this way, compared to approximate solutions for the same cases.

Recently the writer had a research test beam that failed in flexural compression, but that by conventional ultimate strength analysis seemed to be adequately designed for more than the attained load. This beam used high strength steel (nominal yield strength of 75 ksi) with no sharp yield point and a gradually curving stress strain curve in the upper stress level. The steel strain was large because of the large stress and larger still because of the shape of the stress-strain curve. Present design rules are not adapted to this magnitude of yield strength or yield strain. (The ACI Code limits f_y to not over 60 ksi for beams) The basic strain procedure described previously for columns explained the observed beam weakness quite logically.

CONCLUSION

It appears that ultimate strength theory must develop more into a strain theory in establishing steel stresses, at the same time taking advantage of the simple stress block concept in moving from strains to ultimate stresses and loads on concrete.

In this sense possibly one can talk of load-stress relationships, but this is a far cry from the earlier meaning of that phrase. Ultimate strength design must by its very nature develop at least semi-empirically. It bodes well for future use in new situations that it does appear to yield to a logical development from strain relationships.

Journal of the
STRUCTURAL DIVISION
Proceedings of the American Society of Civil Engineers

MOMENT-DISTRIBUTION CONSTANTS FROM CARDBOARD ANALOGS

By Otakar Ondra,[1] F. ASCE

SYNOPSIS

An experimental method of determining moment-distribution and slope-deflection constants for beams with variable moments of inertia is proposed. Simple graphics, especially evolved for the purpose at hand, are used to lay out cardboard templates whose ordinates, areas, and their centroidal distances represent significant parameters of the constants sought. Template areas are evaluated and their centroids are located experimentally. This is equivalent, respectively, to numerical integration and division of one integrated function by another. Thus, the experimental part of the method serves as a mechanical analog. The method is simple, rapid, and sufficiently accurate for office use.

BACKGROUND

The author has previously presented a semi-experimental method[2] of determining the moment-distribution constants for beams with variable moments of inertia. Basically, the method consists of finding several significant parameters of the 1/E I-diagram by weighing three-dimensional 1/E I- and M/E I-solids. Inasmuch as the weighing operations are equivalent to numerical integration, the method is essentially a mechanical analog.

Note.—Discussion open until June 1, 1961. To extend the closing date one month, a written request must be filed with the Executive Secretary, ASCE. This paper is part of the copyrighted Journal of the Structural Division, Proceedings of the American Society of Civil Engineers, Vol. 87, No. ST 1, January, 1961.

[1] Prof. of Civ. Engrg., Manhattan College, New York, N. Y.

[2] "Moment Distribution Constants from Models," by Otakar Ondra, Transactions, Vol. 123, 1958, p. 318.

Perhaps the most interesting aspect of the method is that it affords a means of visualizing the effects of moment of inertia variation upon the factors prerequisite for carrying out moment-distribution or slope-deflection computations. Admittedly, the preparation of the three-dimensional solids and their weighing require certain materials, tools, and instruments which are generally unavailable in an engineering office. In addition to wood, a saw, a weighing scale, etc., the engineer must possess the necessary manual skills to perform the various required operations.

The purpose of this paper is to propose a much simpler method wherein three-dimensional work is reduced to work in a plane. Cardboard and scissors are used instead of wood and saw, and weighing is eliminated. Ratios of integrals or algebraic sums are evaluated experimentally by locating centroids of cardboard templates, readily constructed with the aid of graphics. Because neither special instruments nor skills are required, the new method offers definite possibilities as a useful tool of analysis.

Notation.—The letter symbols adopted for use in this paper are defined where they first appear, in the illustrations or in the text, and are arranged alphabetically, for convenience of reference, in the Appendix.

CARRY-OVER FACTOR

By definition, the carry-over factor of a flexural member is the ratio of the moment induced at the fixed end of the member to the moment causing rotation at the other simply-supported end. In Fig. 1(a), the beam simply supported at a and fixed-ended at b is subjected to a moment M_a at a, causing moment $C_{ab}M_a$ at b in which C_{ab} is the carry-over factor from a to b.

Fig. 1(b) shows a prismatic beam whose depth, d, changes from one value to another. Fig. 1(c) shows the relative E I-values and Fig. 1(d) is the 1/E I-diagram. Area A in Fig. 1(d) is defined as $A = \int_0^L \frac{dx}{EI}$.

It has been shown[2] that the carry-over factor from a to b may be computed from the formula

$$C_{ab} = \frac{Q_a}{J_a} L - 1 \quad \ldots\ldots\ldots\ldots\ldots\ldots (1)$$

in which Q_a is the first (statical) moment of area A taken about the vertical axis through a, and J_a is the second moment of A about the same axis, Fig. 1(d) (the designation "second moment" is preferable to "moment of inertia" to avoid confusion with "I").

Figs. 2(a), 2(b), and 2(c) represent the elevation, top, and pictorial views, respectively, of a solid. Its base is the 1/E I-diagram of the stepped beam in Fig. 1. The plane upper surface of the solid is inclined at an angle γ from the base.

Quantity Q_a used in Eq. 1 may be interpreted either as

$$Q_a = \int_0^L (\frac{1}{EI}\, dx)\, x \quad \ldots\ldots\ldots\ldots\ldots\ldots (2)$$

which is the first moment of area A about a in Fig. 2(b), or as

$$Q_a = \frac{1}{k}\int_0^L \left(\frac{1}{EI}\, kx\right) dx = \frac{1}{k}\int dV = \frac{1}{k}\, V \quad \ldots\ldots\ldots (3)$$

which is (1/k)-times the volume, V, of the solid shown in Fig. 2(c).

Similarly, the expression

$$J_a = \int_0^L \left(\frac{1}{EI}\, dx\right) x^2 \quad \ldots\ldots\ldots\ldots\ldots (4)$$

is the second moment of area A about a in Fig. 2(b), and it is also

$$J_a = \frac{1}{k}\int_0^L \left(\frac{1}{EI}\, kx\, dx\right) x = \frac{1}{k}\, V\, \bar{x} \quad \ldots\ldots\ldots\ldots (5)$$

which is (1/k)-times the first moment of volume V about a in Fig. 2(c). The latter may be expressed as $V\,\bar{x}$ in which $\bar{x}$ is the distance of the centroid of volume V referred to a. If the specific weight of the solid is uniform, $\bar{x}$ is also the distance of the resultant body-force, W, that is, the distance of the center of gravity, from a.

Using the meaning of Q_a and J_a as defined by Eqs. 3 and 5, the ratio Q_a/J_a in Eq. 1 is equivalent to $1/\bar{x}$. By fashioning the solid shown in Fig. 2(c) and its appropriate weighing as has been described,[2] distance $\bar{x}$ may be determined and substituted into Eq. 1.

$$C_{ab} = \frac{Q_a}{J_a}\, L - 1 = \frac{\frac{1}{k}\, V}{\frac{1}{k}\, V\, \bar{x}}\, L - 1 = \frac{L}{\bar{x}} - 1 \quad \ldots\ldots\ldots (6)$$

THE TWO-DIMENSIONAL ANALOG

Fig. 3(a) shows factors 1/E I and k x of the integrand in Eq. 3 juxtaposed in one plane. If the product of each pair of colinear ordinates is effected, (1/E I) (k x), laid off in Fig. 3(b) as ordinate and connected by a line, the plane area bounded by the latter and the axis a-b is equivalent to the volume V in Fig. 2(c) and in Eqs. 3 and 5. It follows that the body-force distance, $\bar{x}$, in Fig. 2(c) is the same as the centroidal distance of the area in Fig. 3(b).

The distance $\bar{x}$ may be determined experimentally by making a cardboard template of the area in Fig. 3(b) and locating its centroid. This is readily accomplished by balancing the template on a knife-edge, or more accurately by suspending it on two non-colinear strings as in the familiar experiment of elementary mechanics. The transformation of the solid into a two-dimensional area of identical equilibrity is the principle of the simplified method.

If preferred, the relation between the carry-over factor, C_{ab}, and the geometric parameters L and $\bar{x}$ of area V in Fig. 3(b) may be derived more readily by direct methods. For example, in an earlier paper of the author's,[2] previously referred to, his Fig. 1 gives the derivation using external work equations and the conjugate-beam method. Clearly, area V in Fig. 3(b) of the present

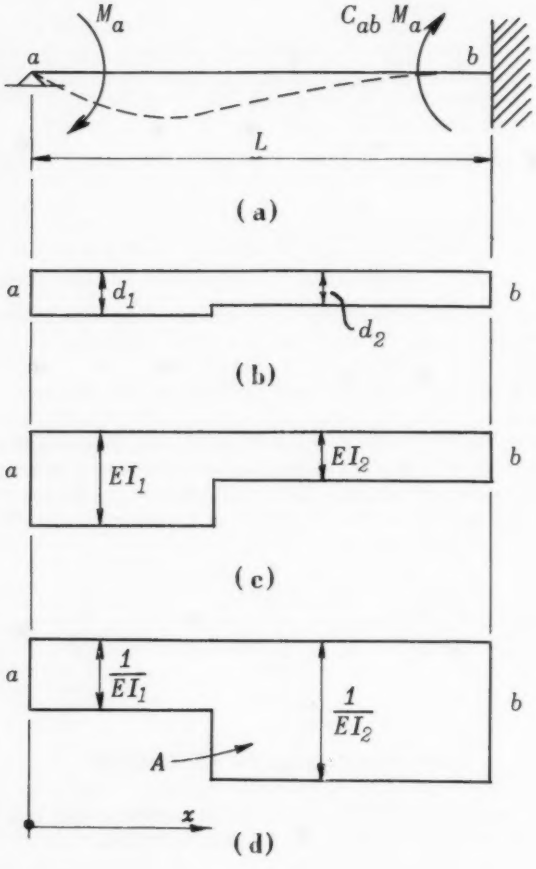

FIG. 1

paper is the load on the conjugate beam for the real beam in the earlier Fig. 1(d). It follows that the ratio of the conjugate-beam reactions, and hence the location of the centroid of V, determine the carry-over factor.

GRAPHIC MULTIPLICATION

The multiplication of ordinates 1/E I by the corresponding ordinates k x may be performed numerically. Inasmuch as the products must be laid out in

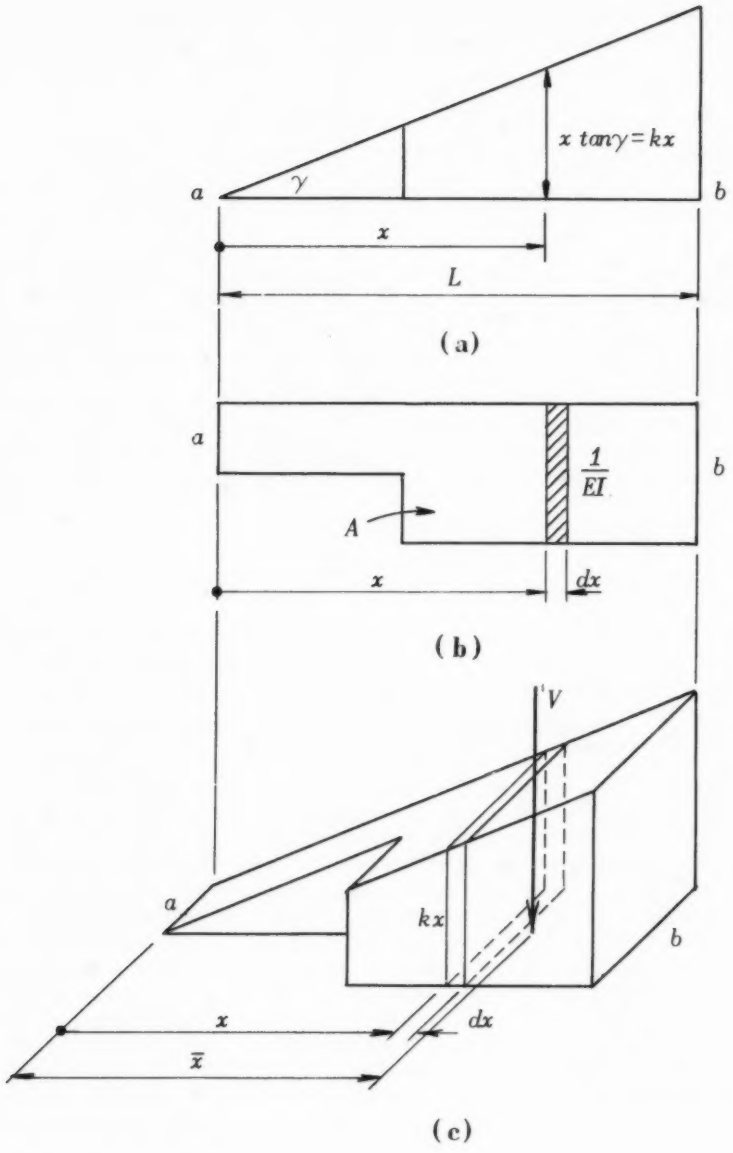

FIG. 2.—VARIOUS VIEWS OF A SOLID

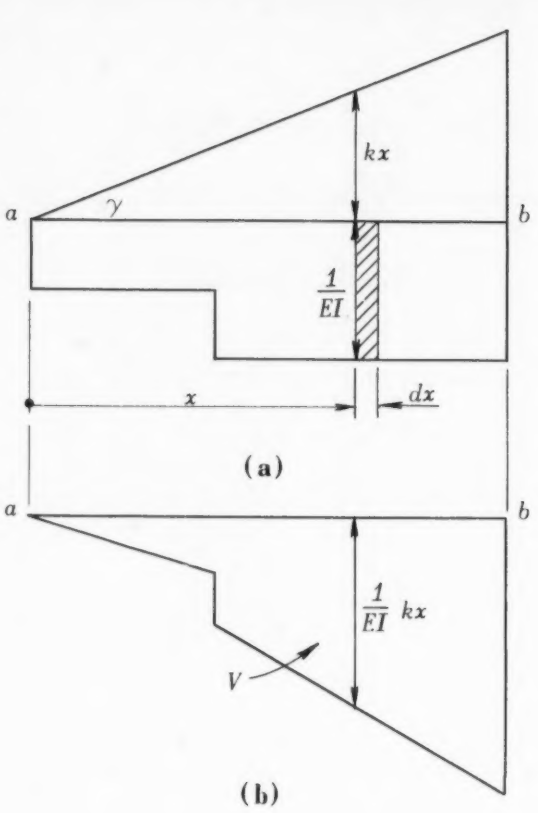

FIG. 3

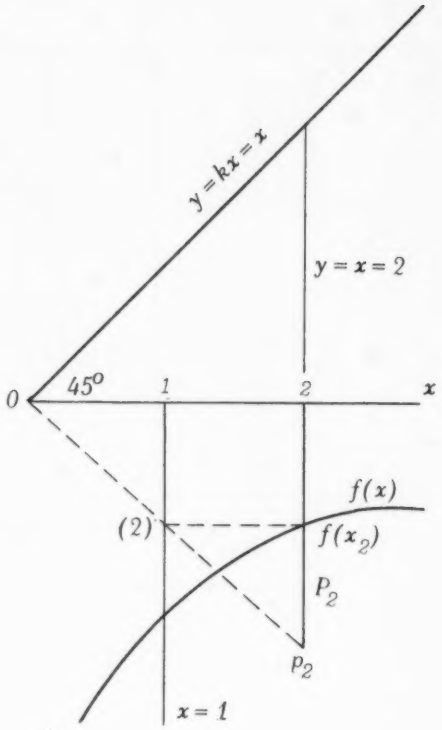

FIG. 4

order to make the cardboard template, both tasks may be conveniently and rapidly accomplished in a single graphic operation.

Graphic multiplication is based on the geometry of similar triangles. In Fig. 4, x is the axis of abscissae, and functions $f(x)$ and $y = k\,x = x$ are as shown. To multiply $f(x_2)$ $(k\,x_2)$, set

$$f(x_2) \quad kx_2 = P_2 \quad \ldots\ldots\ldots\ldots\ldots\ldots (7)$$

or

$$\frac{f(x_2)}{1} = \frac{\frac{1}{k}\,P_2}{x_2} \quad \ldots\ldots\ldots\ldots\ldots\ldots (8)$$

in which the divisor on the left, 1, is a unit of x. If $f(x_2)$ is projected horizontally into 2 on the vertical line $x = 1$, the ray drawn through the origin, 0, and 2 and extended to the vertical at x_2 determines $(1/k)P_2 = \overline{2\,p_2}$.

In Fig. 5 the graphic multiplication is carried out for eight subsequent abscissae x. The manner in which the line $P = f(x)$ $x = F(x)$ is obtained is illustrated for x-values of 2 and 5. The ordinates of P are drawn full-scale, that is, they are read on the same scale as was used to plot the ordinates $f(x)$. However, the scale of the P-ordinates may be controlled as desired, for example, if P is to be obtained to the one-quarter scale, Eq. 7 may be written in the form

$$\frac{f(x_2)}{4} = \frac{\frac{1}{4}\,P_2}{x_2} \quad \ldots\ldots\ldots\ldots\ldots\ldots (9)$$

in which 1/4 is the scale factor. Values of $f(x)$ are projected on the vertical $x = 4$ and rays connecting the origin and the projections, extended, are drawn as is shown for x-values of 3 and 8. The ordinates of the line so constructed, $\frac{P}{4} = \frac{1}{4}\,F(x)$, are the P-ordinates to the one-quarter scale.

To multiply $f(x)$ $(k\,x)$, a comparison of Eqs. 7, 8, and 9 shows that k may be interpreted as a scale factor of the P-ordinates. However, it is significant to note that the abscissa of the centroid, $\bar{x}$, of the area under the P-line is independent of the value of k and any other scale factor (Eq. 6). Consequently any suitable scale factor may be chosen for P, for the experimental purpose herein considered the scale factor need not be taken into account. In practice the choice of the scale is governed by the desirable graphic magnitude of the maximum P-ordinate. In general, this will occur at some fairly high x-value coupled with a large value of 1/E I. A cursory graphic multiplication for one or two such tentative x-values will ascertain the scale factor necessary in order to confine the plot to a desirable size.

The graphic procedure may be further simplified by noting that it is actually unnecessary to plot the line $1/E\,I = f(x)$. Values of $f(x)$ may be plotted directly on the vertical $x = 1$ (or any other vertical if a scale factor is used) and appropriately labeled. Rays are subsequently drawn from the origin through the latter and the P-values are found as before.

GRAPHIC DIVISION

The variation of 1/E I or 1/I values, absolute, or relative, fundamentally affects each of the moment-distribution constants. In standard methods of anal-

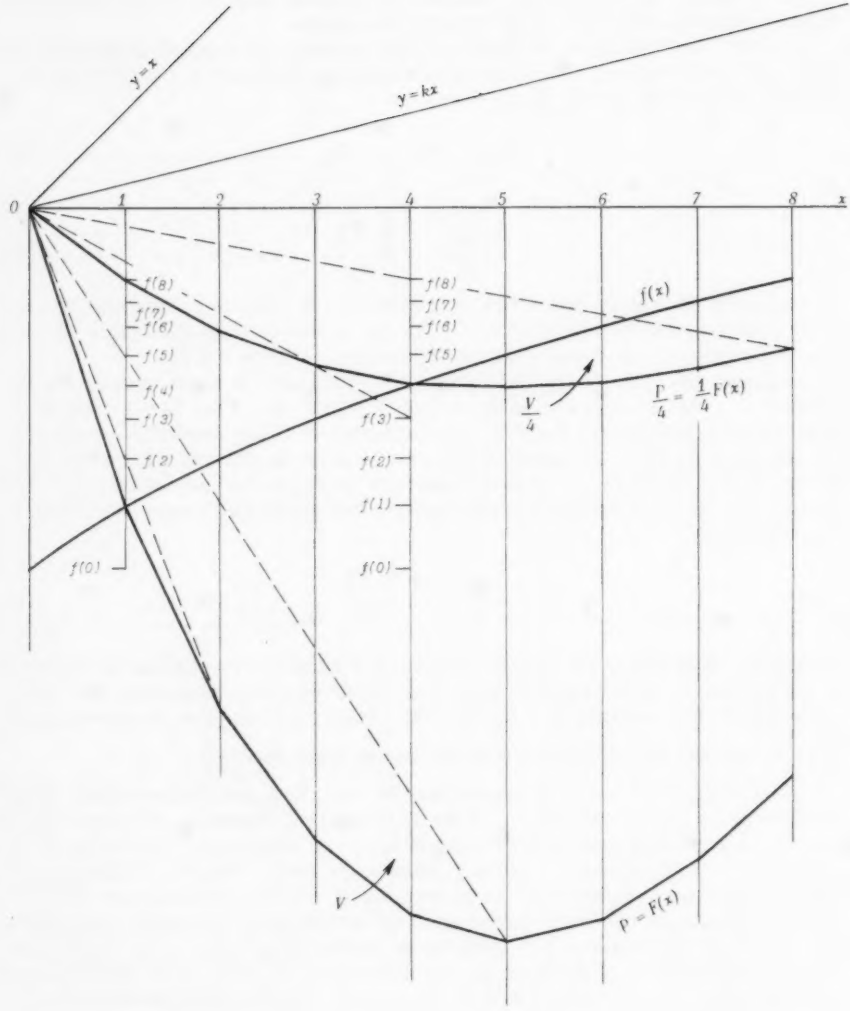

FIG. 5

ysis, values of I and their reciprocals, 1/I, must be computed, then tabulated or plotted, and several properties of the analytic function $1/I = f(x)$ or its geometric diagram are evaluated. It will be shown subsequently that for the purposes considered herein, it is not necessary to compute the reciprocals of the I-values. The I-diagram or the I-values may be used directly as the basis for the graphic construction of the cardboard template. This saves time and minimizes the possibility of numerical error.

To divide values of x by the corresponding values of $I = \phi(x)$, set

$$\frac{x}{\phi(x)} = R \quad \ldots\ldots\ldots\ldots\ldots\ldots \quad (10)$$

and rewrite in the form

$$\frac{x}{R} = \frac{\phi(x)}{1} \quad \ldots\ldots\ldots\ldots\ldots\ldots \quad (11)$$

in which 1 is a unit of $\phi(x)$.

In Fig. 6, bisect the right angle between coordinate axes x and I, and draw the horizontal line I = 1. The construction of Eq. 11 is illustrated for values $x_2 = 2$ and $I_2 = \phi(x_2)$. Project $\phi(x_2)$ horizontally into 2 located on the bisector, hence vertically into [2] located on the line I = 1. Through the origin, 0, of the coordinate axes, draw ray 0-[2] and extend the same to its intersection with the vertical line through x = 2. Point r_2 marks off $R = \overline{2\ r}$ inasmuch as the relationship

$$\frac{2}{R_2} = \frac{\phi(x_2)}{1} \quad \ldots\ldots\ldots\ldots\ldots\ldots \quad (12)$$

which is evident in Fig. 6, satisfies Eq. 11.

The purpose of the bisector in Fig. 6 is to effect graphically the inversion of the I-ordinates into abscissae of the horizontal axis through I = 1. Consequently, the I-diagram and the bisector need not be drawn. The I-values corresponding to values of x may be laid off directly along the line I = 1 and labeled for identification as bracketed values of abscissae x to which they correspond. The rest of the construction remains the same as in Fig. 6.

This simplified graphic procedure is illustrated in Fig. 7 in which a beam with a parabolic intrados and a constant-depth haunch is chosen as an example.

The equation of the intrados-referred to coordinate axes x_c, y_c through the crown point, c, and the depth, d, at any section of the beam are, respectively,

$$y_c = -\frac{x_c^2}{72} \quad \ldots\ldots\ldots\ldots\ldots\ldots \quad (13a)$$

and

$$d = 0.5 - y_c = \frac{36 + x_c^2}{72} \quad \ldots\ldots\ldots\ldots \quad (13b)$$

Depths and relative I-values were computed for sections a unit distance apart and recorded in the figure. A suitable scale is chosen for the I-values and the horizontal I-axis is drawn at the distance of I = 1 below origin 0. Values of I are laid off on that axis and labeled [0], [1], [2], and [3], etc., thus indicating x-values of 0, 1, 2, and 3, etc., with which they are associated. Rays drawn from the origin, 0, through points [1], [2], and [3], etc., intersect verticals at abscissae x = 1, 2, and 3, etc., at points r which determine the ratios $x/I = 1/I_1$, $2/I_2$, and $3/I_3$, etc. The segmented line connecting the thirteen points obtained in the foregoing manner is the line R = x/I. The dotted continuation of the R-line corresponds to the beam whose entire intrados is parabolic.

The scale used for plotting the I-values does not effect the direction of the rays drawn from the origin, 0. If the R-values are to be obtained to a reduced scale, say the one-half scale, either the ordinate I = 1 is halved and the I-scale kept as before, or the I-scale is doubled and the ordinate of the I-axis, I = 1, remains as before.

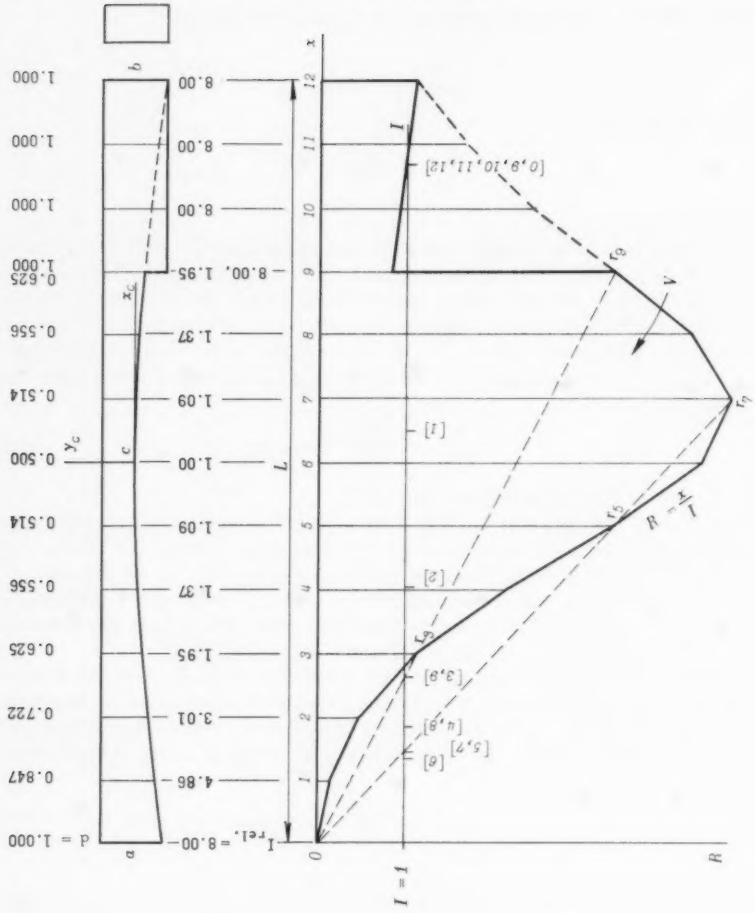
x
b
a
c
d = 1.000
y_c
x_c
L
$I_{rel.}$ = 8.00
I = 1
R
V
$R = \frac{V}{I}$
[0,9,10,11,12]
[1]
[2]
[3,8]
[4,8]
[5,7]
[6]
r_2
r_3
r_5
r_7
r_9
1.000
1.000
1.000
1.000
0.625
0.556
0.514
0.500
0.514
0.556
0.625
0.722
0.847
8.00
8.00
8.00
8.00, 1.95
1.37
1.09
1.00
1.09
1.37
1.95
3.01
4.86

FIG. 7

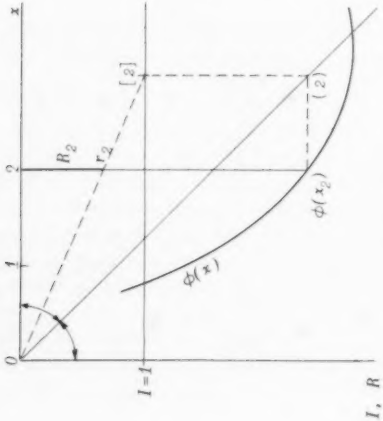
x
R_2
r_2
[2]
(2)
$\Phi(x_2)$
$\Phi(x)$
I = 1
I, R

FIG. 6

The graphic construction of the R-line from previously computed I-values should be done on a sheet of cardboard, bristol board, or similar paper of substantial but uniform thickness. The required template is obtained by cutting out the area bounded by the R-line and the x-axis. The centroid of the area can be accurately and rapidly located in the manner shown schematically in Fig. 8 and explained subsequently.

The template is hung on a pin or thumb tack, 1, passing freely through the paper and embedded in a smooth vertical surface. A weighted thread is wrapped around the pin. Care must be taken to avoid friction between the template and the pin, the vertical surface behind it, and the suspended thread. This can be checked by slightly displacing the suspended template to one side of its position of equilibrium, and when released, the template should oscillate freely.

The orientation of the taut vertical thread relative to the equilibrated template is marked by a dot anywhere along the thread, and the line 1-1 is drawn, connecting the dot and the pin hole. The same procedure is repeated using pin 2 placed at some different position with respect to the template and line 2-2 is obtained. Evidently, the point of intersection of lines 1-1 and 2-2 locates the center of gravity of the template. The accuracy may be checked with the aid of a third pin, 3, as is shown in the third diagram of Fig. 8.

Since the template is made of a material of essentially uniform specific gravity and thickness, the center of gravity also locates the centroid of the area. The centroidal distance, $\bar{x}$, is scaled off and its value substituted into Eq. 6. In the example under consideration, by actual measurement, $\bar{x}$ was found to be 0.555 L, so that Eq. 6 yields

$$C_{ab} = \frac{L}{\bar{x}} - 1 = \frac{L}{0.555L} - 1 = 0.80$$

By equivalent analytic computation based on subdividing the 1/I-diagram into twelve strips of equal lengths Δx and computing $Q_a = \Sigma\, x\, \Delta x/I$ and $J_a = (1/12)\Sigma(\Delta x)^3/I + \Sigma(\Delta x/I)x^2$, Eq. 1 yields

$$C_{ab} = \frac{Q_a}{J_a} L - 1 = \frac{261.48}{1{,}730.92} 12 - 1 = 0.81$$

It is worthwhile to note that the difference between the analytic and analog-results is less than 1.3%. The analog solution (that is, drawing, cutting, and balancing, etc., the template) required approximately 15 min of time. The numerical counterpart was accomplished in slightly less than 1 hr. The task of computing the I-values, which is common to both methods, was not timed. The analytic solution is approximate to the extent that finite differences rather than integration were used. The former approach is the standard method of determining carry-over factors for beams with continuously varying I. Since twelve strips were also used in the analog method, the two solutions have a common basis for the comparison of accuracy and time expended.

In general, aside from the small errors inherent to any graphic or experimental method of analysis, the accuracy of the analog method depends somewhat on the number of segments Δx used in obtaining the P- or R-lines. As this number is increased, the area under either line, $\sum_0^L (x\, \Delta x)/I$, approaches the correct value, $\int_0^L (x\, dx)/I$. It will be found by actual use of the method

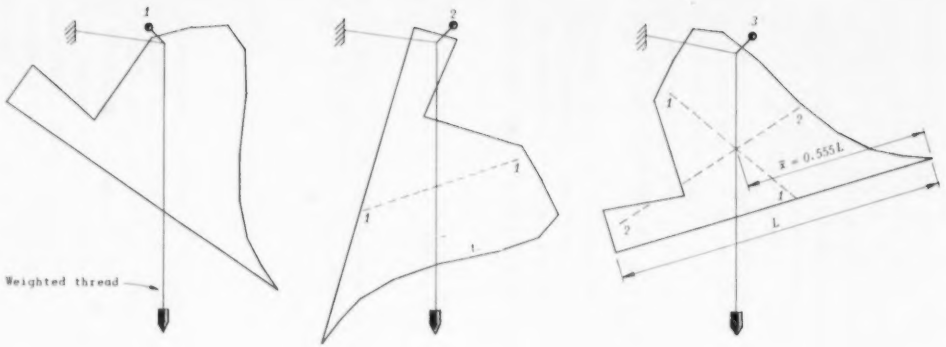
1
Weighted thread
2
1
1
1
3
1
2
$\bar{x} = 0.555L$
1
2
L

FIG. 8

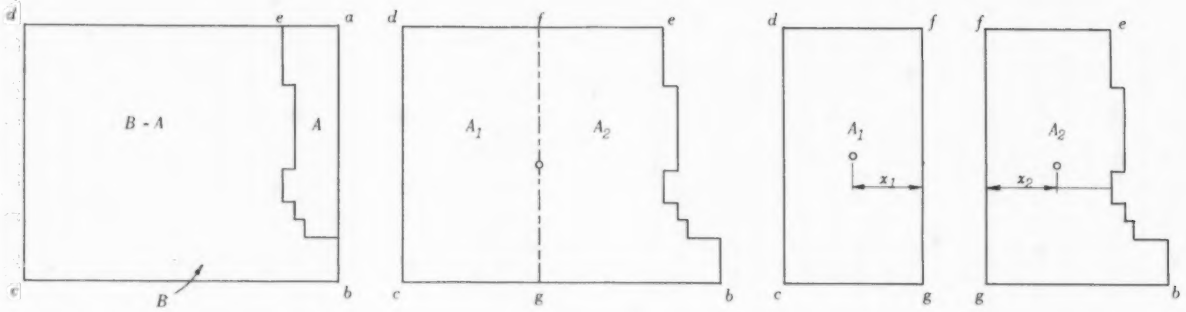
d
e
a
B - A
A
c
B
b
(a)
d
f
e
A_1
A_2
c
g
b
(b)
d
f
A_1
x_1
c
g
(c)
f
e
A_2
x_2
g
b
(d)

FIG. 10

that the graphic construction of the template is so simple and rapid that it hardly matters whether 10, 12, and 16 or more elements are used. Since the work of balancing the template is the same regardless of its make up, the degree of the controllable part of the accuracy depends on one's decision as to how many elements will be used. Obviously, this number should be larger for beams

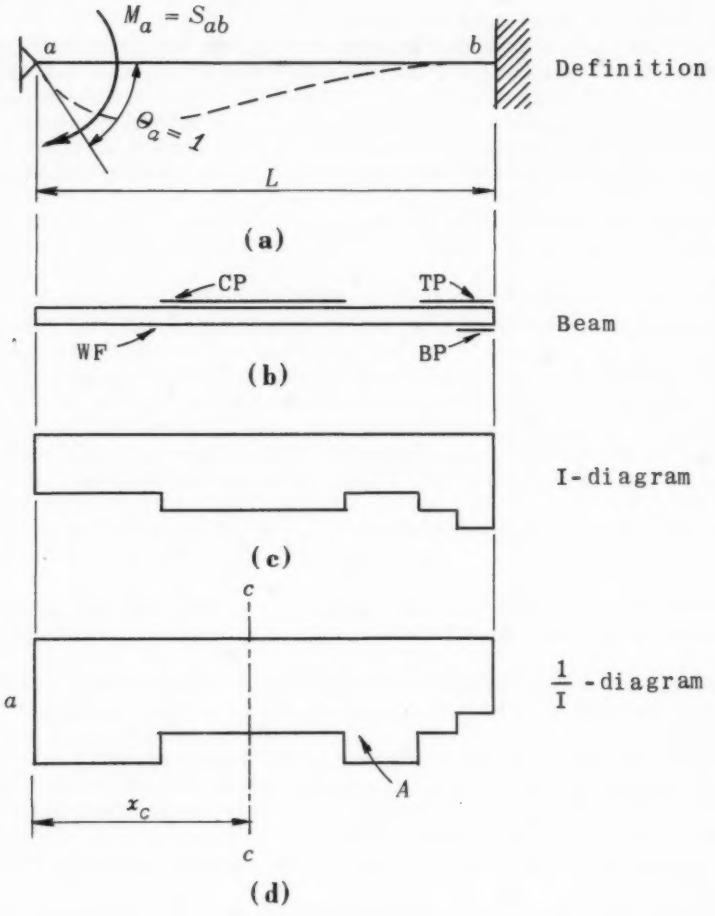

FIG. 9

with a rapidly changing depth. In practice, the task of computing I-values at closely spaced sections may be simplified by constructing the P- or R-line for larger intervals. The line is then replaced by a continuous curve drawn tangent to the segmented line.

In the case of stepped or cover-plated beams, the sole potential source of small errors lies in the graphic and experimental nature of the analog method.

STIFFNESS FACTOR

The stiffness factor, S, at the simply supported end of a flexural member is defined as the moment required to rotate that end through a unit angle while the other end is held fixed. In Fig. 9(a), M_a is S_{ab}, the stiffness factor at end a of the beam a-b, when θ_a is one radian.

In the Hardy Cross method of moment distribution,[3] an unbalanced moment acting on a joint is distributed among the members meeting at the joint in proportion to the distribution factors, $S_n/\Sigma S$, in which S_n is the stiffness factor at the joint-end of the member under consideration, and ΣS is the sum of the stiffness factors at the joint-end of the members framed into the joint.

It has been shown[2] that the stiffness factor may be computed from the formula

$$S_{ab} = \frac{1}{A - \frac{Q_a^2}{J_a}} \quad \ldots\ldots\ldots\ldots\ldots\ldots \quad (14)$$

The stiffness factor is absolute or relative depending on whether absolute or relative I-values are used in Eq. 14. It is observed that for the purposes of moment-distribution, computations relative S-values may be used.

The term Q_a^2/J_a in Eq. 14 may be written as $Q_a\,(Q_a/J_a)$, or, according to Eq. 6, $Q_a/\bar{x}$. But Q_a is the first moment of area A about a (Eq. 2), and may therefore be set equal to $A\,x_c$, in which x_c is the distance of the centroid of area A from a. Consequently, Eq. 14 may be written in the form

$$S_{ab} = \frac{1}{A - \frac{A\,x_c}{\bar{x}}} = \frac{\bar{x}}{A\,(\bar{x} - x_c)} \quad \ldots\ldots\ldots\ldots \quad (15)$$

Distance $\bar{x}$ appeared in Eq. 6 and its analog-evaluation has already been explained and illustrated. Quantities A and x_c may be found in the following manner.

Fig. 9(b) shows a WF beam with cover-plate CP, tie-plate TP, and bearing-plate BP. Relative I- and 1/I-diagrams are shown in Figs. 9(c) and 9(d), respectively.

Refer to the schematic diagrams in Fig. 10. Beginning with a rectangular sheet of cardboard, a-b-c-d, of area B square inches (say, 10.00 in by 8.00 in), Fig. 10(a), the 1/I-diagram is drawn to scale as is shown. Next, the template for area A is cut out with a razor blade. The centroid of A is located in the same manner as was done in Fig. 8, and the centroidal distance, x_c, Fig. 9(d), is scaled off.

Likewise, the centroid of template e-b-c-d of area (B - A) is found experimentally and the centroidal axis is drawn as is shown in Fig. 10(b) (dashed line f-g). Next, the template of Fig. 10(b) is cut into two parts, Figs. 10(c) and 10(d), and the areas of the parts are denoted by A_1 and A_2. The centroidal distance of A_1, x_1, is found by direct measurement; that of A_2, denoted by x_2, is found experimentally.

---

[3] "Analysis of Continuous Frames by Distributing Fixed-End Moments," by Hardy Cross, Transactions, ASCE, Vol. 96, 1932, p. 1.

Evidently, the following relationships hold in Fig. 10:

$$A_1 x_1 = A_2 x_2 = (B - A - A_1) x_2 \quad \ldots\ldots\ldots \quad (16)$$

from which

$$A = B - A_1 - A_1 \frac{x_1}{x_2} \quad \ldots\ldots\ldots\ldots \quad (17)$$

Areas B and A_1 are rectangular and can be computed from measured sides with a high degree of accuracy. Centroidal distance x_1 is obtained with precision by direct measurement. Centroidal distance x_2 can be determined very accurately by the method of Fig. 8.

Aside from purely numerical computations, area A could also be determined in other ways (for example, from the measured size and weight of sheet a-b-c-d and the weight of template A). However, aside from being impractical, it was conclusively established that the weighing is frequently unreliable.

It is advantageous to determine the absolute rather than relative value of area A if fixed-end moments are to be found later. Fixed-end moments result from loads placed on the member considered or from joint-displacements caused by settlement or temperature change.

Relative values of areas A for two consecutive members free of loads and transverse joint-displacements, such as members c-b and c-d in Fig. 11(a), suffice for the moment-distribution method.

To determine relative stiffness factors of members c-b and c-d, lay out their 1/E I-templates to scale as is shown in Fig. 11(b). (A simple case of I-variation is chosen to illustrate the procedure. Obviously, an equivalent numerical solution would be more expedient here.) Locate the centroid of (A_{cb} + A_{cd}) by the method of Fig. 8, and scale off centroidal distance x_c, Fig. 11(b). Separate areas A_{cb} and A_{cd} by cutting through c, locate their centroids by the method of Fig. 8, and scale off centroidal distances x_{cb} and x_{cd}. Taking first moments about c yields

$$A_{cb} x_{cb} - A_{cd} x_{cd} = -(A_{cb} + A_{cd}) x_c \quad \ldots\ldots\ldots \quad (18)$$

from which

$$\frac{A_{cb}}{A_{cd}} = \frac{x_{cd} - x_c}{x_{cb} + x_c} = \frac{1}{r} \quad \ldots\ldots\ldots\ldots \quad (19)$$

Applying Eq. 17, relative stiffness factors are

$$S_{cb} = \frac{\bar{x}_{cb}}{\bar{x}_{cb} - x_{cb}} \quad \ldots\ldots\ldots\ldots \quad (20)$$

and

$$S_{cd} = \frac{\bar{x}_{cd}}{r(\bar{x}_{cd} - x_{cd})} \quad \ldots\ldots\ldots\ldots \quad (21)$$

CARRY-OVER AND STIFFNESS FACTORS AT END b

The factors at end b are expressed by formulas analogous to Eqs. 6 and 14, namely,

$$C_{ba} = \frac{Q_b}{J_b} L - 1 \quad \ldots\ldots\ldots\ldots \quad (22)$$

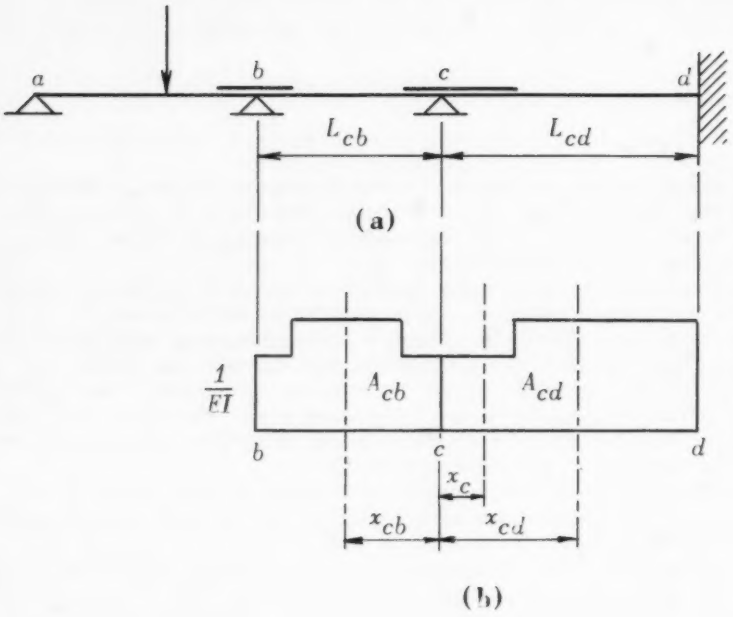

FIG. 11

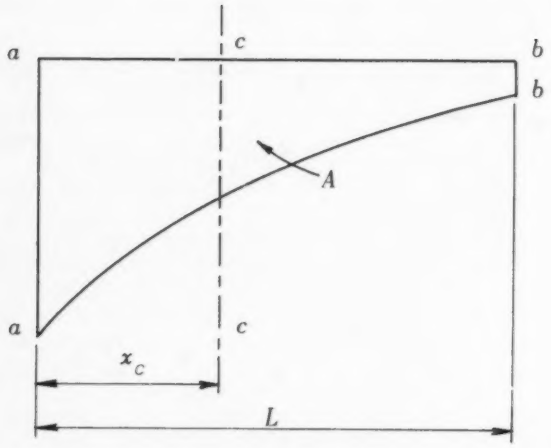

FIG. 12

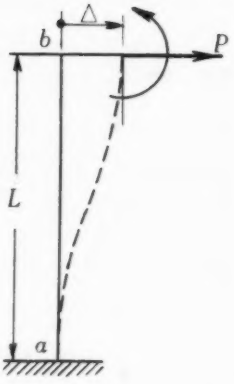

FIG. 13

and

$$S_{ba} = \frac{1}{A - \frac{Q_b^2}{J_b}} \quad \ldots\ldots\ldots\ldots\ldots\ldots \quad (23)$$

If the physical make up of the member (its I-values) is symmetrical about the mid-span, the carry-over and stiffness factors are the same, respectively, for ends a and b. If the member is non-symmetrical, factors C_{ba} and S_{ba} may be evaluated by applying to end b the procedure outlined for end a, that is, the origin of abscissae x is placed at b, the corresponding P- or R-lines are plotted, etc. It is emphasized that the centroidal distance, x-barred, when referred to b, is not equal to $L - \bar{x}$.

However, factors C_{ba} and S_{ba} may be determined more rapidly from the parameters already established in evaluating C_{ab} and S_{ab} in the subsequent manner.

In Fig. 12, c-c is a centroidal axis of area A, parallel to a-a and b-b. The following relationships evidently hold:

$$Q_a = A\,x_c \quad \ldots\ldots\ldots\ldots\ldots\ldots \quad (24)$$

$$Q_b = A\,(L - x_c) \quad \ldots\ldots\ldots\ldots\ldots\ldots \quad (25)$$

$$J_a = J_c + A\,x_c^2 \quad \ldots\ldots\ldots\ldots\ldots\ldots \quad (26)$$

and

$$J_b = J_c + A\,(L - x_c)^2 \quad \ldots\ldots\ldots\ldots\ldots\ldots \quad (27)$$

Substituting for J_c obtained from Eq. 26 into Eq. 27 yields

$$J_b = J_a + A\,L(L - 2x_c) \quad \ldots\ldots\ldots\ldots\ldots\ldots \quad (28)$$

Combining Eqs. 6 and 26 leads to

$$J_a = A\,x_c\,\bar{x} \quad \ldots\ldots\ldots\ldots\ldots\ldots \quad (29)$$

Substituting for J_a expressed by Eq. 29 into Eq. 28 results in

$$J_b = A\left[L^2 - x_c(2L - \bar{x})\right] \quad \ldots\ldots\ldots\ldots\ldots\ldots \quad (30)$$

Substituting into Eq. 22 for Q_b and J_b given by Eqs. 25 and 30 yields

$$C_{ba} = \frac{x_c(L - \bar{x})}{L^2 - x_c(2L - \bar{x})} \quad \ldots\ldots\ldots\ldots\ldots\ldots \quad (31)$$

Similarly, Eq. 23 combined with Eqs. 25 and 30 leads to

$$S_{ba} = \frac{L^2 - x_c(2L - \bar{x})}{A x_c(\bar{x} - x_c)} \quad \ldots\ldots\ldots\ldots (32)$$

MODIFIED STIFFNESS FACTOR

The modified stiffness factor at end a of a simply supported beam a-b, S'_{ab}, is the moment which, when applied at a will cause that end to rotate through a unit angle. The use of the modified stiffness factor expedites moment-distribution computations for structures which are externally simply supported.

The author has previously shown[2] that the modified stiffness factor can be computed from the formula

$$S'_{ab} = \frac{L^2}{J_b} \quad \ldots\ldots\ldots\ldots\ldots (33)$$

Substituting for J_b from Eq. 30 results in

$$S'_{ab} = \frac{L^2}{A\left[L^2 - x_c(2L - \bar{x})\right]} \quad \ldots\ldots\ldots\ldots (34)$$

Similarly, the formula for the modified stiffness factor at end b is

$$S'_{ba} = \frac{L^2}{J_a} \quad \ldots\ldots\ldots\ldots\ldots (35)$$

which, upon substitution for J_a from Eq. 29, becomes

$$S'_{ba} = \frac{L^2}{A x_c \bar{x}} \quad \ldots\ldots\ldots\ldots\ldots (36)$$

SHEAR STIFFNESS AND FLEXIBILITY

The shear stiffness of a member a-b, S_s, is the transverse force P required to cause a unit transverse displacement, $\Delta = 1$, between ends a and b, held fixed against rotation. In Fig. 13, force P is the shear stiffness when Δ is unity.

It has been shown[2] that the shear stiffness is given by the formula

$$S_s = \frac{P}{\Delta} = \frac{1}{J_c} \quad \ldots\ldots\ldots\ldots\ldots (37)$$

Substituting for J_c obtained from Eq. 26 and for J_a given by Eq. 29 transforms Eq. 37 into

$$S_s = \frac{1}{A x_c(\bar{x} - x_c)} \quad \ldots\ldots\ldots\ldots (38)$$

Flexibility, F, is the reciprocal of shear stiffness, that is, the transverse displacement, Δ, between ends a and b caused by a unit transverse force P.

Therefore,

$$F = J_c = A x_c(\bar{x} - x_c) \quad \ldots\ldots\ldots\ldots \quad (39)$$

Relative shear-stiffness and flexibility values may be used in sidesway analysis of rigid frames. Absolute values must be used when analyzing structures for the effect of settlement of supports or temperature change.

FIXED-END MOMENTS IN BEAMS

Concentrated Load.—Column-analogy formulas[4] will be used to develop the cardboard-analog procedure for determining fixed-end moments. In Fig. 14(a), the moments at a and b are, respectively,

$$M_a^F = \frac{W}{A} - \frac{W e}{J_c} x_c \quad \ldots\ldots\ldots\ldots \quad (40)$$

and

$$M_b^F = -P(L - KL) + \left[\frac{W}{A} + \frac{W e}{J_c}(L - x_c)\right] \quad \ldots\ldots \quad (41)$$

in which x_c and J_c are properties of A as previously defined,

$$W = \int_0^{L-KL} \frac{M\,dx}{EI} = \int_0^{L-KL} \frac{Px}{EI}\,dx \quad \ldots\ldots\ldots\ldots \quad (42)$$

is the area under the (M/E I)-diagram for beam a-b cut back to a statically determinate one by removing the fixed support at a; it is also the volume of the solid, Fig. 14(b), whose base has widths equal to the (1/E I)-values and a plane upper surface rising as Px;

$$e = KL + \bar{x}_w - x_c \quad \ldots\ldots\ldots\ldots\ldots \quad (43)$$

is the eccentricity of W, that is, the horizontal distance of the centroid of W from the centroidal axis, c-c, of A.

Referring to Eq. 42, a plane template may be constructed for W by multiplying values of 1/E I by values of x. The graphic multiplication is performed in exactly the same manner as was done in Fig. 5 except that it begins at point k. In Fig. 14(c), two W-templates are constructed for load P = 1 placed at k_1 (solid line) and at k_2 (dashed line). If preferred, templates W_1 and W_2 may also be obtained by graphic division of x-values by the corresponding values of E I. In either case, relative E I- or I-values may be used.

The W-template is cut out, its centroid is located by the method of Fig. 8, and centroidal distance $\bar{x}_W$ is scaled off. Assuming that x_c is known from stiffness-factor computations, eccentricity, e, may be readily computed from Eq. 43.

---

4 "Theory of Modern Steel Structures," by L. E. Grinter, The Macmillan Co., New York, Vol. II, 1937, p. 216.

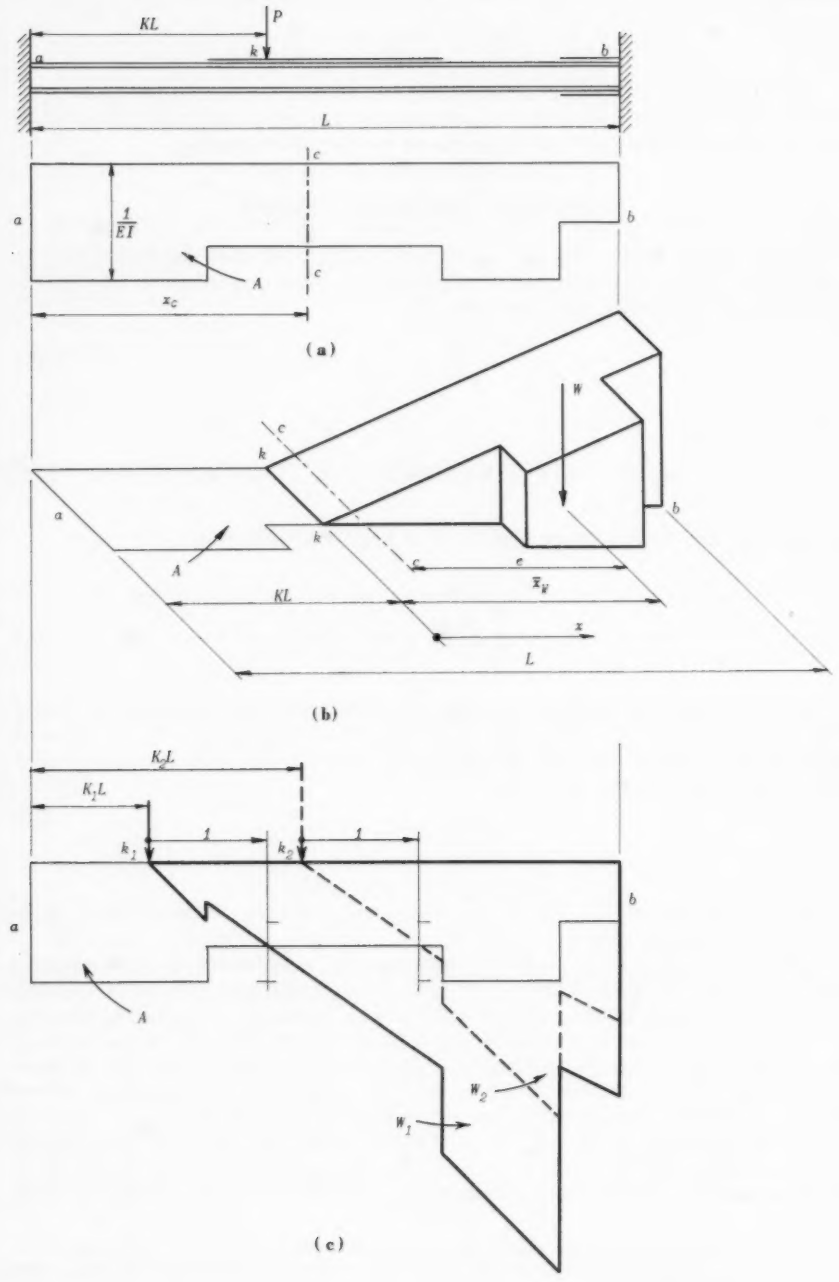
KL
P
k
a
b
L
c
a
$\frac{1}{EI}$
b
A
c
x_c
(a)
W
c
k
a
k
A
c
e
$\bar{x}_W$
KL
x
L
b
(b)
K_2L
K_1L
1
1
k_1
k_2
a
b
A
W_2
W_1
(c)

FIG. 14

The function W may be evaluated by the method of Fig. 10 and Eq. 17, in which W replaces A.

Substituting into Eq. 40 for e given by Eq. 43 and for J_c obtained by combining Eqs. 26 and 29 leads to

$$M_a^F = \frac{W}{A} \frac{\bar{x} - \bar{x}_w - KL}{\bar{x} - x_c} \quad \ldots\ldots\ldots\ldots (44)$$

Function (x/E I) in Eq. 42 may be constructed graphically to any suitable scale that will yield a W-template of desired proportions. It will be recalled that in graphic multiplication, the scale of the product-function is governed by the selection of the abscissa, x = 1, Fig. 5 or Fig. 14, x = 4, Fig. 5, etc., onto whose ordinate the dependent variable, 1/E I, is projected. Similarly, when graphic division is used, the choice of the horizontal line, I = 1, Fig. 7, I = 1/4, etc., along which the I-values are laid off determines the scale to which ordinates R are obtained.

The value of W as used in Eq. 44 is the value obtained experimentally by the method of Fig. 10, multiplied by the scale factor (for example, 4, if the (x/E I)-function is constructed to the one-quarter scale), and by the load intensity, P.

The term W, defined by Eq. 42, is a function of 1/E I and L, as is A in Eq. 44. It follows that the scales for 1/E I and (L - K L) in the W-template [Fig. 14(c)] should be the same, respectively, as the scales for 1/E I and L in the A-template, Fig. 10(a). If different scales are chosen in constructing the two templates, the scales must be correlated when evaluating Eq. 44. The correlation is effected by applying an appropriate scale factor in Eq. 44.

Suppose that in the case of template A, the span, L, of the beam is laid off as λ_A-inches, a unit of 1/E I (absolute or relative) is plotted as i_A-inches, and that in the case of the W-template, (L - K L) is laid off as λ_W-inches, and a unit of 1/E I is plotted as i_W-inches. Then the numerical values of A and W as found independently of each other in the manner described in Fig. 10 are converted to the true ratio-value, $|W/A|$, which must be used in Eq. 44 as

$$\left|\frac{W}{A}\right| = \frac{i_A \lambda_A^2 (1 - K)^2}{i_W \lambda_W^2} P \frac{W}{A} \quad \ldots\ldots\ldots\ldots (45)$$

An application of Eq. 45 is illustrated in the following example. For the sake of simplicity, assume I = 1/5 = constant, and K = 0.5, Fig. 15(a). Let $\lambda_A = 10$, $i_A = 0.4$, Fig. 15(b); $\lambda_W = 8$, and $i_W = 0.3$, Fig. 15(c).

The experimental evaluation of A by means of Eq. 17 and the procedure illustrated in Fig. 10, and of W determined in the like manner, would yield A and W expressed in square inches. In the simple case under consideration, however, both will be obtained algebraically.

In Fig. 15(b),

$$A = (\lambda_A)(5\, i_A) = (10)(2) = 20$$

and in Fig. 15(c),

$$W = \frac{1}{2}(\lambda_W)\left(\frac{5\, i_W}{1} \lambda_W\right) = \frac{1}{2}(8)\left(\frac{5 \times 0.3}{1} \times 8\right) = 48$$

Substituting into Eq. 45 results in

$$\left| \frac{W}{A} \right| = \frac{(0.4)(10\,\lambda_w)(1 - 0.5)^2}{(0.3)\,8^2} \quad P \quad \frac{48}{20} = \frac{1}{8} \quad P\lambda_w$$

Reference to Fig. 7 shows that graphic division is not effected by the scale chosen for the I-values as long as the horizontal line on which the I-values are

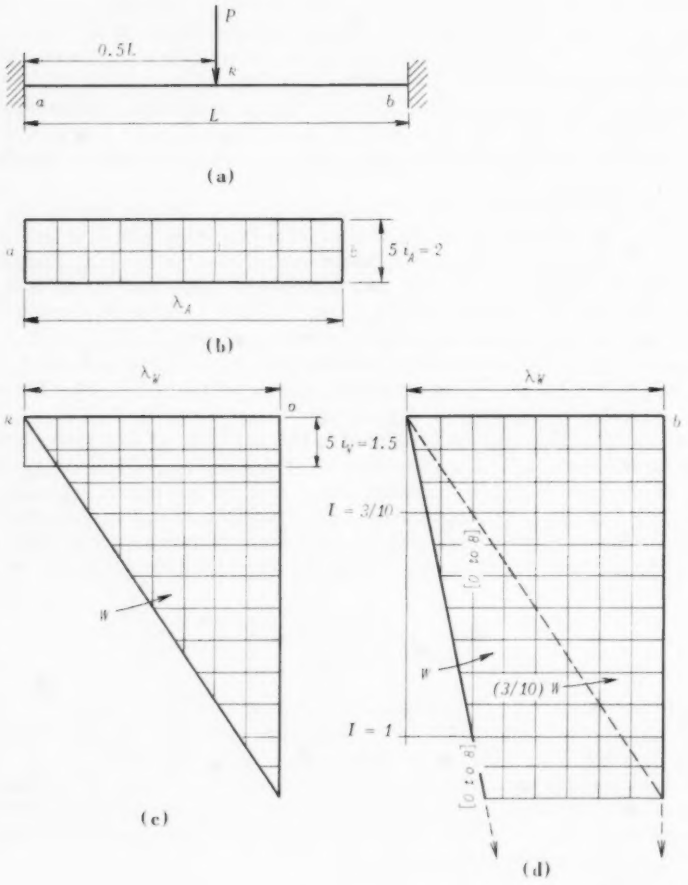

FIG. 15

laid off is drawn at I = 1. This becomes evident when one realizes that, say, doubling the I-scale would move the horizontal line to twice its present distance below the x-axis in Fig. 7, as it would also move the bracketed points plotted along that line to twice their present distance from the R-axis. Consequently, if graphic division is used to construct the W-template, Fig. 15(d), the horizontal line I = 1 and the segment I = 1/5 terminating at [0 to 8] may be laid off

to any scale. Since the resulting template is affected only by the λ_W-scale, i_W in Eq. 45 and the subsequent computations is replaced by 1. Based on the alternate W-template in Fig. 15(d) and simple computations, W is 160, and $|W/A|$ is found to be (1/8) P λ_W as before.

In actual experimental practice, however, the W-template in Fig. 15(d) would be of impractical proportions and therefore, a scale reduction would be desirable. Using a scale-reduction factor of 3/10 (dashed construction lines in Fig. 15(d)) results in a template which is identical with that of Fig. 15(c). The value to be substituted for W on the right side of Eq. 45 would be

$$(48)(10/3) = 160,$$

the value of i_W in the same equation remaining 1.

Refer again to Eq. 44. Although the second fractional expression on the right side is dimensionless, consideration must be given to the x-scales (λ-lengths) of the three templates, A, V and W from which the four parameters were determined. In general, any three parameters in the fractional expression under consideration may be adjusted to the scale of the fourth, or all four parameters may be converted to values corresponding to unit span-lengths, $\lambda = 1$. The span-lengths are the lengths of the respective templates with the exception of parameter $\bar{x}_W$, for which the span-length is the template length increased by K L.

The (1/E I)-scales have no effect upon the position of the centroids in the x-direction so that their correlation is not necessary.

Uniformly Distributed Load, w, over Entire Span.— The fixed-end moments caused by a uniformly distributed load, Fig. 16, are

$$M_a^F = \frac{W}{A} - \frac{W e}{J_c} x_c \quad \ldots\ldots\ldots\ldots\ldots (46)$$

and

$$M_b^F = -\frac{w L^2}{2} + \left[\frac{W}{A} + \frac{W e}{J_c}(L - x_c)\right] \quad \ldots\ldots\ldots (47)$$

The expression for W is

$$W = \int_0^L \frac{M\,dx}{E I} = \int_0^L \frac{w x^2}{2 E I}\,dx \quad \ldots\ldots\ldots\ldots (48)$$

in which M is the bending moment at any distance x in the beam cut back to a statically determinate condition by removing the support at a.

Eq. 48 may be written as

$$W = \frac{w}{2}\int_0^l \frac{x^2}{E I}\,dx = \frac{w}{2} J_a \quad \ldots\ldots\ldots\ldots (49)$$

Substituting for J_a from Eq. 29 into Eq. 49 results in

$$W = \frac{w}{2} A x_c \bar{x} \quad \ldots\ldots\ldots\ldots\ldots\ldots (50)$$

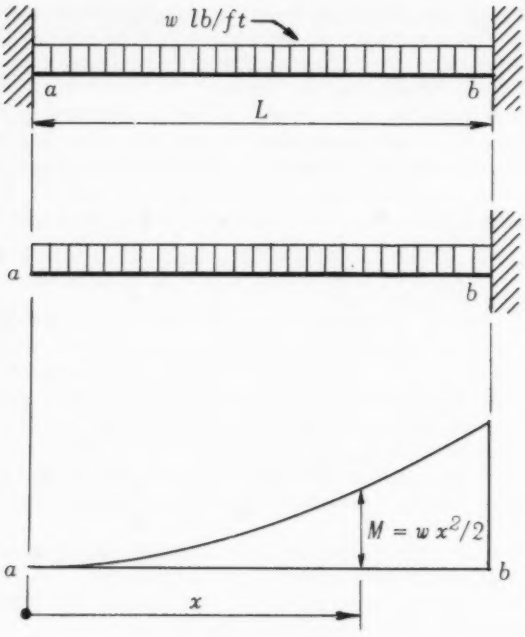

FIG. 16

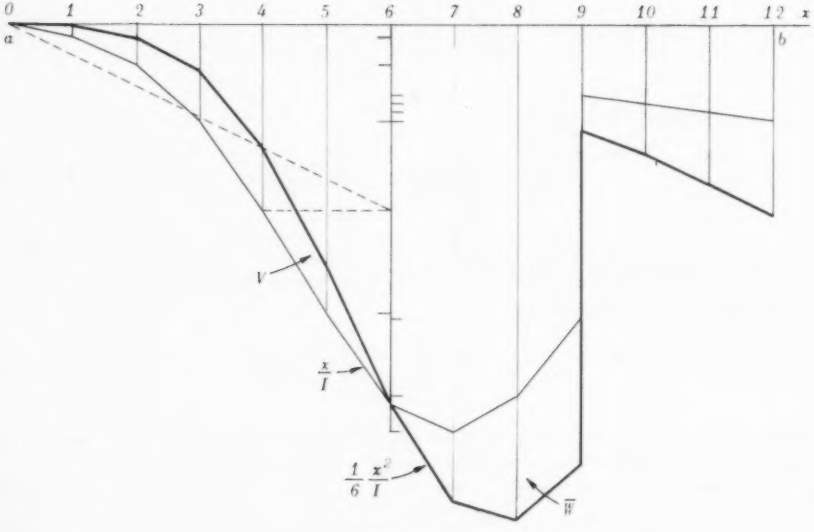

FIG. 17

Substituting for W from Eq. 50 in Eq. 46 and replacing J_c by its equivalent obtained by combining Eqs. 26 and 29 leads to

$$M_a^F = \frac{w}{2} x_c \bar{x} \frac{\bar{x} - x_c - e}{\bar{x} - x_c} \quad \ldots\ldots\ldots\ldots (51)$$

Parameters $\bar{x}$ and x_c have already been encountered in the analog-evaluation of the carry-over and stiffness factors, and will therefore be considered known. The only parameter that remains to be determined is e, the eccentricity, which is defined as the x-distance of the centroid of the (M/E I)-diagram from the centroidal axis, c-c, for area A.

According to Eq. 48, if a template representing the integral $\int_0^L \frac{x^2\,dx}{E\,I}$ is prepared, the x-distance of its centroid from any vertical reference axis is the same as the x-distance of the centroid of the (M/E I)-diagram from that axis. The template can be constructed from the V-template (Figs. 3, 5 and 7) by multiplying its ordinates by the corresponding abscissae. This multiplication by the x-values amounts to considering the V-template area to be what area A is when constructing V.

The graphic construction for the beam and V-template of Fig. 7 is shown in Fig. 17, in which the ordinates are obtained to one-sixth scale. Accordingly, utilizing Eq. 49, the resulting template is, nearly,

$$\bar{W} = \frac{1}{6} \int_0^{12} \frac{x^2}{I}\,dx = \frac{2\,E}{6\,w}\,W \quad \ldots\ldots\ldots\ldots (52)$$

The subsequent step, not illustrated, consists of cutting out the template and locating its centroid by the experimental method of Fig. 8. The centroidal distance, $\bar{x}_{\bar{W}}$, is scaled off. Since this distance is independent of factors 2, E, 6, and w, each of which pertains to the ordinates of either $\bar{W}$ or W (Eq. 52), distance $\bar{x}_{\bar{W}}$ is the same for both $\bar{W}$ and W. Therefore, the eccentricity, e, of W is

$$e = \bar{x}_{\bar{w}} - x_c \quad \ldots\ldots\ldots\ldots (53)$$

which, substituted into Eq. 51 results in

$$M_a^F = \frac{w}{2} x_c \bar{x} \frac{\bar{x} - \bar{x}_{\bar{w}}}{\bar{x} - x_c} \quad \ldots\ldots\ldots\ldots (54)$$

Although it is advantageous to utilize the V-template in the foregoing construction, a two-fold graphic multiplication by x may be readily performed without actually drawing or tracing the V-outline. The procedure is illustrated in Fig. 18 in which $f(x_2)$ is multiplied by x = 2 once, and the product, $\overline{2 - p'}_2$, is thereupon multiplied by x = 2 once more, so that $2^2 f(x_2) = \overline{2 - p''}_2$. Points p'' so obtained and connected define the boundary of the required template. A scale reduction may be effected in either one or both multiplications by projecting the multiplicand on the vertical at abscissae $x > 1$.

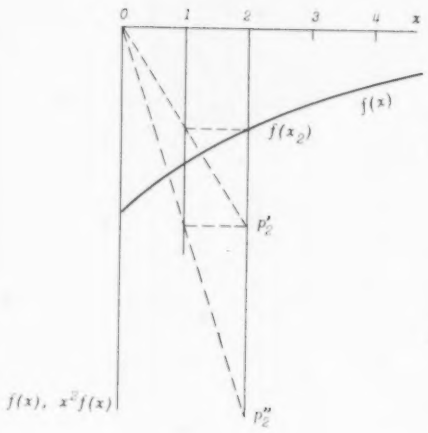

FIG. 18

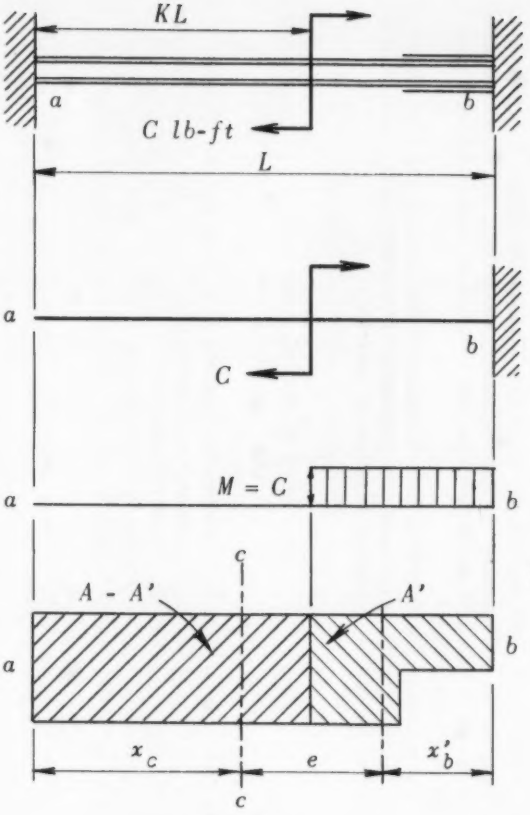

FIG. 19

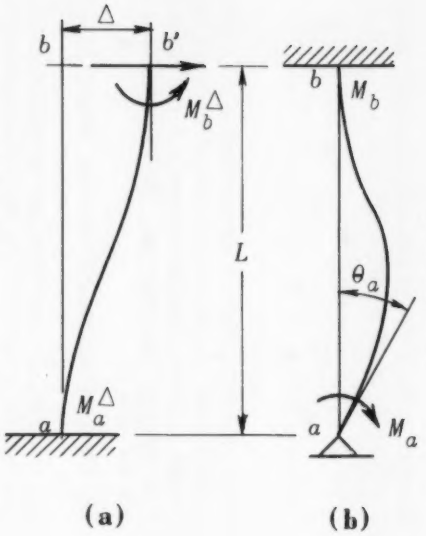

FIG. 20

Couple or Eccentric Longitudinal Load.—The fixed-end moments caused by couple or moment, C, Fig. 19, are

$$M_a^F = -\left[\frac{W}{A} - \frac{W\,e}{J_c}\,x_c\right] \quad \ldots\ldots\ldots\ldots\ldots (55)$$

$$M_b^F = C - \left[\frac{W}{A} + \frac{W\,e}{J_c}(L - x_c)\right] \quad \ldots\ldots\ldots\ldots (56)$$

in which

$$W = \int \frac{M\,dx}{EI} = \int_{KL}^{L} \frac{C\,dx}{EI} = C\,A' \quad \ldots\ldots\ldots\ldots (57)$$

in which A' is the area under the (1/E I)-diagram from K L to L.

Since the bending moment in the beam cut back to a statically determinate one is constant, the eccentricity, e, of W is the distance of the centroid of area A' from axis c-c. Centroidal distance x'_b for template A' is found experimentally by applying the procedure of Fig. 8. Then

$$e = L - x_c - x'_b \quad \ldots\ldots\ldots\ldots\ldots (58)$$

Substituting from Eqs. 57 and 58 into Eq. 55 leads to

$$M_a^F = -C\,\frac{A'}{A}\,\frac{\bar{x} + x'_b - L}{\bar{x} - x_c} \quad \ldots\ldots\ldots\ldots (59)$$

FIXED-END MOMENTS IN BEAMS CAUSED BY IMPRESSED DISTORTIONS

Relative Transverse Displacement between Ends a and b, Fig. 20(a).—It can be readily shown (for example, by conjugate-beam or column-analogy methods of analysis) that fixed-end moments caused by transverse displacement, Δ, between ends a and b are

$$M_a^\Delta = \frac{\Delta}{A\,(\bar{x} - x_c)} \quad \ldots\ldots\ldots\ldots\ldots (60)$$

and

$$M_b^\Delta = \frac{\Delta\,(L - x_c)}{A\,x_c\,(\bar{x} - x_c)} \quad \ldots\ldots\ldots\ldots\ldots (61)$$

Rotation of One End, a, of the Beam, Fig. 20(b).—From the definition of the stiffness factor at a, Fig. 9(a), it follows that moment M_a required to cause rotation θ_a at a is

$$M_a = S_{ab}\,\Theta_a \quad \ldots\ldots\ldots\ldots\ldots (62)$$

The moment required to hold end b fixed is

$$M_b = C_{ab} S_{ab} \Theta_a \quad \ldots\ldots\ldots\ldots\ldots (63)$$

MOMENT-DISTRIBUTION CONSTANTS OF PROTOTYPE

In general, the values of the constants determined with the aid of cardboard templates must be adjusted to express the constants of the prototype. The fundamental dimensions in the construction of templates are lengths, L or λ, and 1/E I-values, plotted as scaled lengths in a rectangular coordinate system.

Centroidal x-distances, scaled off from the templates, must be multiplied by the scale to which the template-length represents the corresponding length

TABLE 1

Constant (1)	Designation; Template-Determined Value (2)	Equation (3)	Prototype-Value (4)
Carry-Over Factor	C_{ab}	6	C_{ab}
Stiffness Factor	S_{ab}	15	$\frac{1}{m.n} S_{ab}$
Modified Stiffness Factor	S'_{ab}	34	$\frac{1}{m.n} S'_{ab}$
Shear Stiffness	S_s	38	$\frac{1}{m^3.n} S_s$
Flexibility	F	39	$m^3.n\ F$
Fixed-End Moment, P-load	M^F_a	44	$m\ M^F_a$
Fixed-End Moment, w-load	M^F_a	51	$m^2\ M^F_a$
Fixed-End Moment, C-load	M^F_a	59	M^F_a
Fixed-End Moment, Δ-displacement	M^{Δ}_a	60	$\frac{1}{m^2.n} M^{\Delta}_a$
Fixed-End Moment, θ_a-displacement	$S_{ab}\ \theta_a$	62 & 15	$\frac{1}{m.n} S_{ab}\theta_a$

in the prototype. Since ratios of like quantities are dimensionless, they retain the same value when applied to the prototype. Areas of templates, computed in square inches, must be multiplied by the scales of the two fundamental dimensions.

Let 1 in. of template length represent m-inches of span of the prototype, and 1 in. of ordinate represent 1-(1/pound-square inches) of 1/E I. Table 1

shows the various moment-distribution constants determined by cardboard analogs, and constants adjusted for the prototype.

CONCLUSIONS

The practicability and accuracy of the method described in this paper was tested by a group of fifty senior civil engineering students at Manhattan College, New York, N. Y. The moment-distribution constants for one of two complex structures (a three-span continuous steel beam with fifteen different I-values, and a two-span concrete bridge frame with varying I) were determined by each student with the aid of cardboard templates. To provide a check, several students and the writer also computed the constants by analytic methods.

In general, an excellent correlation was found to exist between the experimental and analytic results. Occasional discrepancies when encountered were traced to one or more of the following causes:

1. Gross errors in the initial computations of I-values.
2. Use of unsuitable template material (corrugated cardboard, ordinary writing paper).
3. Choice of very small m-scales (templates less than 4 in. long).
4. Poor drawing technique, crudely constructed or cut out templates.

Notwithstanding the aforementioned sources of error, the correlation between template and analytic results was generally well within 5%, with the exception of fixed-end moments caused by concentrated or distributed loads where differences of up to 10% were not uncommon. In the latter case, the discrepancy is not necessarily or entirely due to the analog technique. An inspection of the column-analogy formulas on which the working formulas of the cardboard analog method are based, shows that differences of quantities of comparable order of magnitude are involved.[2] Thus, both the analytic and experimental results are sensitive, respectively, to the accuracy with which the several terms are computed or measured.

For all practical purposes, the cardboard analog-method is sufficiently accurate. It is also highly reliable since little opportunity exists for gross errors.

The principle of the method can be applied to determine the deflections of beams with constant or variable moment of inertia, and of statically determinate or indeterminate structures in general.

ADDITIONAL REFERENCES

"The Determination of Moment Distribution Constants of Members with a Variable Moment of Inertia," by O. Ondra, thesis presented to Lehigh University, at Bethlehem, Pa., in 1955, in partial fulfilment of the requirements for the degree of Doctor of Philosophy.

APPENDIX.—NOTATION

C = carry-over factor

c = crown point

d = depth

E = modulus of elasticity

e = eccentricity

F = flexibility

I = rectangular moment of inertia

J = second moment

P = force

Q = statical moment

S = stiffness factor

V = volume

W = resultant body force

x = distance

$\bar{x}$ = distance of centroid of volume V referred to a; distance of center of gravity from a

Δ = displacement

θ = rotation

Journal of the
STRUCTURAL DIVISION
Proceedings of the American Society of Civil Engineers

DISCUSSION

Note.—This paper is a part of the copyrighted Journal of the Structural Division, Proceedings of the American Society of Civil Engineers, Vol. 87, No. ST 1, January, 1961.

MATRIX SOLUTION OF BEAMS WITH VARIABLE MOMENT OF INERTIA[a]

Closure by Ming L. Pei

MING L. PEI,[1] M. ASCE.—Many interesting questions were brought up by the discussers. The following is an attempt to clarify these points:

An Alternate Derivation of the Matrix Formula.—Instead of the finite-difference approach, the problem may be considered from the integral-equation approach. The governing equations of the simple beam are two second-order differential equations

$$\frac{d^2M}{dx^2} = q \qquad M(0) = M(L) = 0 \ldots\ldots\ldots\ldots (1)$$

and

$$\frac{d^2y}{dx^2} = \frac{M}{E\,I} \qquad y(0) = y(L) = 0 \ldots\ldots\ldots\ldots (15)$$

Since these two equations are identical in form, they can be solved in the same manner in succession, as two integral equations

$$M = \int A(x,z)\, q(z)\, dz \ldots\ldots\ldots\ldots\ldots\ldots (28)$$

and

$$y = \int A(x,z)\, \frac{M(z)}{E\,I(z)}\, dz \ldots\ldots\ldots\ldots\ldots\ldots (29)$$

where $A(x,z)$ is known as the Green's Function of the differential equation (15, 6). The problem is then reduced to the search of the Green's Function. The matrix $[A]$ is, in fact, this Green's Function in finite-difference form, and actually represents the exact solution, in closed form, of the finite-difference equations. Hence our formulas

$$[M] = [A]\ [q\,h] \ldots\ldots\ldots\ldots\ldots\ldots (11)$$

and

$$[Y] = [A] \left[\frac{M}{E\,I}\, h\right] \ldots\ldots\ldots\ldots\ldots\ldots (21)$$

Weighting Function.—At the expense of additional computations, we may insert a weighting function, or weighting matrix $[W]$ (called concentration matrix by Fenves) in the above formulation.

$$[M] = [A]\,[W]\,[q\,h] \ldots\ldots\ldots\ldots\ldots\ldots (30)$$

---

[a] October, 1959, by Ming L. Pei.

[1] Assoc. Prof. of Civ. Engrg., City College of New York. Currently, visiting Assoc. Prof. of Civ. Engrg., Univ. of Mich.

and

$$[Y] = [A]\,[W]\,[\frac{M}{E\,I}\,h] \quad \ldots\ldots\ldots\ldots\ldots \quad (31)$$

A large variety of weighting matrices may be used. The following have been suggested.

Pei

$$[W] = \begin{bmatrix} 1 & & & & & & \\ & 1 & & & & & \\ & & \cdot\cdot & & & & \\ & & & \cdot\cdot & & & \\ & & & & \cdot\cdot & & \\ & & & & & 1 & \\ & & & & & & 1 \end{bmatrix} = [I] \quad \ldots\ldots\ldots\ldots \quad (32)$$

Simpson's Rule

$$[W] = \frac{1}{3}\begin{bmatrix} 4 & & & & & & \\ & 2 & & & & & \\ & & 4 & & & & \\ & & & \cdot\cdot & & & \\ & & & & \cdot\cdot & & \\ & & & & & \cdot\cdot & \\ & & & & & & 2 \\ & & & & & & & 4 \end{bmatrix} \quad \ldots\ldots\ldots\ldots\ldots \quad (33)$$

Lagrangian Interpolation (n = 5)

$$[W] = \frac{5}{288}\begin{bmatrix} 75 & & & & \\ & 50 & & & \\ & & 50 & & \\ & & & 75 & \end{bmatrix} \quad \ldots\ldots\ldots\ldots\ldots \quad (34)$$

Clough-Fenves

$$[W] = \frac{1}{6}\begin{bmatrix} 4 & 1 & & & & & \\ 1 & 4 & 1 & & & & \\ & \cdots & & & & & \\ & & \cdots & & & & \\ & & & 1 & 4 & 1 & \\ & & & & 1 & 4 & \end{bmatrix} \quad \ldots\ldots\ldots\ldots\ldots\ldots \quad (35)$$

Fenves-Richards

$$[W] = \frac{1}{12}\begin{bmatrix} 10 & 1 & & & & & \\ 1 & 10 & 1 & & & & \\ & \cdots & & & & & \\ & & \cdots & & & & \\ & & & 1 & 10 & 1 & \\ & & & & 1 & 10 & \end{bmatrix} \quad \ldots\ldots\ldots\ldots\ldots \quad (36)$$

Clough

$$[W] = \frac{1}{12}\begin{bmatrix} 3.5 & 3 & -0.5 & & & \\ 1 & 10 & 1 & & & \\ & & \cdots & & & \\ & & & \cdots & & \\ & & & 1 & 10 & 1 \\ & & & -0.5 & 3 & 3.5 \end{bmatrix} \quad \ldots\ldots\ldots\ldots (37)$$

Szabo

$$[W] = \frac{1}{6}\begin{bmatrix} 2+\frac{2I_1}{I_2} & 1 & & & \\ \frac{I_1}{I_2} & 2+\frac{2I_2}{I_3} & 1 & & \\ & & \cdots & & \\ & & & \cdots & \end{bmatrix} \quad \ldots\ldots\ldots\ldots (38)$$

Szabo's weighting matrix depends on the values of moments of inertia, and cannot be combined with [A] before the writing of the machine program. Furthermore, the values of moments of inertia at half-intervals are required, which is awkward. Finally, this weighting matrix displays a peculiar asymmetry, which should not be present in weighting matrices.

Weighting matrices (Eqs. 32 through 37) should give better answers than the unit matrix used by the writer. The increased accuracy is obtained at the expense of additional computation, and a slightly longer program, if the problem is to be done on the computer. To be consistent, it would seem that the same weighting matrix should be used both in Eq. 30 and Eq. 31.

Computer Program.—Fenves raises the question of how many storage locations are required to program the writer's formulas. It appears at first that nearly n^2 locations are needed to store [A]. Actually, it is not necessary to store [A] which can be generated, as it is needed, by the following formula

$$a_{ij} = i\,\frac{(n-j)}{n} \qquad i < j \quad \ldots\ldots\ldots\ldots\ldots (39a)$$

and

$$a_{ij} = j\,\frac{(n-i)}{n} \qquad i > j \quad \ldots\ldots\ldots\ldots\ldots (39b)$$

The writer has written a program in MAD (Michigan Algorithm Decoder, a fast compiler developed by the University of Michigan Computing Center) for the IBM 704 computer which is shown in Fig. 6. Such a program can be constructed to compute deflections with n = 1,000 on any computer having 4,000 memory locations. The program is quite short, and did not use special matrix subroutines. The program has been included in a larger program as its subroutine. It would require considerable sophistication to write as short a program using Newmark's Method.

Newmark's Method.—Newmark's Method gives an extremely efficient algorithm for solving the sets of equations

$$[B] = [M]\,[q\ h] \quad \ldots\ldots\ldots\ldots\ldots (6)$$

and

$$[B] = [Y]\left[\frac{Mh}{EI}\right] \quad \ldots\ldots\ldots\ldots\ldots\ldots \quad (18)$$

It is fast because it takes advantage of the fact that [B] is a tri-diagonal matrix. The algorithm is described recently by (17). The writer's scheme simply "plugs" the given values into the formulas

$$[M] = [A]\ [q\ h] \quad \ldots\ldots\ldots\ldots\ldots\ldots \quad (11)$$

and

$$[Y] = [A]\left[\frac{M\,h}{E\,I}\right] \quad \ldots\ldots\ldots\ldots\ldots\ldots \quad (21)$$

In spite of this, Newmark's Method can be faster if all the deflections are required.

```
R     BEAM DEFLECTIONS BY MATRIX FORMULA

      READ FORMAT INPUT,L,N,INER(1)...INER(N-1)
      READ FORMAT INPUT1,Q(1)...Q(N-1)
      PRINT FORMAT TITLE
      PRINT FORMAT DATA,INER(1)...INER(N-1)
      PRINT FORMAT DATA,Q(1)...Q(N-1)
      EQUIVALENCE (INER, Y)
      INTEGER I,J,R,S,N
      ME=1.0
      THROUGH ABLE, FOR I=1,1,I.G.(N-1)
      MOM(I) = 0
      THROUGH ABLE, FOR J = 1,1,J.G.(N-1)
      WHENEVER I .G. J
      MOM(I)=MOM(I)+J*(N-I)*Q(J)/INER(I)
      OTHERWISE
      MOM(I)=MOM(I)+I*(N-J)*Q(J)/INER(I)
\BLE  END OF CONDITIONAL
      THROUGH BAKER,FOR R=1,1,R.G.(N-1)
      Y(R)=0
      THROUGH BAKER,FOR S=1,1,S.G.(N-1)
      WHENEVER R .G. S
      Y(R)=Y(R)+S*(N-R)*MOM(S)*L.P.3/(N.P.5*ME)
      OTHERWISE
      Y(R)=Y(R)+R*(N-S)*MOM(S)*L.P.3/(N.P.5*ME)
BAKER END OF CONDITIONAL
      DIMENSION Y(100),MOM(100),Q(100),INER(100)
      PRINT FORMAT DATA,Y(I)...Y(N-1)
      VECTOR VALUES TITLE=$1H1,S38,44HDEFLECTIONS OF SIMPLE BEAM BY
     1 MATRIX FORMULA//*$
      VECTOR VALUES INPUT =$S40,F10.4,I10/9F7.4*$
      VECTOR VALUES INPUT1 = $9F7.4*$
      END OF PROGRAM
```

FIG. 6

Clough's Method.—The writer cannot agree with Clough's comments regarding his method (16). His derivation of flexibility matrix is certainly not as straight forward as he claims. After obtaining a 2n by 2n flexibility matrix, he then arbitrarily reduces it to an n by n matrix for computational use. Time will tell whether these methods will be accepted by the profession.

Remarks.—The writer has not been able to locate Szabo's Hungarian paper (14). His later papers (12,13) deal with the analysis of orthogonal gridwork structures, and do not seem to discuss deflections of beams with variable moments of inertia.

Reggini kindly called to the writer's attention two papers (10,11) published in Argentina where the same idea is explored. The writer wishes to thank all the discussors for their interest in the paper.

Acknowledgments.—The computer program mentioned herein was written while the writer was serving as Visiting Associate Professor at the University of Michigan under the sponsorship of the Ford Foundation Project on Computers, Donald L. Katz, Director. Carnahan gave assistance in MAD programming techniques. Their generous supports are gratefully acknowledged.

Errata.—Page 11, line 1, Eq. 23 should read Eq. 22. Page 11, Example 5, the reciprocal of [h/E I] is given instead of [h/E I].

REFERENCES

10. "Determinacion Numerica De La Rigidez Angular De Una Viga," by H. C. Reggini, Centro Est. de Ing. Serie 4.31, No. 4/8, Argentine.

11. "Vibraciones De Flexion De Una Viga," by H. C. Reggini, Centro Est. de Ing. Vol. 127, No. 637, pp. 101-113, 1959, Argentine.

12. "Stahlbeton - Tragerrostdecken," by J. Szabó, Bautechnik, p. 220, July, 1957.

13. "Die Berchnung von Brucken - Tragerrosten," by J. Szabó, Stahlbau, p. 141, June, 1958.

14. "Application of the Matrix Theory to the Calculation of Continuous Beams," by J. Szabó, Acta Technica Scientiarum Hungaricae, Tomus XVI, fase. 1-2, 1957.

15. "Matrix Analysis of Beams," by R. W. Clough, ASCE, Vol. 84, No. EM 1, January, 1958.

16. "Methods of Mathematical Physics," by Courant and Hilbert, Vol. 1, pp. 351-386.

17. "Inversion of Band Matrices," by S. O. Asplund, 2nd ASCE Conference on Electronic Computation, September, 1960.

ULTIMATE LOAD THEORY FOR CONCRETE FRAME ANALYSIS[a]

Closure by A. L. L. Baker

A. L. L. BAKER.[1]—The contributions of the several discussers are greatly appreciated. Since the discussions refer to design criteria, it may be appropriate to offer a general reply. Many tests have shown that full ultimate resistance can develop at all critical sections of a statically indeterminate reinforced concrete structure before failure occurs at one of them. But computations and tests also show that cases are possible in which some critical sections fail by excessive strain, before others have attained full strength. Hence, critical sections must be designed to be able to deform inelastically before failure, an amount compatible with the relative stiffnesses and deformations of the influential frame members. However, the $(n + 1)$th hinge by appropriate reinforcement design can be made to form at a load only very slightly greater than that which produces the nth hinge. A more difficult problem for the designer is to decide what alternative distributions of load may occur and be critical. Here the statistical approach is of great interest, and could be used as an aid in deciding what loading conditions and hinge positions to adopt as sound design criteria. Having decided on certain load distributions as possible critical, each case requires investigation to ensure adequate strength when the nth hinge forms. It would not be wise to risk the possibility of failure due to strain incompatibility. Research may, of course, eventually show that the present recommendations of design criteria are a little too cautious, and that further simplifying assumptions can be justified.

---

[a] November, 1959, by A. L. L. Baker.
[1] Prof., Concrete Tech., Univ. of London, London, England.

ANALYSIS OF RIGID FRAMES BY ELECTRONIC COMPUTATION[a]

Closure by Ardis White

ARDIS WHITE,[1] M. ASCE.—The discussion by King has considerably increased the value of the original paper, as he added a number of ideas which were very pertinent to the subject matter, but were not included in the paper. King has asked about the time and equipment involved in preparing data for entry into the computer. A special form is used for presenting the data, and about 5 min is required by the engineer to fill out this form. An additional 10 min or so is used by the key-punch operator in punching data cards for the IBM 650. Feeding the program deck and data cards into the computer requires about 5 min or less, and the actual computation consumes about 10 min. Printing out the results requires about 5 min or less.

The program is coded in SOAP, including SIR, with sine, cosine, and square root functions. About 12 man-weeks were involved in writing the program; coding and debugging each required about 1 additional week.

The writer wishes to express his appreciation to Arthur McMorris, whose encouragement and assistance was so vary valuable during preparation of the paper.

[a] November, 1959, by Ardis White.

[1] Assoc. Prof., Univ. of Houston, Houston, Tex.

VIERENDEEL BENTS WITH NONPRISMATIC MEMBERS[a]

Closure by S. L. Lee and F. P. Wiesinger

S. L. LEE,[1] M. ASCE and F. P. WIESINGER,[2] M. ASCE.—The writers agree with Rogers that approximate solutions are often necessary and sometimes indespensable in engineering practice. The approximate method used by Rogers as an illustration of his remarks was originally suggested by Saliger.[3] In using this method, however, the location of the imaginary hinges in the chord member (or cross member) should not be in the ratio of the squares of the stiffnesses of the adjacent cross members (or chord members), as stated in Rogers' discussion, but in the ratio of their square roots. The latter was apparently used in the numerical work of the discussion with the exception of the hinge location in the cross members, which cannot be verified.

It is most unfortunate that the method presented in the paper under discussion, which deals only with Vierendeel bents with equal chord stiffness and symmetrical cross members, is not applicable to Rogers' example in which the chord stiffnesses are different. The latter, however, can be readily treated by means of another method of analysis suggested elsewhere by the writers.[4]

It should be emphasized here that the method presented in this paper involves simple expressions and yields correct solutions with a speed of convergence rapid enough for office practice.

Corrections.—In the original paper, on p. 60, the second equation from the bottom should read

$$P = \frac{2M'_E - 2M'}{\overline{AB}} = \frac{-2M_E + 2M}{\overline{CD}}$$

On p. 61, in the tenth line from the bottom $K_O = E_O\, I/L$ should be replaced by $K_O = E\, I_O/L$ and, in the following line, D by C. In Fig. 6 on p. 66, the directions of all the forces should be reversed.

---

[a] December, 1959, by S. L. Lee and F. P. Wiesinger.

[1] Prof. of Civ. Engrg. Northwestern Univ., Evanston, Ill.

[2] Natl. Science Foundation Faculty Fellow, Northwestern Univ., and Asst. Prof. of Civ. Eng., Univ. of Illinois, Chicago, Ill.

[3] "Der Eisenbetonbau," by R. Saliger, 6 Aufl., Krõner, Leipzig, 1933. See also Beton-Kalendar, 1945-1950, XXXIX Jahrgang, Wilhelm Ernst & Sohn, Berlin, 1949, p. 237.

[4] "Moment - Distribution Analysis of Vierendeel Bents with Inclined Chords of Unequal Stiffnesses," by S. L. Lee and F. P. Wiesinger, Proceedings, I.C.E., Paper No. 6490 (to be published).

DISCONTINUITY STRESSES IN BEAMS ON ELASTIC FOUNDATIONS[a]

By R. S. Alwar

R. S. ALWAR.[4]—An interesting iterative procedure for the evaluation of stresses in beams on elastic foundations with discontinuous loadings has been suggested.

If the differential equation for the deflection curve of the beam on an elastic foundation is solved by the classical method, the number of simultaneous equations to be dealt with would be 4 n, where n is the number of discontinuities in loading. This, as the author himself has pointed out, is quite cumbersome. It is rather unfortunate that Penzien has not mentioned in his introduction the existence and utility of the operational methods in solving such discontinuity problems. With this method, the number of simultaneous equations to be dealt with is only two, whatever the number of discontinuities. A paper on the application of the operational method to simple beam problems by William T. Thompson is available.[5] Recently the writer[6] applied the operational technique to problems of beams on elastic foundations in which beams with arbitrary discontinuous loading was also considered.

By applying the Laplace transformation, the ordinary differential equation is reduced to a simpler form, usually a linear algebraic equation. This simple equation is then solved for a transition function from which the desired solution to the original differential equation is obtained by the use of inverse Laplace transforms.

In addition the load functions that are used in the transformation method provide, in the case of beams with arbitrary discontinuous loading, a very convenient tool for arriving at the solution, in a continuous form, and in a single process, for deflection, moment, and foundation reaction at any point in the beam.

There is one more point of particular interest and that is in contrast to the 4 n simultaneous equations, involved in the classical method, which Penzien has referred to, this method needs the solution of only two simultaneous equations, whatever the number of discontinuities.

---

[a] April, 1960, by Joseph Penzien.

4 Research Fellow, Civ. and Hydr. Engrg. Sect., Indian Inst. of Science, Bangalore-12.

5 Journal of the Franklin Inst., 1949.

6 "Solution of Problems in Beams on Elastic Foundations by the Method of LaPlace Transformation," by R. S. Alwar, A Journal of the Institution of Engineers, India, Vol. XL, No. 12, Part 1, August, 1960.

REINFORCED CONCRETE PAVEMENTS FOR AIRPORTS[a]

Discussion By Gordon K. Ray,[8] F. ASCE, and William G. Westall,[9] M. ASCE

GORDON K. RAY,[8] F. ASCE and WILLIAM G. WESTALL,[9] M. ASCE.—In advocating the use of steel reinforcement in concrete airport pavements, the author draws upon three principal sources for his argument. These are:

1. Highway pavement performance.
2. Corps of Engineers tests on reinforced concrete pavement.
3. Theoretical assumptions.

The purpose of this discussion is to objectively examine each of these.

To keep the subject in proper perspective, it must be recognized that the use of reinforcement in highway pavements is but one of several methods being tried by highway engineers in their continuing search for a design that will provide optimum balance between economy and performance. The principle involved is well stated by an ACI committee in its report on concrete slab dimensions:[10]

> "Determination of the proper length of concrete pavement slabs involves a consideration of several factors, some of which depend upon longitudinal slab stresses, however produced, and others upon the pavement design, construction, maintenance, and past performance under traffic. All of the factors involved must be so balanced against each other that the slab length finally chosen will result in optimum pavement performances. The economic phase of the problem is important and optimum performance must be attained at a cost which, although not necessarily the minimum, does not, however, exceed the benefit produced."

The fact that several state highway departments build reinforced concrete in relatively long panels does not necessarily validate this practice under the criteria quoted previously. Using cement-treated subbases, California and several other states are building concrete pavements with relatively short joint spacing and without dowels for load transfer. The first pavement built on this design in California has shown excellent performance for 14 yr.[11] Nevertheless, the statement used previously also applies here: the successful use of this design does not validate it as the optimum. It must be assumed that each of the many design methods now used by highway construction agencies was

---

[a] May, 1960, by August W. Compton.

[8] Mgr., Paving Bureau, Portland Cement Assoc., Chicago, Ill.

[9] Supervising Engr., Airfield Program, Portland Cement Assoc., Chicago, Ill.

[10] "Considerations in the Selection of Slab Dimensions," ACI 53-24, American Concrete Inst.

[11] "Construction Practices on Cement-Treated Subgrades for Concrete Pavements," by F. N. Hveem, presented at 39th Annual Meeting, Highway Research Bd.

adopted in an attempt to obtain a balanced relationship between performance and economy. It appears likely that results from the AASHO Road Test near Ottawa, Ill. will cause revision of some current highway design practices.

Following a comparison of joint spacing in reinforced and non-reinforced pavements, the author states in the last paragraph of his introduction:

> "Both types of design have been used and are now being used for airport pavements. Reasons for using or not using reinforcement are the same as those for highways. Of course, they should be. The volume of traffic on airport pavements is much less than on highways but the wheel loads are many times greater."

The conclusions reached in this quotation are subject to question. Because of a combination of factors, the reasons for using reinforcement in highway pavements cannot be applied without exception to airport pavements. Some of these factors will be discussed because of their special significance.

Compton has pointed out that the traffic volume is much less on airport pavements than on highways. This difference in frequency of loading will bear closer examination.

Airport traffic controllers have estimated that, even under ideal conditions, 1,000 to 1,200 operations per day would equal the maximum rate of utilization of one runway by transport type aircraft. This daily rate is purely theoretical because it is based on the highest hourly rate possible. It does not take into account the reduced rate during weather minimums, nor allow for the slack hours of operation. In actual practice, the number of daily operations will be considerably below the theoretical maximum. Even if it is assumed that an airport pavement might be trafficked 1,000 times daily, this is less than the hourly rate on a busy urban expressway or freeway. Whereas it is true that only a relatively small percentage of the total number of vehicles on the highway will equal or exceed the loading for which the pavement was designed, this is also true of the aircraft that use airport pavements. Considering their much greater traffic volume, highway pavements probably are subjected to the maximum allowable loads with greater frequency than airport pavements are subjected to loads of any kind.

The manner in which loads are applied to pavements is a critical factor in the development of design criteria. Westergaard and others have demonstrated that loading at the free edge of a concrete pavement creates stresses of greater magnitude than interior loading where pavement continuity is provided by load transfer between joints. Airport pavements are seldom, if ever, subjected to loading along a free or unsupported edge. On highways, however, wheels of the heaviest vehicles travel close to the outer edge of the pavement.

Considering their high traffic volume with load channelization at the pavement edge, it must be concluded that highway pavements are subjected to more severe conditions of loading than are airport pavements. The reasons for using reinforcement in highway pavements are not equally applicable to airport pavements.

The author refers frequently (and logically) to Corps of Engineers test data. During the past twenty years the Corps has invested more than $10,000,000 in research and engineering investigations for the development of valid design procedures for airfield pavements. During the same period of time, as the construction agency for the Air Force, they have designed and constructed some $3,000,000,000 worth of military airfield pavements. Probably the Corps of

Engineers has more experience than any other agency in the design, construction, and performance evaluation of pavements built for modern aircraft.

It is interesting, then, to look at their reasons for performing tests on reinforced concrete pavements. In a paper James P. Sale and Ronald L. Hutchinson summed it up as follows:[12]

> "The increased thicknesses (up to 22 inches) required for the 100,000-pound loading at the higher number of coverages being applied, caused increased attention to be focused on methods for reducing these thicknesses through steel reinforcement or prestressing of the pavements. . . . Although it was realized that generally a reinforced rigid pavement would be more costly than an equivalent strength non-reinforced rigid pavement, there was a definite need for such a design criteria to produce some way in which certain pavement thicknesses could be reduced to meet surface grade requirements for different thicknesses in the various traffic areas and, when strengthening an existing pavement, it was impossible to meet surface grade requirements without either removing and replacing large areas of pavements or over-designing certain areas."

Significantly, the reinforced design criteria was developed for the purpose of meeting certain special conditions and no unsatisfactory performance of plain concrete pavement was cited. On the contrary, this statement was included in the same report:

> "The rigid pavement design procedures developed in the investigational program have produced pavements with a proven record of adequacy from the standpoint of construction feasibility, structural capacity, surface smoothness and durability for support of such propeller-driven aircraft as the B-29 and B-36 and more recently for the B-47 and B-52 jet bomber aircraft."

In view of their vast experience in all phases of engineering relating to airfield pavements, it is of further interest to note that the Corps of Engineers design manual[13] (with changes to March 1960) requires reinforced concrete pavement only to meet certain conditions and not as general design criteria.

Much of the author's argument is predicted on assumptions regarding the behavior of concrete pavements built without reinforcement or dowels. It is implied that these pavements can be expected to develop uncontrolled cracking, joint faulting, and general deterioration. This behavior pattern has not been confirmed by engineers who have made performance evaluation surveys of airport pavements that are in service.

Plain concrete pavements that were adequately designed and built under good construction procedures have not developed harmful cracks even under prolonged usage at capacity loading. This is well illustrated in the Corps of Engineers report[14] on the performance of test sections at Sharonville, Ohio.

---

12 "Development of Rigid Pavement Design Criteria for Military Airfields," by James P. Sale and Ronald L. Hutchinson, Journal of the Air Transport Div., Proceedings, ASCE, Vol. 85, 1959.

13 "Engineering and Design, Rigid Airfield Pavements," EM 1110-45-303, Corps of Engrs., Dept. of the Army, February, 1958.

14 "Heavy Wheel Load Traffic on Concrete Airfield Pavements," by Frank M. Mellinger, James P. Sale, and Thurman R. Wathan, Proceedings, 36th Annual Meeting of the Highway Research Bd.

These test sections, which included various thicknesses of reinforced and plain concrete pavements, were subjected to 90,000 repetitions of a 100,000-lb twin-wheel loading. The under-designed sections of each type of pavement cracked and broke up under the load repetitions. The fact that the reinforced pavement survived longer after the appearance of a crack seems to have led to conclusions regarding the benefits of reinforcement. However, two of the non-reinforced sections were the only test pavements which did not crack under a number of load repetitions considered the equivalent of 10 yr of traffic.

It has been demonstrated that dowels across contraction joints improve the performance of highway pavements that carry a large volume of heavy truck traffic. As previously discussed, the loading on airport pavements does not approach the highway frequency.

Regarding the assumption that dowels are required to prevent joint faulting in concrete airport pavements, reference is again made to Corps of Engineers design criteria which reflects the information collected in their long-term study of pavement performance. The Corps design manual[13] sets forth these requirements:

> "Dowels will be required across the last three transverse dummy joints back from the ends of all runways, and similar dowel requirements may be included for the ends of other large paved areas where local experience indicates that they are needed."

It is true that the Federal Aviation Agency, requires[15] dowels across contraction joints in aprons, taxiways and the ends of runways "to provide an increased margin of safety with respect to load transfer in these critical areas." This appears to be a carry-over from their 1948 criteria which was published at a time when the effect on pavement of multiple-wheel landing gears was not well understood. The cost of installing dowels, except at free pavement ends, cannot be justified based on airport pavement performance. Within the past several years, the writers have made detailed surveys of millions of square yards of concrete airfield pavements designed and constructed by the Corps of Engineers. These pavements supported all types of military aircraft including the heaviest jet bombers. Even on Air Force training bases, where heavy bomber traffic was at the saturation point, there was no evidence of contraction joint faulting or other pavement defects that could be attributed to the omission of dowels across contraction joints. Built without expansion joints except at abutting structures, airport pavements are restrained from movement to such an extent that aggregate interlock is retained at contraction joints.

Based on his assumption that contraction joints in airport pavements require dowels for proper performance, the author has presented the hypothesis that a reduction of the number of contraction joints will result in financial savings which can be applied to the cost of reinforcement in the longer panels.

This argument loses validity in view of the completely adequate performance of airport pavements built without dowels at the contraction joints. It was stated, also, that a saving in maintenance costs would result from reinforced pavement with fewer joints to maintain. The fallacy of this theory has been conclusively demonstrated by the performance of joints placed between long reinforced panels. Excessive movement, resulting in large joint openings, has made it impossible to keep the joints sealed. The infiltration of noncompressible ma-

---

15 "Airport Paving," U. S. Dept. of Commerce, Civ. Aeronautics Administration, October, 1956.

terial into the wide joint openings has caused spalling of concrete along the edges. Attempts to maintain the joints under these conditions have resulted in more maintenance effort than is required for the normal joint spacing in non-reinforced concrete pavement.

The plain concrete pavements built under Corps of Engineers criteria have provided the clean, smooth surfaces required for the operation of modern jet aircraft. Joint openings are minimized by the shorter panels and the infiltration of foreign material is prevented. The possibility of jet engine damage from spalled particles is thus eliminated.

The great weights and peculiar gear configurations of military aircraft have caused the Corps of Engineers to become concerned over the possibility that the pavement thicknesses required may eventually exceed the limits of construction feasibility. This concern need not extend to the pavements required for civil aircraft. The current jet transports, equipped with dual-tandem landing gears, require only about 10 in. to 14 in. of plain concrete pavement even in the critical areas of loading such as taxiways and runway ends. In pavement strength criteria for the various classes of airports, the FAA has seen fit to provide for pavement strength considerably above the current aircraft requirements. This provides a form of insurance against future increases in aircraft weights. For example, at Dulles International Airport, the critical areas of concrete pavement are 15 in. in thickness. This provides sufficient pavement strength to support operations of a 500,000-lb aircraft equipped with the dual-tandem type gear of the 300,000-lb current jet transports. The possibility of these pavements becoming overloaded within the foreseeable future is extremely remote. The pavement thickness is well within the construction capabilities of modern methods and equipment.

This discussion is not intended in any way to disparage the value of steel reinforcement in concrete pavement where conditions justify its use. There is little evidence that the additional cost of reinforcement can be justified for airport pavements. The use of long reinforced panels may be in some ways objectionable from an operational standpoint. Properly designed plain concrete pavement has been proved entirely adequate by many years of performance.

STABILITY PROBLEMS OF COMPRESSED STEEL MEMBERS AND ARCH BRIDGES[a]

Discussion by S. O. Asplund

S. O. ASPLUND,[15] F. ASCE.—The Engesser-Vianello iteration[16] has proved quite useful in solving elastic buckling problems. The work needed depends on the number of iterations required and that is determined by the precision of the terminating estimate (Eq. 29(b)) of the buckling load. This estimate is of general importance and it may perhaps be appropriate to discuss it herein.

Generally speaking the buckling deflections η of an arch are soluble from a homogeneous differential equation

$$g(\eta) + H\,h(\eta) = 0 \quad \ldots\ldots\ldots\ldots\ldots\ldots \quad (56)$$

with boundary conditions; g and h are self-adjoint linear differential expressions with variable coefficients. For certain "eigen-values" λ_i of the horizontal force H this boundary value problem has non-zero solutions η_i:

$$g(\eta_i) + \lambda_i\,h(\eta_i) = 0 \quad \ldots\ldots\ldots\ldots\ldots\ldots \quad (57)$$

In the Engesser-Vianello method a roughly chosen approximation $\eta^{(1)}$ satisfying the boundary conditions is substituted into the second term of Eq. 56 and an improved solution $\eta = \eta^{(2)}$ is solved by numerical or graphical integration from Eq. 56:

$$g(\eta^{(2)}) = -\,H\,h(\eta^{(1)}) \quad \ldots\ldots\ldots\ldots\ldots\ldots \quad (58)$$

and the boundary conditions. This new function $\eta^{(2)}$ is posed as a better approximation and again substituted in the second term of Eq. 56. The solution is repeated.

H. A. Schwartz[17] investigated the convergence of such iterations. Assuming convergence, J. J. Koch[18] proved the intuitive formula

$$\lim_{n\to\infty} \eta^{(n-1)}/\eta^{(n)} = \lambda_1/H = \nu \quad \ldots\ldots\ldots\ldots\ldots\ldots \quad (59)$$

The "eigenfunctions" η_i are orthogonal and can be normalized:

$$\int \eta_i\,h(\eta_j)\,dx = \delta_{ij} \quad \ldots\ldots\ldots\ldots\ldots\ldots \quad (60a)$$

and

$$\int \eta_i\,g(\eta_j)\,dx = \lambda_i\,\delta_{ij} \quad \ldots\ldots\ldots\ldots\ldots\ldots \quad (60b)$$

---

[a] June, 1960 by Georg Wastlund.

[15] Prof., Chalmers Inst. of Tech., Gothenberg S., Sweden.

[16] F. Engesser, Öst. Ing. u. Arch, Ver. 1893, p. 506.

[17] H. A. Schwartz, Ges. Math. Abh. I, Berlin 1890, p. 241-265.

[18] J. J. Koch, Proc. 2nd Int. Congr. Appl. Mech., Zürich 1926, p. 213.

where $\delta_{ij} = 0$ for $i \neq j$ and $\delta_{ij} = 1$ for $i = j$. All integrals here written are assumed to be extended from $x = 0$ to $x = L$.

Any roughly posed displacement $\eta^{(1)}$ satisfying the boundary conditions can now be expressed by a Fourier series

$$\eta^{(1)} = \Sigma \eta_{fi}^{(1)} \eta_i \quad \ldots\ldots\ldots\ldots\ldots\ldots (61a)$$

and

$$\eta_{fi} = \int \eta^{(1)} h(\eta_i)\, dx \quad \ldots\ldots\ldots\ldots\ldots\ldots (61b)$$

Substituting Eqs. 61 and 57 into Eq. 58 we obtain

$$g(\eta^{(2)}) = -H \Sigma \eta_{fi}^{(1)} h \eta_i = \Sigma (H/\lambda_i) \eta_{fi}^{(1)} g(\eta_1) \quad \ldots\ldots\ldots (62)$$

or if $\eta^{(2)}$ satisfies the boundary conditions

$$\eta^{(2)} = \Sigma_i (H/\lambda_i) \eta_{fi}^{(1)} \eta_i \quad \ldots\ldots\ldots\ldots\ldots (63)$$

Repeating this we obtain

$$\eta^{(n)} = \Sigma_i (H/\lambda_i)^{n-1} \eta_{fi}^{(1)} \eta_i \quad \ldots\ldots\ldots\ldots\ldots (64)$$

and

$$\eta^{(n)} = (H/\lambda_1)^{n-1} \eta_{f1}^{(1)} \eta_1 + (H/\lambda_2)^{n-1} \eta_{f2}^{(1)} \eta_2 + \ldots \quad \ldots\ldots\ldots (65)$$

When n is large and $\lambda_2, \lambda_3, \ldots >> \lambda_1$ that is always the case for fixed arches, only the first term of Eq. 65 needs to be considered and we find, proving Eq. 59,

$$\eta^{(n-1)}/\eta^{(n)} = \lambda_1/H \quad \ldots\ldots\ldots\ldots\ldots\ldots (66)$$

Still, after a limited number n of iterations, the two curves $\eta^{(n-1)}$ and $\eta^{(n)}$ are not perfectly affine, so the value (Eq. 59) of the buckling safety factor will depend on the special abscissa at which the displacements $\eta^{(n-1)}$ and $\eta^{(n)}$ are measured. It has therefore been suggested to use the ratio of the integrals of η over the span

$$\nu_s^{(n)} = \int \eta^{(n-1)} dx / \int \eta^{(n)} dx \quad \ldots\ldots\ldots\ldots\ldots (67)$$

but it is seen by Eq. 65 that this value is not always the best. The lowest buckling mode being antisymmetric we have $\int \eta_1\, dx = 0$ and by Eq. 65 we obtain a too-high safety factor

$$\nu_s^{(n)} = \eta^{(n-1)}/\eta^{(n)} \to \lambda_2/H \quad \ldots\ldots\ldots\ldots\ldots (68)$$

To avoid this, absolute values of η can be used in Eq. 67. However, to be certain that a correct limit is approached the writer suggests adopting, for terminating buckling safety, the ratio

$$\nu^{(n)} = \int \eta^{(n-1)}\, \eta^{(n)} dx / \int \eta^{(n)} \eta^{(n)} dx \quad \ldots\ldots\ldots\ldots (69)$$

Inserting the first terms of Eq. 65 we obtain

$$\nu^{(n)} = \frac{\Sigma (H/\lambda_i)^{2n-3} \eta_{fi}^{(1)} \int \eta_i^2\, dx}{\Sigma (H/\lambda_i)^{2n-2} \eta_{fi}^{(1)} \int \eta_i^2\, dx} \to \frac{\lambda_1}{H} \quad \ldots\ldots\ldots\ldots (70)$$

The writer has applied the ratio (Eq. 69) to Engesser-Vianello approximations of problems with known exact solutions and found that it is very easy to apply numerically and that it yields surprisingly accurate results. These examples show, for instance, that two iterations using Eq. 69 gives a more accurate estimate than three iterations using Eq. 59.

DYNAMIC RESPONSE OF ELASTO PLASTIC FRAMES[a]

By A. A. Eremin

A. A. EREMIN,[4] M. ASCE.—In his conclusion Penzien stated, "Stiffness provided by secondary components such as walls, partitions, stairwells, and so on, are primarily responsible for the apparent ability of many existing structures to withstand strong motion earthquakes."

It should be noted that when rigid walls or stairwells are used as damping members in a structure they should be designed to give a uniform variation of elasto-plastic rigidity in the structure. In Fig. 2 there has been shown the diagram of elasto-plastic stress-strain variation. It would be interesting if Penzien would indicate the repeated stress-strain loop that resulted form a dynamic vibrating force. Generally it is considered that the strain in steel beyond the yield point does not recover in a short period of time.

The graphs of dynamic stresses superimposed over the spectra of stresses for the El Centro earthquake in Fig. 5 to 12 is a valuable contribution. It is interesting to note that at the greater dynamic stresses, as shown on the figures, the effect of damping stresses is increased whereas the graphs in Fig. 13 show that at the increased dynamic stresses the damping stresses are decreased.

---

[a] July, 1960, by Joseph Penzien.

[4] Assoc. Bridge., Bridge Dept., Calif. State Highways, Sacramento, Calif.

ERRATA

Journal of the Structural Division

Proceedings of the American Society of Civil Engineers

July 1960

p. 119. In line 2 of Eq. 41 change $L^3\ b/\pi^2$ to $L^4\ b/\pi^2$. In line 3 of Eq. 41 change $L^2\ \bar{z}/\pi^2$ to $L^4\ \bar{z}/\pi^2$.

p. 121. In line 2 of Eq. 47 change I_{xy} to I_{zx}. In line 2 of Eq. 48 remove the first parentheses and insert a parentheses prior to the term 1/A. In line 5 of Eq. 48 insert a bracket just after the first minus sign and another bracket just prior to the first bracket that was printed originally. In line 5 of Eq. 48 change the denominator $n\ \pi\ E\ I_{xy}$ to $n^2\pi^2\ E\ I_{xy}$. In line 6 of Eq. 48 insert a bracket just after the first plus sign and insert a bracket just prior to the term s_{jn}.

August 1960

p. 111. Delete the first paragraph of the discussion by Mr. Newson and replace it with

> Mr. Bonasia has presented a very interesting paper on a subject which is current and has especial significance for the younger engineer because it is fairly easy to understand; and, if called upon to do so, the younger engineer should have no trouble solving the kind of problem with which the paper is concerned.

October, 1960

p. 57. Eq. 7 should be written

$$M_{ab} = -Q_a\ \theta_a \quad \ldots\ldots\ldots\ldots\ldots\ldots \quad (7)$$

p. 62. Eq. 21b should be written

$$M_{bc} = K_{bc}\ \left(4\ \theta_b + 2\ \theta_c\right) = 2\ K_{bc}\ \theta_b \quad \ldots\ldots\ldots \quad (21b)$$

p. 68. Eq. 35b should be written

$$2\ K_{bc}\ \theta\ b + \left(K_{cd}\ A'_{cd} + 4\ K_{bc} + 4\ K_{cf}\right)\ \theta_c + 2\ K_{cf}\ \theta_f - K_{cd}\ C_{cd}\ c_{cd}\ \frac{\Delta\ ab}{L_{cd}} = 0 \quad \ldots\ldots\ldots\ldots \quad (35b)$$

Eq. 35d should be Eq. 35c; Eq. 35e should be Eq. 35d.

p. 69. The proper Fig. 8 should be as follows:

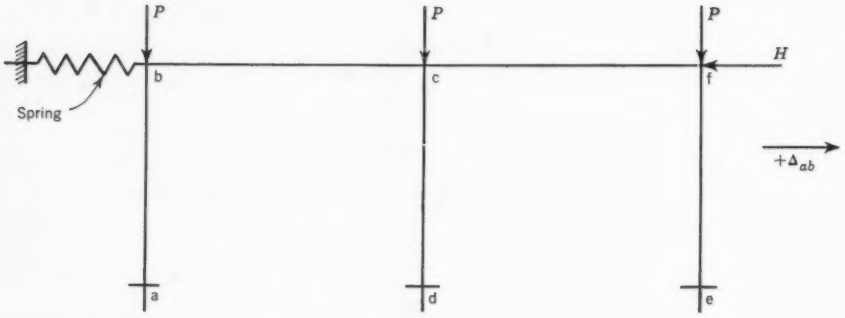

pgs. 69-70. Eq. 36 should be written as follows:

$$\frac{K_{ab}}{L_{ab}} C_{ab}\, c_{ab}\, \theta_b + \frac{K_{cd}}{L_{cd}} C_{cd}\, c_{cd}\, \theta_c + \frac{K_{ef}}{L_{ef}} C_{ef}\, c_{ef}\, \theta_f$$

$$- \left(\frac{K_{ab}}{L_{ab}^2} C_{ab}\, c'_{ab} + \frac{K_{cd}}{L_{cd}^2} C_{cd}\, c'_{cd} + \frac{K_{ef}}{L_{ef}^2} C_{ef}\, c'_{ef} \right.$$

$$\left. - \frac{P_{ab}}{L_{ab}} - \frac{P_{cd}}{L_{cd}} - \frac{P_{ef}}{L_{ef}} + k \right) \Delta_{ab} = H = 0 \quad \ldots\ldots \quad (36)$$

there is no Eq. 36b.

p. 73. Eq. 43 should be written as

$$\frac{\mu}{H} = \frac{y_i^{(n+1)}}{y_i^{(n)}}$$

p. 88. Change Eqs. 1a, 1b and 1c to,

$$dA = t\, dx \quad \ldots\ldots\ldots\ldots\ldots\ldots \quad (1a)$$

$$dy = \frac{a}{12}\, dx \quad \ldots\ldots\ldots\ldots\ldots\ldots \quad (1b)$$

$$dx = \frac{a}{12}\, dy \quad \ldots\ldots\ldots\ldots\ldots\ldots \quad (1c)$$

p. 102. Change "reaction" to "the section"

PROCEEDINGS PAPERS

The technical papers published in the past year are identified by number below. Technical-division sponsorship is indicated by an abbreviation at the end of each Paper Number, the symbols referring to: Air Transport (AT), City Planning (CP), Construction (CO), Engineering Mechanics (EM), Highway (HW), Hydraulics (HY), Irrigation and Drainage (IR), Pipeline (PL), Power (PO), Sanitary Engineering (SA), Soil Mechanics and Foundations (SM), Structural (ST), Surveying and Mapping (SU), and Waterways and Harbors (WW), divisions. Papers sponsored by the Department of Conditions of Practice are identified by the symbols (PP). For titles and order coupons, refer to the appropriate issue of "Civil Engineering." Beginning with Volume 82 (January 1956) papers were published in Journals of the various Technical Divisions. To locate papers in the Journals, the symbols after the paper number are followed by a numeral designating the issue of a particular Journal in which the paper appeared. For example, Paper 2703 is identified as 2703(ST1) which indicates that the paper is contained in the first issue of the Journal of the Structural Division during 1961.

VOLUME 86 (1960)

JANUARY: 2331(EM1), 2332(EM1), 2333(EM1), 2334(EM1), 2335(HY1), 2336(HY1), 2337(EM1), 2338(EM1), 2339(HY1), 2340(HY1), 2341(SA1), 2342(EM1), 2343(SA1), 2344(ST1), 2345(ST1), 2346(ST1), 2347(ST1), 2348(EM1)[c], 2349(HY1)[c], 2350(ST1), 2351(ST1), 2352(SA1)[c], 2353(ST1)[c], 2354(ST1).

FEBRUARY: 2355(CO1), 2356(CO1), 2357(CO1), 2358(CO1), 2359(CO1), 2360(CO1), 2361(PO1), 2362(HY2), 2363(ST2), 2364(HY2), 2365(SU1), 2366(HY2), 2367(SU1), 2368(SM1), 2369(HY2), 2370(SU1), 2371(HY2), 2372(PO1), 2373(SM1), 2374(HY2), 2375(PO1), 2376(HY2), 2377(CO1)[c], 2378(SU1), 2379(SU1), 2380(SU1), 2381(HY2)[c], 2382(ST2), 2383(SU1), 2384(ST2), 2385(SU1)[c], 2386(SU1), 2387(SU1), 2388(SU1), 2389(SM1), 2390(ST2)[c], 2391(SM1)[c], 2392(PO1)[c].

MARCH: 2393(IR1), 2394(IR1), 2395(IR1), 2396(IR1), 2397(IR1), 2398(IR1), 2399(IR1), 2400(IR1), 2401(IR1), 2402(IR1), 2403(IR1), 2404(IR1), 2405(IR1), 2406(IR1), 2407(SA2), 2408(SA2), 2409(HY3), 2410(ST3), 2411(SA2), 2412(HW1), 2413(WW1), 2414(WW1), 2415(HY3), 2416(HW1), 2417(HW3), 2418(HW1)[c], 2419(WW1)[c], 2420(WW1), 2421(WW1), 2422(WW1), 2423(WW1), 2424(SA2), 2425(SA2)[c], 2426(HY3)[c], 2427(ST3)[c]

APRIL: 2428(ST4), 2429(HY4), 2430(PO2), 2431(SM2), 2432(PO2), 2433(ST4), 2434(EM2), 2435(PO2), 2436(ST4), 2437(ST4), 2438(HY4), 2439(EM2), 2440(EM2), 2441(ST4), 2442(SM2), 2443(HY4), 2444(ST4), 2445(EM2), 2446(ST4), 2447(EM2), 2448(SM2), 2449(HY4), 2450(ST4), 2451(HY4), 2452(HY4), 2453(EM2), 2454(EM2), 2455(EM2)[c], 2456(HY4)[c], 2457(PO2)[c], 2458(ST4)[c], 2459(SM2)[c].

MAY: 2460(AT1), 2461(ST5), 2462(AT1), 2463(AT1), 2464(CP1), 2465(CP1), 2466(AT1), 2467(AT1), 2468(SA3), 2469(HY5), 2470(ST5), 2471(SA3), 2472(SA3), 2473(ST5), 2474(SA3), 2475(ST5), 2476(SA3), 2477(ST5), 2478(HY5), 2479(SA3), 2480(ST5), 2481(SA3), 2482(CO2), 2483(CO2), 2484(HY5), 2485(HY5), 2486(AT1)[c], 2487(CP1)[c], 2488(CO2)[c], 2489(HY5)[c], 2490(SA3)[c], 2491(ST5)[c], 2492(CP1), 2493(CO2).

JUNE: 2494(IR2), 2495(IR2), 2496(ST6), 2497(EM3), 2498(EM3), 2499(EM3), 2500(EM3), 2501(SM3), 2502(EM3), 2503(PO3), 2504(WW2), 2505(EM3), 2506(HY6), 2507(WW2), 2508(PO3), 2509(ST6), 2510(EM3), 2511(EM3), 2512(ST6), 2513(HW2), 2514(HY6), 2515(PO3), 2516(EM3), 2517(WW2), 2518(WW2), 2519(EM3), 2520(PO3), 2521(HY6), 2522(SM3), 2523(ST6), 2524(HY6), 2525(HY6), 2526(HY6), 2527(IR2), 2528(ST6), 2529(HW2), 2530(IR2), 2531(HY6), 2532(EM3)[c], 2533(HW2)[c], 2534(WW2), 2535(HY6)[c], 2536(IR2)[c], 2537(PO3)[c], 2538(SM3)[c], 2539(ST6)[c], 2540(WW2)[c].

JULY: 2541(ST7), 2542(ST7), 2543(SA4), 2544(ST7), 2545(ST7), 2546(HY7), 2547(ST7), 2548(SU2), 2549(SA4), 2550(SU2), 2551(HY7), 2552(ST7), 2553(SU2), 2554(SA4), 2555(ST7), 2556(SA4), 2557(SA4), 2558(SA4), 2559(ST7), 2560(SU2)[c], 2561(SA4)[c], 2562(HY7)[c], 2563(ST7)[c].

AUGUST: 2564(SM4), 2565(EM4), 2566(ST8), 2567(EM4), 2568(PO4), 2569(PO4), 2570(HY8), 2571(EM4), 2572(EM4), 2573(EM4), 2574(SM4), 2575(EM4), 2576(EM4), 2577(HY8), 2578(EM4), 2579(PO4), 2580(EM4), 2581(ST8), 2582(ST8), 2583(EM4)[c], 2584(PO4)[c], 2585(ST8)[c], 2586(SM4)[c], 2587(HY8)[c].

SEPTEMBER: 2588(IR3), 2589(IR3), 2590(WW3), 2591(IR3), 2592(HW3), 2593(IR3), 2594(IR3), 2595(IR3), 2596(HW3), 2597(WW3), 2598(IR3), 2599(WW3), 2600(WW3), 2601(WW3), 2602(WW3), 2603(WW3), 2604(HW3), 2605(SA5), 2606(WW3), 2607(SA5), 2608(ST9), 2609(SA5)[c], 2610(IR3), 2611(WW3)[c], 2612(ST9)[c], 2613(IR3)[c], 2614(HW3)[c].

OCTOBER: 2615(EM5), 2616(EM5), 2617(ST10), 2618(SM5), 2619(EM5), 2620(EM5), 2621(ST10), 2622(EM5), 2623(SM5), 2624(EM5), 2625(SM5), 2626(SM5), 2627(EM5), 2628(EM5), 2629(ST10), 2630(ST10), 2631(PO5)[c], 2632(EM5)[c], 2633(ST10), 2634(ST10), 2635(ST10)[c], 2636(SM5)[c].

NOVEMBER: 2637(ST11), 2638(ST11), 2639(CO3), 2640(ST11), 2641(SA6), 2642(WW4), 2643(ST11), 2644(HY9), 2645(ST11), 2646(HY9), 2647(WW4), 2648(WW4), 2649(WW4), 2650(ST11), 2651(CO3), 2652(HY9), 2653(HY9), 2654(ST11), 2655(HY9), 2656(HY9), 2657(SA6), 2658(WW4), 2659(WW4)[c], 2660(SA6), 2661(CO3), 2662(CO3), 2663(SA6), 2664(CO3)[c], 2665(HY9)[c], 2666(SA6)[c], 2667(ST11)[c].

DECEMBER: 2668(ST12), 2669(IR4), 2670(SM6), 2671(IR4), 2672(IR4), 2673(IR4), 2674(ST12), 2675(EM6), 2676(IR4), 2677(HW4), 2678(ST12), 2679(EM6), 2680(ST12), 2681(SM6), 2682(IR4), 2683(SM6), 2684(SM6), 2685(IR4), 2686(EM6), 2687(EM6), 2688(EM6), 2689(EM6), 2690(EM6), 2691(EM6)[c], 2692(ST12), 2693(ST12), 2694(HW4)[c], 2695(IR4)[c], 2696(SM6)[c], 2697(ST12)[c].

VOLUME 87 (1961)

JANUARY: 2698(PP1), 2699(PP1), 2700(HY1), 2701(SA1), 2702(SU1), 2703(ST1), 2704(ST1), 2705(SU1), 2706(HY1), 2707(HY1), 2708(HY1), 2709(PO1), 2710(HY1), 2711(HY1), 2712(ST1), 2713(HY1), 2714(PO1), 2715(ST1), 2716(HY1), 2717(SA1), 2718(SA1), 2719(SU1)[c], 2720(SA1)[c], 2721(ST1), 2722(PP1)[c], 2733(PO1)[c], 2724(HY1)[c], 2725(ST1)[c].

c. Discussion of several papers, grouped by divisions.

AMERICAN SOCIETY OF CIVIL ENGINEERS

OFFICERS FOR 1961

PRESIDENT

GLENN W. HOLCOMB

VICE-PRESIDENTS

Term expires October 1961:
CHARLES B. MOLINEAUX
LAWRENCE A. ELSENER

Term expires October 1962:
DONALD H. MATTERN
WILLIAM J. HEDLEY

DIRECTORS

Term expires October 1961:
THOMAS J. FRATAR
EARL F. O'BRIEN
DANIEL B. VENTRES
CHARLES W. BRITZIUS
WAYNE G. O'HARRA
FRED H. RHODES, JR.
N. T. VEATCH

Term expires October 1962:
ELMER K. TIMBY
SAMUEL S. BAXTER
THOMAS M. NILES
TRENT R. DAMES
WOODROW W. BAKER
BERNHARD DORNBLATT

Term expires October 1963:
ROGER H. GILMAN
HENRY W. BUCK
EARLE T. ANDREWS
JOHN B. SCALZI
JOHN D. WATSON
HARMER E. DAVIS

PAST PRESIDENTS

Members of the Board

FRANCIS S. FRIEL
FRANK A. MARSTON

EXECUTIVE SECRETARY
WILLIAM H. WISELY

TREASURER
E. LAWRENCE CHANDLER

ASSISTANT SECRETARY
DON P. REYNOLDS

ASSISTANT TREASURER
LOUIS R. HOWSON

PROCEEDINGS OF THE SOCIETY

HAROLD T. LARSEN
Manager of Technical Publications

PAUL A. PARISI
Editor of Technical Publications

MARVIN L. SCHECHTER
Associate Editor of Technical Publications

IRVIN J. SCHWARTZ
Assistant Editor of Technical Publications

COMMITTEE ON PUBLICATIONS

THOMAS M. NILES, *Chairman*

WAYNE G. O'HARRA, *Vice-Chairman*

BERNHARD DORNBLATT
HENRY W. BUCK
JOHN D. WATSON
HARMER E. DAVIS